BST

BioScience Trends

IRCA
BSSA

IACMHR

www.biosciencetrends.com

BioScience Trends is one of a series of peer-reviewed journals of the International Research and Cooperation Association for Bio & Socio-Sciences Advancement (IRCA-BSSA) Group and is published bimonthly by the International Advancement Center for Medicine & Health Research Co., Ltd. (IACMHR Co., Ltd.) and supported by the IRCA-BSSA and Shandong University China-Japan Cooperation Center for Drug Discovery & Screening (SDU-DDSC).

BioScience Trends devotes to publishing the latest and most exciting advances in scientific research. Articles cover fields of life science such as biochemistry, molecular biology, clinical research, public health, medical care system, and social science in order to encourage cooperation and exchange among scientists and clinical researchers.

BioScience Trends publishes Original Articles, Brief Reports, Reviews, Policy Forum articles, Case Reports, News, and Letters on all aspects of the field of life science. All contributions should seek to promote international collaboration.

Editorial Board

BioScience Trends

Editorial and Head Office

Pearl City Koishikawa 603, 2-4-5 Kasuga, Bunkyo-ku,
Tokyo 112-0003, Japan

Tel: +81-3-5840-8764, Fax: +81-3-5840-8765
E-mail: office@biosciencetrends.com
URL: www.biosciencetrends.com

Editorial Board Members

CONTENTS   *Volume 9, Number 5, 2015*

CONTENTS   (*Continued*)

Guide for Authors

Copyright

Policy Forum

Human resources for health development: toward realizing Universal Health Coverage in Japan

Hidechika Akashi[1],*, Yasuyo Osanai[2], Rumiko Akashi[3]

[1] *Bureau of International Health Cooperation, National Center for Global Health and Medicine, Tokyo, Japan;*
[2] *Center Hospital, National Center for Global Health and Medicine, Tokyo, Japan;*
[3] *Department of Social Work, Meijigakuin University, Tokyo, Japan.*

Summary	Human resources are an important factor in establishing universal health coverage (UHC). We examined Japan's health policies related to development of human resources for health (HRH) toward establishing UHC, and tried to formulate a model for other countries wanting to introduce UHC through reviewing existing data and documents related to Japan's history in developing HRH. In the results, there were four phases of HRH development in Japan: Phase 1 involved a shortage of HRH; Phase 2 was characterized by rapid production of less-educated HRH; Phase 3 involved introduction of quality improvement procedures such as upgrade education for nursing staff or licensing examination for physicians; Phase 4 was characterized by a predominance of formal health professionals. To encourage transition between these phrases, Japan utilized several procedures, including: (*i*) offering shorter professional education, (*ii*) fewer admission requirements for professional education, (*iii*) widespread location of schools, and (*iv*) the aforementioned quality improvement procedures. Japan was able to introduce UHC during Phase 3, and Japanese health indicators have improved gradually through these phases. Consequently, the government of Japan focused on increasing the quantity of HRH through relaxed admission requirements, shorter education periods, and increasing the numbers of educational facilities, before introducing UHC. Subsequently, the government began focusing on improving quality through procedures such as upgrade education or licensing examination programs to enable less-educated HRH to become fully educated professionals. For governments wanting to introduce UHC, the Japanese model can be a suitable option for HRH development, particularly in resource-poor countries.

Keywords: Japan, human resources for health (HRH), universal health coverage (UHC), quantity, quality, nurse, auxiliary nurse, physician

1. Introduction

Universal health coverage (UHC) has been announced as one of the important topics in the post-Millennium Development Goal (MDG) agenda (*1*). Japan has gained international recognition for its outstanding achievement of UHC during the second half of the 20th century (*2*). Japan established UHC in 1961 with the completion of its universal health insurance ("kokumin kaihoken") system (*2-4*). However, a universal health insurance system, which enables the whole population to have financial access to health care services, is not sufficient for establishing UHC. Indeed, establishment of UHC would require a formal health service provision system including an adequate health workforce as suggested by the World Health Organization (WHO) in its six building-block model of an effective health system (*5*). Blockages in health systems, including a critical shortage of skilled, motivated, and geographically distributed health workers, can lead to inefficient and ineffective health coverage (6).

There are some cross-sectional studies of human resources development toward UHC in several countries (*7,8*). Similarly, there are other articles on the

*Address correspondence to:
Dr. Hidechika Akashi, Bureau of International Health Cooperation, National Center for Global Health and Medicine, 1-21-1 Toyama, Shinjuku-ku, Tokyo 162-8655, Japan.
E-mail: hakashi@it.ncgm.go.jp

chronological history on human resource development in the health care system of Japan (*9*), but these present neither its fundamental meaning in relation to UHC development nor a model for UHC establishment. Ikegami and Buchan (*10*) discussed health policies in introducing licensed practical nurses (*i.e.*, auxiliary nurses), which were important for promoting UHC; however, there are few articles like theirs. In this paper, we examine how Japan attained UHC from a human resource perspective through reviewing existing publications and data on the Japanese history of human resources for health development. More specifically, we discuss human resource development with a focus on physicians and nurses because these health personnel are the main providers of medical services, and attempt to extract from this discussion important lessons and a schematic explanation of human resource development to provide a method of enabling such development towards UHC in other countries.

2. Chronological changes on the production of health service providers

2.1. *Nurses*

The following phases, listed chronologically, of nursing staff production in Japan were identified.

Phase 1 "Health workforce shortage": This phase, starting at around World War II (WWII), was characterized by a decrease in the number of nurses (*11*).

Phase 2 "Rapid production of auxiliary nurses": The Government of Japan (GOJ) implemented shorter nursing education programs (*i.e.*, auxiliary nurse education programs ["jun-kangoshi"], a form of two-year specialty education), while increasing the number of schools offering these programs from around 300 in the early 1950s to over 400 in the mid-1950s and over 500 in the late 1950s (*12*). The number of auxiliary nursing schools continuously increased after 1961, reaching over 700 in the mid-1960s. The number of prefectures with such schools increased from 41 in 1958 to 47 later on; eventually, every prefecture had them (*12-14*). These shorter programs were organized by local physicians' associations or hospitals, and were located throughout each prefecture, including in rural areas. Auxiliary nurse licenses were issued by prefectural governors. Using this strategy, the number of auxiliary nurses increased dramatically from less than 10,000 in the 1940s and early 1950s to around 70,755 in 1961 and 133,811 in 1969; the number of registered nurses (*i.e.*, completed a three-year program) plateaued at around 110,000 in the 1950s and 60s (*11*).

Phase 3 "Quality improvement through upgrade education": During Phase 2 (in 1959), the GOJ began offering upgrade courses for auxiliary nurses (two-year program), thereby enabling auxiliary nurses to become registered nurses. Additionally, the production

of formally educated nurses also increased.

Phase 4 "Predominance of formal nurses": This phase was characterized by a marked reduction in nurses with two-year educations, causing nurses with formal educations (more than three-year education) to become the predominant human resource for health; such nurses included bachelors of nursing course (four-year) graduates.

2.2. *Physicians*

The GOJ employed similar steps for physicians as for nurses. Before WWII, Japanese medical education included a six-year course for medical doctors and four-year vocational education courses.

Phase 1 "Health workforce shortage": Before WWII, there was a clear physician shortage; indeed, from 1912-1931, only 40,000 physicians were working (*11*). The number of medical schools was nine in 1888, and 17 in 1919 (*15*).

Phase 2 "Rapid production of less-educated physicians": The GOJ increased the number of medical doctors to reduce the wartime shortage. Thus, from 1939-1945, they increased the number of medical schools and three-year extra-affiliated schools of medicine (which offered shorter courses than the medical schools) (*15,16*). Accordingly, the number of admissions to medical schools increased from 3,078 students (1935) to 10,533 (1945) (*11*); female students were also accepted (*16*). The number of medical schools was 26 in 1939, and 69 in 1945 (*15*). The annual number of graduates from medical schools and extra-affiliated schools increased from around 50,000 (1932-1936) to over 60,000 (1937-1941) (*11*). This increase was not planned to introduce UHC but rather to account for wartime shortages in personnel; however, these procedures indirectly influenced introduction of UHC.

Phase 3 "Quality improvement phase through national licensing examination": After WWII (1945), physicians who had completed a three-year education returned to Japan, thus increasing the number from 13,833 in 1945 to 65,301 in 1946 and 70,636 in 1947 (*11*). It was thought that they would spread throughout Japan by returning to their hometowns. Subsequently, the national licensing examination was introduced in 1947; all medical school graduates had to pass this examination. Additionally, in 1948, medical universities became the only authorized medical schools. As such, graduates of three-year education courses had to pass a physician's preparatory examination and undergo one year of clinical training to ensure they were at the same level as medical school graduates (*15*).

Phase 4 "Predominance of formal physicians": The number of medical university graduates (*i.e.*, the six-year education) increased gradually, with the number of physicians reaching 104,732 in 1961 and 116,568 in 1969 (*11*) – over eight times the number in 1945.

These trends in the numbers of physicians, nurses, and auxiliary nurses are shown in Figure 1 (*11*). Based on our data analysis of physicians and nurses, a schematic explanation of their development processes is shown in Figure 2. Notably, many health indicators such as mortality rates from pneumonia and tuberculosis and the infant mortality rate (which was 76.7 in 1947 and 28.6 in 1961) improved gradually over the studied period; however, we observed increasing trends in mortality rates from cancers, cerebrovascular diseases, and cardiac diseases during that same period (*4,17*).

3. Strategies on health workforce development

Based on the Japanese experience, we extracted the following strategies on health workforce development.

3.1. *Focusing on quantity instead of quality*

3.1.1. *Shorter professional education*

Shorter education courses – such as extra-affiliated schools of medicine for physicians and auxiliary nursing education courses for nursing staff – were introduced in Phase 2. For example, with nursing staff, rather than expanding the number of three-year courses, the GOJ increased the number of two-year courses,
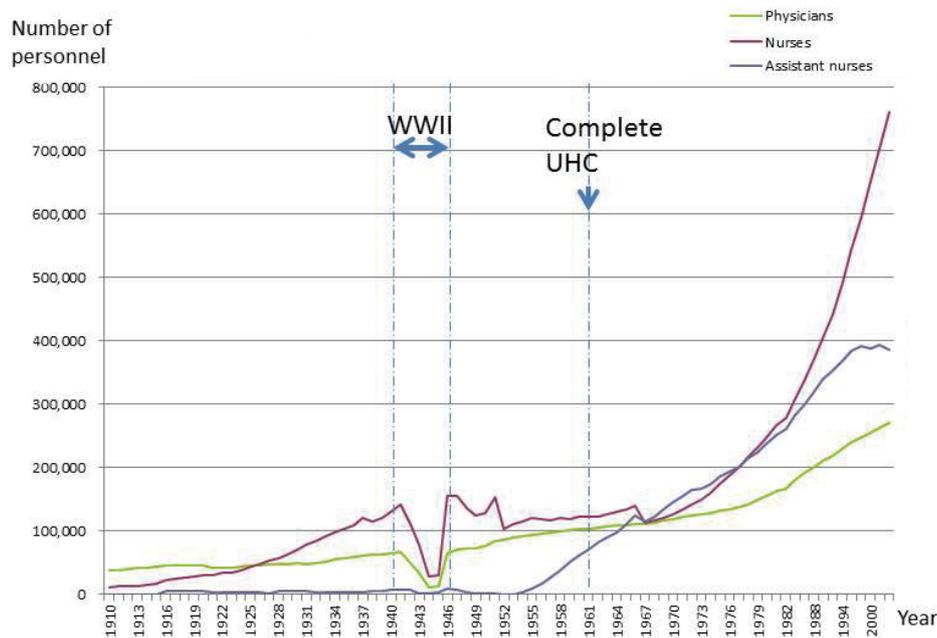
**Figure 1. Trends of human resources for health in Japan.** WWII: World War Second, UHC: Universal Health Coverage.
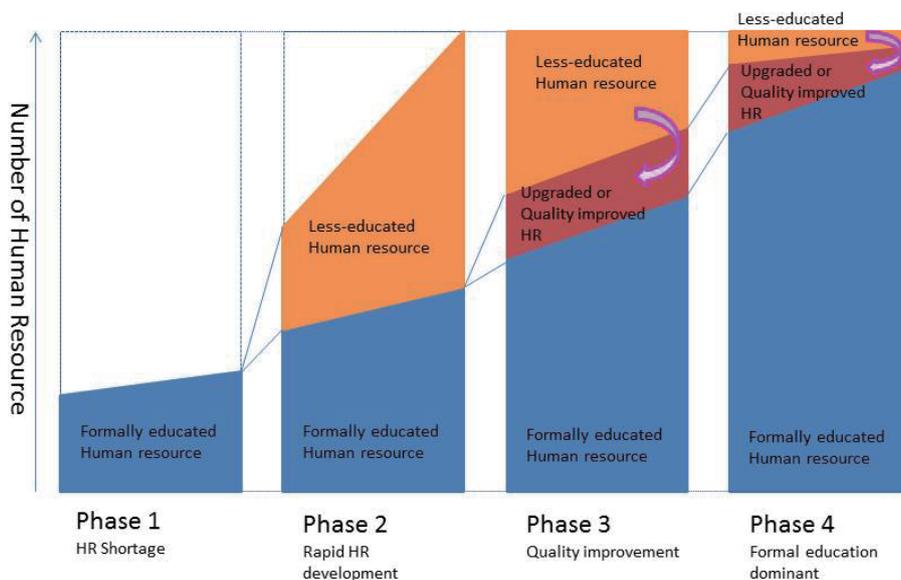
Figure 2. Schematic framework for human resource development to address its shortage. HR: Human Resources, Arrows in the figure mean "conversion" from less-educated HR to quality improved HR through up-grading course education, licensing examination, or other quality improvement procedures.

that is, auxiliary nursing schools (*12*). For physicians, a similar strategy was observed, although the expansion of shorter courses was to account for wartime shortages. In other words, the GOJ began rapid production of less-educated physicians with three-year educations instead of six-year ones before 1945 during wartime (Phase 2). Additionally, special medical schools for women were opened to serve people inside of Japan. Then, many physicians, including those less-educated ones, returned to Japan just after the end of WWII (Figure 1), and they covered almost the entire country after 1946.

3.1.2. *Fewer admission requirements for professional education*

Admission requirements for auxiliary nursing courses were only a basic education (*i.e.*, junior-high school graduates), whereas ordinary nursing courses required at least a high school graduation. There were few high school graduates during the study period; specifically, the admission rate to high school was 42.5% in 1950, 51.5% in 1955, 57.7% in 1960, and 70.7% in 1965 (*18*). This seems to have occurred in other countries as well. In Cambodia, there are few nursing student candidates with high school education, especially in rural areas (*19*).

However, we did not observe reduced admission requirements to medical schools for physicians' education (*15*).

3.1.3. *Widespread school locations*

Widespread schools can contribute to an increasing health workforce. For nurses, one of the reasons for this expansion in schools was that auxiliary nursing schools were usually established in hospitals by local physicians' associations in rural prefectures of Japan. This was because rural local hospitals under the physicians' associations required cheaper labor, and thus wanted to produce such relatively less qualified nurses by themselves. Another reason was that less-educated students seemed to predominantly inhabit rural areas just after WWII. This phenomenon meant that the GOJ began establishing schools throughout the country, although the quality of education in such nursing schools varied. "Those who had stayed longer in rural areas had settled and integrated well within their community" (*20*); therefore, it can be said that the local recruitment of students is important for staff retention in remote areas. However, it is important to consider how these schools are distributed, because it has been reported that this increase in nursing institutions could only be accomplished by deepening geographical imbalances in human resource distribution (*7*).

For physicians, 69 schools (including 18 universities and 51 relevant special schools) in 1945 were widely distributed covering almost the entire country (*15*).

3.2. *Shifting from quantity to quality*

Ikegami and Buchan pointed out that Japan's focus on quantity was an important factor for UHC introduction (*10*). This unique Japanese approach of producing auxiliary nurses may be appropriate for increasing the amount of health personnel in rural areas. However, in 1957, once auxiliary nurses had spread throughout the country, Japan introduced education upgrades for two-year courses, thereby allowing auxiliary nurses to become registered nurses (Phase 3). These upgrade courses have continued until the present. Through these processes, registered nurses gradually became the predominant human resource for health, and the four-year nursing university education was introduced (Phase 4). In these last two phases, the GOJ shifted the focus of its policy from increasing the quantity to increasing the quality of the health workforce. For physicians, the GOJ certified less-educated physicians as fully educated physicians via a licensing examination rather than providing an upgraded education (Phase 3).

3.3. *Limitation*

There are some problems in focusing solely on quantity rather than quality of an individual health workforce to ensure the quality of medical services. However, less-educated health personnel may be better than no health personnel or harmful procedures practiced by some traditional healers.

The year that UHC began in Japan, 1961, was during Phase 3. During this period, some health indicators improved such as the mortality rates for pneumonia or tuberculosis. However, we cannot conclude that the increases in the health workforce were responsible for these improvements, because streptomycin, chest X-rays, improved nutrition, etc. were introduced during that time, which contributed to a reduction in tuberculosis in Japan (*21*).

4. Conclusion

The Japanese process of introducing UHC is said to have been a complicated and unique case; however, it appears that human resource development was largely responsible and its process can be simplified as we have shown. In other words, before introducing UHC, the GOJ focused on increasing the quantity of health and medical professionals via less stringent admission requirements and shorter professional education courses delivered at institutions covering the entire country. Then, quality improvement procedures such as upgraded courses or quality assurance licensing examinations were introduced to allow existing human resources to be recognized as fully educated professionals. Governments wanting to introduce UHC may be able to use this Japanese model as a means of

human resource development, especially in resource-poor countries..

References

1. United Nations, General Assembly. The road to dignity by 2030: Ending poverty, transforming all lives and protecting the planet. Synthesis report of the Secretary-General on the post-2015 sustainable development agenda. 2014. A/69/700.
2. Reich MR, Ikegami N, Shibuya K, Takemi K. 50 years of pursuing a healthy society in Japan. Japan Universal Health Care at 50 Years. Lancet. 2011; 378:1051-1053.
3. Campbell JC, Ikegami N, Tsugawa Y. The political-historical context of Japanese health care. Universal Health Coverage for Inclusive and Sustainable Development, Lessons from Japan. A World Bank Study. World Bank Group, Washington DC, USA, 2014; pp. 15-26.
4. Research Group, Japan International Cooperation Agency (JICA). Japan's experiences in public health and medical systems: towards improving public health and medical systems in developing countries. Institute for International Cooperation, JICA, Tokyo, Japan, 2005; pp. 15-18.
5. World Health Organization. Everybody's business. Strengthening health systems to improve health outcomes. WHO's framework for action. WHO Document Production Services, Geneva, Switzerland, 2007.
6. Save the Children. Universal health coverage: A commitment to close the gap. Save the Children, London, UK, 2013; pp. 24-25.
7. Roo M, Rao KD, Kumar AKS, Chatterjee M, Sundararaman T. India: Towards Universal Health Coverage 5. Human Resources for Health in India. Lancet. 2011; 377:587-598.
8. Anand S, Fan VY, Zhang J, Zhang L, Ke Y, Dong Z, Chen LC. Health System Reform in China 5. China's human resources for health: quantity, quality, and distribution. Lancet. 2008; 372:1774-781.
9. Japan International Cooperation Agency (JICA). Consideration on human resource development for health in Japan. JICA, Tokyo, Japan, 2013. (in Japanese)
10. Ikegami N, Buchan J. Licensed Practical Nurse: One option for expanding the nursing workforce in Japan. Universal Health Coverage for Inclusive and Sustainable Development, Lessons from Japan. A World Bank Study. World Bank Group, Washington DC, USA, 2014; pp. 133-148.
11. Statistics Bureau, Ministry of Internal Affaires and Communications. Historical statistics of Japan. Medical Care Personnel (1874-2004). Ministry of Internal Affaires and Communications, Tokyo, Japan, 2013. (in Japanese)
12. Nursing Division, Health Policy Bureau, Ministry of Health, Labor and Welfare. 60-year history of Act on Public Health Nurses, Midwives and Nurses. The Japan Nurse Association Publishing Company, Tokyo, Japan, 2009. (in Japanese)
13. Nursing Division, Health Policy Bureau, Ministry of Health and Welfare. Statistical data on nursing service in Japan. The Japan Nurse Association Publishing Company, Tokyo, Japan, 1979. (in Japanese)
14. Nursing Division, Health Policy Bureau, Ministry of Health, Labor and Welfare (MOHLW). Annual Nursing Report. MOHLW, Tokyo, Japan, unpublished data. 1953. (in Japanese)
15. Sakai T, Sawai T, Takizawa T, Fukushima O, Shimada K. Historical development of the systems of medical education and medical licensure and its effect on medical schools in Japan. Medical education. 2010; 41:337-346. (in Japanese)
16. Kamiya A. Medical education during the 15-years war in Japan, Journal of 15-years War and Japanese Medical Science and Service. 2007; 7: 1-12. (in Japanese)
17. Ministry of Health, Labor and Welfare. Vital statistics. *http://www.mhlw.go.jp/toukei/list/dl/81-1a2.pdf* (in Japanese). (accessed April 25, 2015).
18. Tokunaga T, Kamiyo H, Kitakaze K, Fuchigami T. The history of school education systems in Japan.- 100's year history on education system in Japan. National Institute of Educational Policy Research, Tokyo, Japan, 2012. (in Japanese).
19. Suzuki S. Historical change and issues on continuous education for midwives in Cambodia. Aichi Prefectural College of Nursing and Health, Nagoya, Japan, 2005; pp. 13-16. (in Japanese)
20. Mutale W, Ayles H, Bond V, Mwanamwenge MT, Balabanova D. Measuring health workers' motivation in rural health facilities: Baseline results from three study districts in Zambia. BMC Human Resources for Health. 2013;11:8. *http://www.human-resources-health.com/content/11/1/8.* (accessed June 11, 2013).
21. Ikeda K, Nadaoka Y, Kurashina S. (2003). A digital history of tuberculosis control in 20th Century Japan - Preparation of mortality data of vital statistics - Ann. Rep. Tokyo Metr. Inst. P.H. 2003;54:365-369. (in Japanese)

Associating liver partition and portal vein ligation (ALPPS): Taking a view of trails

Takeshi Takamoto, Yasuhiko Sugawara*, Takuya Hashimoto, Masatoshi Makuuchi

Divisions of Hepato-Biliary-Pancreatic and Liver Transplantation, Japanese Red Cross Medical Center, Tokyo, Japan.

Summary	Associating liver partition and portal vein ligation (ALPPS) is introduced as a modified two-staged hepatectomy for advanced liver malignancies, which requires extended hepatectomy with very small future remnant liver volume. It is characterized by rapid and large growth of future remnant liver and potential of widening the indication of curative resection with extended major hepatectomy for liver malignancies. It showed, however, much higher morbidity and mortality than extended hepatectomy after portal vein embolization. Here, we review the literatures and examine the role of ALPPS in Japan, where zero mortality after hepatectomy is highly expected.

Keywords: ALPPS, Japan, hepatectomy, liver malignancies, liver volume, portal vein embolization

1. Introduction

The ultimate goal for liver surgeons in performing hepatectomy for hepatobiliary malignancies is complete resection of tumors with zero mortality. The morbidity and mortality after liver resection are associated with insufficient remnant liver volume and its function. Therefore, several methods to increase the future remnant liver volume before major hepatectomy, including portal vein embolization (*1*), ligation (*2*), sequential arterial and portal vein embolizations (*3*), and two-staged hepatectomy (*4*), were introduced. These techniques, however, usually required 2-8 weeks interval before completing the entire clearance of tumor burden in the liver and the risk of tumor progression during the period might be critical especially among the patients with borderline resectable tumors or oncologically aggressive tumors (*5,6*).

In 2011, Baumgart and colleagues reported *in situ* liver splitting through the umbilical ligament with concomitant right portal vein ligation, achieving future liver remnant (FLR) hypertrophy in 9 days in two-stage right trisectionectomy (*7*). A multi-institutional study was immediately started and 25 patients with marginally resectable liver malignancies were included (*8*). In the first operation, surgical exploration, right portal vein ligation and *in situ* splitting of the liver parenchyma along the falciform ligament were performed. Limited resections for tumors in future remnant liver were performed if necessary. Then after a median interval of days (range: 5-28 days) waiting period, the right trisegmentectomy was completed as second operation. The volume of the left lateral lobe was increased in a median volume ratio of 74% (range: 21%-192%), which is rather larger comparing with the increasing volume ratio of 10-20% in several weeks after portal vein embolization (PVE). The morbidity ratio was, however, up to 68% and 14% of the patients were died within a short follow-up period of 180 days in median (range: 60-776 days) after surgery (*8*).

This new technique is named as "associating liver partition and portal ligation for staged hepatectomy (ALPPS)" and several authors demonstrated successful cases with the similar procedures (Table 1). Most of all the following studies showed 60% or more increment of remnant liver volume and 100% R0 resection rate. Nevertheless, the postoperative short-term outcome is not satisfactory showing that high incidence of morbidity (mostly over 50%), postoperative liver failure (around 20%), and in-hospital mortality was up to 10-20%. An international registry study, in which 56 institutions from all over the world took part, showed the result of analyzing 202 patients (141 patients with

*Address correspondence to:
Dr. Yasuhiko Sugawara, Divisions of Hepato-Biliary-Pancreatic Surgery and Liver Transplantation, Japanese Red Cross Medical Center. 4-1-22 Hiroo, Shibuya-ku, Tokyo 150-8935, Japan.
E-mail: yasusugatky@gmail.com

Table 1. Review of literature on ALPPS

Items	Year	n	Diagnosis	Liver Regeneration[*] (%)	Interval (days)	Morbidity (%)	Hepatic Insufficiency (%)	Sepsis (%)	Bile leakage (%)	In-Hospital Mortality (%)
Schnitzbauer	2012	25	HCC 3 Mets 16	74	9	64	-	20	24	12
Sala	2012	10	HCC 1 Mets 7	82	7	40	20	-	-	0
Alvarez	2013	15	HCC 1 Mets 13	78	7	53	20	-	20	0
Li	2013	9	Mets 3	87	13	16	22	22	22	22
Schadde	2014	48	HCC 3 CRLM 26	74	-	-	-	-	9.3	15
Knoefel	2013	7	-	65	6	71	0			0
Gauzolino (variations)	2013	4	CRLM 4	27.8	7	75	0	-	25	0
Robles (ALTPS)	2014	22	HCC 1 Mets 20	63	11	63	23	-	23	9
Ratti	2014	6	CRLM 3	58.3	7.5	50	0	-	-	17
Gall (RALPP)	2015	5	CRLM 5	62.3	21.8	20	0	0	0	0

HCC: hepatecellular carcinoma, Mets: metastatic liver tumors, CRLM: colorectal liver metastases, ALTPS: tourniquet in the umbilical fissure and right portal vein occlusion, RALPP: radio-frequency-assisted liver partition with portal vein ligation. [*] Liver regeneration ratio is showed as the ratio of increased volume to the future remnant liver volume before first operation.

colorectal liver metastases) who underwent ALPPS from 2012-2013 (*9*). Median future remnant liver volume ratio was increased from 21% to 40% for standardized future liver remnant (sFLR) within a median of 7 days. Ninety-day mortality was 9%. Severe complications including mortalities (Clavien-Dindo ≥ IIIb) occurred in 27% of patients.

Although this procedure is discussed vigorously in famous journals of surgery, the practical advantage of ALPPS is still under debate because it showed a high morbidity and mortality rate and the oncological benefits of the aggressive resection are not proven.

2. Problems of ALPPS

The ALPPS is potentially effective procedure for patients who requires super extended liver resection to achieve curative resection of extensive liver malignancies. The most notable phenomenon is the rapid liver hypertrophy. Schadde *et al*. calculated the speed of liver hyperatrophy during the waiting period before final hepatectomy and showed that the extrapolated growth rate was 11 times higher in ALPPS (34.8 cc/day; interquartile range 26-49) compared with PVE/PVL (3 cc/day; IQR2-6; *p* = 0.001). Attention should be paid, however, to the difference of waiting periods between ALPPS (1-2 weeks) and PVE/PVL (4-8 weeks) in order not to overestimate the impact of ALPPS on liver hypertrophy. The kinetic growth curve of liver regeneration is always convex upward.

The enlarged volume of liver is not always parallel to the increment of liver function, as is often the case with recipients of living-donor liver transplantation who show considerably enlarged transplanted liver graft and are suffering persistent liver insufficiency with hyperbilirubinemia. The effect of inflammation in the ischemic and congestive area in the part of liver with vascular modulation can induce the edema of liver.

An experimental model using mice gave important information about the mechanism of accelerated hypertrophy in ALPPS (*10*). In the experiment, the mice which underwent either transection or PVL alone received plasma from ALPPS-treated mice or the mice which were subjected to splenic, renal, or pulmonary ablation instead. Injury to other organs or ALPPS-plasma injection combined with PVL induced liver hypertrophy similar to ALPPS. This result supports the hypothesis that liver damage after the first procedure of ALPPS raises inflammatory signals and promotes the liver hypertrophy.

It might be misunderstood that no ischemic area except for a small part of transected segment IV or limited resections are remained in the first operation. Portal flow in veno-occlusive area (congestive area), however, becomes hepatofugal (*11*) and the congestive area can theoretically change to ischemic when the portal vein was occluded. The process of liver splitting along the Rex-Cantlie's line or right side of falciform ligament is always accompanied with division of hepatic venous tributaries and congestive area appears.

Therefore, larger area than expected can change to be necrotic after the first operation accordingly and such complete devascularized area may become a source of severe sepsis (*12*). The occurrence of bile leakage in ALPPS is reported up to around 20%, which is much higher than that in ordinary hepatectomy (< 5%) (*13*). As several authors commented that bile leakage was associated with sepsis, it is possible that bile leakage in ALPPS reflects a large area of liver parenchymal necrosis, because the dark red colored discharge from the necrotic area in liver usually contains high levels of bilirubin.

Although complete resection of liver malignancy by ALPPS procedure is safely achieved, the long-term benefit of aggressive surgical treatment is still unclear, especially for the patients with multiple bilobar colorectal liver metastases or hilar cholangiocarcinoma progressing into the peripheral biliary tree.

3. Modification of ALPPS

According to the original procedure of ALPPS, most of the procedures were performed in the first operation and the right liver and ischemic segment IV put in the plastic bag was removed in second operation. Several modifications of the first operation to lower invasive procedure were proposed aiming at reducing the damage and obtaining better patient's condition with same rapid liver hypertrophy before second operation. Robles *et al.* introduced a liver tourniquet ligation method instead of splitting liver. A tourniquet was positioned around Rex-Cantlie's line between the right and middle hepatic veins used in the hanging maneuver and it was knotted tightly on a groove 1 cm deep which was made along the Rex-Cantlie's line. They showed 61% (33-189%) increasing of FLR after 7days and liver failure ratio was 23% and two of included 22 patients were died after the second operation (*14*). Machado *et al.* reported that total laparoscopic right portal vein ligation combined with *in situ* splitting is feasible (*15*). Gall *et al.* reported 5 cases of radio-frequency ablation along Rex-Cantlie's line instead of splitting liver. This procedure showed better liver regeneration ratio than PVE (64.3% *vs.* 24.8%) and no mortality among all the included 5 cases. Petrowsky *et al.* showed improved postoperative morbidity and mortality and similar rapid future remnant liver hypertrophy by modifying the liver splitting procedure, *i.e.*, by switching from complete transection to a well-defined partial transection (> 50% of the transection surface). They hypothesized that sparing complete liver splitting can reduce the liver injury after the first operation by rescuing the "deportalized" part of the liver from congestion and ischemia (*16*).

4. ALPPS in Japan

Several high volume centers in Japan adopt ALPPS as an option of aggressive treatment for advanced colorectal liver metastases. It is difficult, however, to find a sign of the prevailing tide of ALPPS. The high mortality rate up to 10-20% in ALPPS cannot be easily accepted in Japan because the mortality rate of hepatectomy is reported less than 2% in a nationwide surveillance program and most of high volume center perform hepatectomy with nearly zero mortality (*17*). Furthermore, there is little limitation for performing portal vein embolization. A few institution indicated liver partition for patients who had insufficient volume increase and impaired liver function after portal vein embolization as an extension of ALPPS (*18*).

As Kokudo *et al.* pointed out that the ALPPS procedure can be said as a clinical study still under phase I (*19*), the most important issue is to modify this procedure safer and to establish indication criteria to select the cohort of patients who have best risk-benefit balance to adopt this procedure.

References

1. Makuuchi M, Thai BL, Takayasu K, Takayama T, Kosuge T, Gunven P, Yamazaki S, Hasegawa H, Ozaki H. Preoperative portal embolization to increase safety of major hepatectomy for hilar bile duct carcinoma: A preliminary report. Surgery. 1990; 107:521-527.
2. Broering DC, Hillert C, Krupski G, Fischer L, Mueller L, Achilles EG, Schulte am Esch J, Rogiers X. Portal vein embolization *vs.* portal vein ligation for induction of hypertrophy of the future liver remnant. J Gastrointest Surg. 2002; 6:905-913.
3. Aoki T, Imamura H, Hasegawa K, Matsukura A, Sano K, Sugawara Y, Kokudo N, Makuuchi M. Sequential preoperative arterial and portal venous embolizations in patients with hepatocellular carcinoma. Arch Surg. 2004; 139:766-774.
4. Adam R, Laurent A, Azoulay D, Castaing D, Bismuth H. Two-stage hepatectomy: A planned strategy to treat irresectable liver tumors. Ann Surg. 2000; 232:777-785.
5. Kokudo N, Tada K, Seki M, Ohta H, Azekura K, Ueno M, Ohta K, Yamaguchi T, Matsubara T, Takahashi T, Nakajima T, Muto T, Ikari T, Yanagisawa A, Kato Y. Proliferative activity of intrahepatic colorectal metastases after preoperative hemihepatic portal vein embolization. Hepatology. 2001; 34:267-272.
6. Hayashi S, Baba Y, Ueno K, Nakajo M, Kubo F, Ueno S, Aikou T, Komokata T, Nakamura N, Sakata R. Acceleration of primary liver tumor growth rate in embolized hepatic lobe after portal vein embolization. Acta Radiol. 2007; 48:721-727.
7. Baumgart J, Lang S, Lang H. A new method for induction of liver hypertrophy prior to right trisectionectomy: A report of three cases. HPB (Oxford). 2011; 13(Suppl):72-73.
8. Schnitzbauer AA, Lang SA, Goessmann H, *et al.* Right portal vein ligation combined with *in situ* splitting induces rapid left lateral liver lobe hypertrophy enabling 2-staged extended right hepatic resection in small-for-size settings. Ann Surg. 2012; 255:405-414.
9. Schadde E, Ardiles V, Robles-Campos R, Malago M,

Machado M, Hernandez-Alejandro R, Soubrane O, Schnitzbauer AA, Raptis D, Tschuor C, Petrowsky H, De Santibanes E, Clavien PA. Early survival and safety of ALPPS: First report of the International ALPPS Registry. Ann Surg. 2014; 260:829-836.

10. Schlegel A, Lesurtel M, Melloul E, Limani P, Tschuor C, Graf R, Humar B, Clavien PA. ALPPS: From human to mice highlighting accelerated and novel mechanisms of liver regeneration. Ann Surg. 2014; 260:839-846.

11. Sano K, Makuuchi M, Miki K, Maema A, Sugawara Y, Imamura H, Matsunami H, Takayama T. Evaluation of hepatic venous congestion: Proposed indication criteria for hepatic vein reconstruction. Ann Surg. 2002; 236:241-247.

12. Tanaka K, Endo I. ALPPS: Short-term outcome and functional changes in the future liver remnant. Ann Surg. 2015; 262:e88-89.

13. van den Broek MA, van Dam RM, Malago M, Dejong CH, van Breukelen GJ, Olde Damink SW. Feasibility of randomized controlled trials in liver surgery using surgery-related mortality or morbidity as endpoint. Br J Surg. 2009; 96:1005-1014.

14. Robles R, Parrilla P, Lopez-Conesa A, Brusadin R, de la Pena J, Fuster M, Garcia-Lopez JA, Hernandez E. Tourniquet modification of the associating liver partition and portal ligation for staged hepatectomy procedure. Br J Surg. 2014; 101:1129-1134.

15. Machado MA, Makdissi FF, Surjan RC. Totally laparoscopic ALPPS is feasible and may be worthwhile. Ann Surg. 2012; 256:e13.

16. Petrowsky H, Gyori G, de Oliveira M, Lesurtel M, Clavien PA. Is partial-ALPPS safer than ALPPS? A single-center experience. Ann Surg. 2015; 261:e90-92.

17. Imamura H, Seyama Y, Kokudo N, Maema A, Sugawara Y, Sano K, Takayama T, Makuuchi M. One thousand fifty-six hepatectomies without mortality in 8 years. Arch Surg. 2003; 138:1198-1206.

18. Tschuor C, Croome KP, Sergeant G, Cano V, Schadde E, Ardiles V, Slankamenac K, Claria RS, de Santibanes E, Hernandez-Alejandro R, Clavien PA. Salvage parenchymal liver transection for patients with insufficient volume increase after portal vein occlusion − an extension of the ALPPS approach. Eur J Surg Oncol. 2013; 39:1230-1235.

19. Kokudo N, Shindoh J. How can we safely climb the ALPPS? Updates in surgery. 2013; 65:175-177.

Original Article

A systematic review and meta-analysis of feasibility, safety and efficacy of associating liver partition and portal vein ligation for staged hepatectomy (ALPPS) versus two-stage hepatectomy (TSH)

Zhipeng Sun[1,2], Wei Tang[2,*], Yoshihiro Sakamoto[2], Kiyoshi Hasegawa[2], Norihiro Kokudo[2]

[1] *Oncology Surgery Department, Peking University Ninth School of Clinical Medicine (Cancer Centre, Beijing Shijitan Hospital, Capital Medical University), Beijing, China;*
[2] *Hepato-Biliary-Pancreatic Surgery Division, Department of Surgery, Graduate School of Medicine, The University of Tokyo, Tokyo, Japan.*

Summary   **This meta-analysis aimed to review the regeneration rate of future liver remnant (FLR) and perioperative outcomes after associating liver partition and portal vein ligation for staged hepatectomy (ALPPS) and two-stage hepatectomy (TSH). A web search was performed in "MEDLINE", "EMBASE", and "SCIENCE DIRECT" databases using both subject headings (MeSH) and truncated word to identify all the articles published that related to this topic. Pooled risk ratios were calculated for categorical variables and mean differences for continuous variables using the fixed-effects and random-effects models for meta-analysis. Three studies involved 282 patients, of whom 234 were in the TSH group and 48 in the ALPPS group. Morbidity was experienced in 56.3% patients in the ALPPS group and 36.1% in the TSH group. There was a statistical difference (RR = 1.08; Z = 3.24; 95% CI, p = 0.001). Second surgeries were performed successfully in 79.1% patients in the portal vein embolization (PVE) group and 100% in the ALPPS group. There was a statistical difference (Z = 2.48; 95% CI, p = 0.01). The mean regeneration rate of FLR in the ALPPS group was 56.4% compared with 52.8% in the TSH group. There was no statistical difference (95% CI, p = 0.34). So from the outcome of this meta-analysis, TSH had a similar remnant liver regeneration ability compared to ALPPS while the morbidity and mortality rates were relatively low. Cancer progression while waiting for the staged liver resection after portal vein embolization was a drawback for TSH.**

Keywords: *Associating liver partition and portal vein ligation for staged hepatectomy (ALPPS), portal vein embolization (PVE), two-staged Hepatectomy (TSH), liver regeneration*

1. Introduction

During the period of associating liver partition and portal vein ligation for staged hepatectomy (ALPPS) surgery promotion, there were always comparisons with conventional Two-Stage Hepatectomy (portal vein embolization and staged hepatectomy, TSH), which don't need laparotomy and liver parenchyma partition in the first surgery. Some researchers found that TSH had a similar remnant liver regenerative effect compared to ALPPS while the morbidity and mortality rates were relatively low (*1-3*). There were already 3 randomized control trials comparing the two surgeries up to now that we have summarized as follows.

The major difference between ALPPS and TSH is the extra liver parenchyma partition in ALLPS, which may result in fast remnant liver regeneration. The procedure of cancer-bearing liver partition may also reduce the chance of tumor invasion to the remnant liver (*4*). The major deficit of conventional two-stage hepatectomy is that the speed of future remnant liver

*Address correspondence to:
Dr. Wei Tang, Hepato-Biliary-Pancreatic Surgery Division, Department of Surgery, Graduate School of Medicine, The University of Tokyo, 7-3-1 Hongo, Bunkyo-ku, Tokyo 113-8655, Japan.
E-mail: tang-sur@h.u-tokyo.ac.jp

(FLR) regeneration is not very high. It's rarely over 50% for 4-8 weeks. About 1/10 patients who underwent portal vein embolization as the first surgery of TSH lost the second hepatic resection surgery opportunity while waiting for FLR regeneration (*5*) because of cancer progress. So conventional TSH now is widely used for hilar cholangiocarcinoma, which grows slowly compared with hepatic cancer. The purpose of this systematic review and meta-analysis was to compare ALPPS with TSH to evaluate feasibility, safety and efficacy.

2. Materials and Methods

2.1. *Procedure of data collection*

The databases of "MEDLINE", "EMBASE", and "SCIENCE DIRECT" were searched for articles published up to the date of Oct 15th, 2015 using the medical subject headings (MeSH) terms "portal vein ligation", "PVE", "staged hepatectomy", "staged liver resection", "liver resection", "two-stage hepatectomy",

"TSH", "associating liver partition and portal vein ligation for staged hepatectomy" and "ALPPS" (Figure 1). There were no language restrictions. Relevant articles were reviewed and duplicates were removed. Articles unrelated to ALPPS, TSH as well as abstracts were excluded. Full-text articles were assessed for eligibility. Editorials and commentary articles as well as case reports were excluded. Studies reporting on up to three patients were classified as case reports. Patients were carefully screened for double reporting, after exclusion of those patients, a quantitative synthesis and meta-analysis was performed.

All patients who underwent liver resection for malignant tumors in both normal and cirrhotic livers were included. Inclusion criteria for searching were studies evaluating the use of TSH and ALPPS for elective liver resection.

2.2. *Types of outcome measures*

The morbidity rate, second surgery finish rate, FLR regeneration rate of TSH and ALPPS were measured.
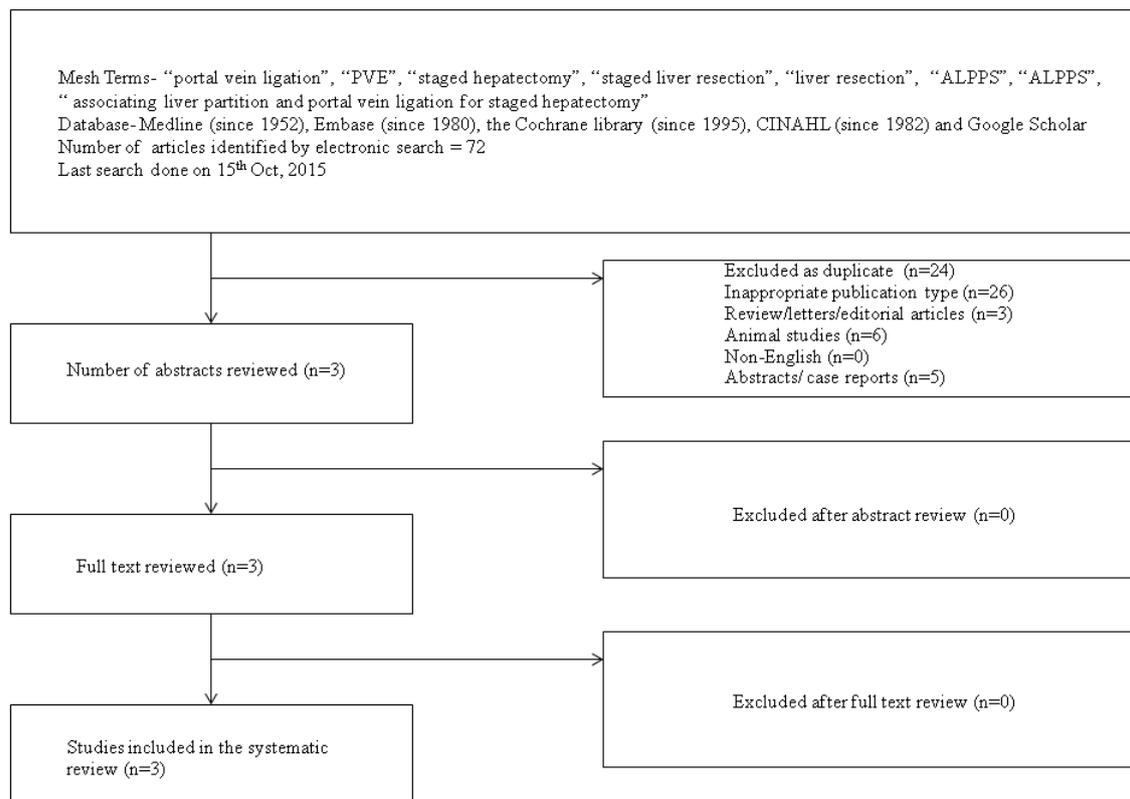
Figure 1. Prisma flowchart of databases searched, strategy used, and exclusions performed for "ALPPS" and "TSH". Randomized and case-controlled studies, irrespective of language, country of origin, hospital, blinding, sample size, or publication status that compared ALPPS and TSH were included in this review. The databases of "MEDLINE", "EMBASE", and "SCIENCE DIRECT" were searched for articles published up to the date of Oct 15th, 2015 using the medical subject headings (MeSH) terms "portal vein ligation", "PVE", "staged hepatectomy", "staged liver resection", "liver resection", "two-stage hepatectomy", "TSH", "associating liver partition and portal vein ligation for staged hepatectomy" and "ALPPS". Relevant articles were reviewed and duplicates were removed. Articles unrelated to ALPPS, TSH as well as abstracts were excluded. Full-text articles were assessed for eligibility. Editorials and commentary articles as well as case reports were excluded. Studies reporting on up to three patients were classified as case reports. Patients were carefully screened for double reporting.

2.3. *Statistical analysis*

Statistical analysis was performed using Review Manager Version 5.2 software (Cochrane Collaboration). The risk ratio (RR) with 95% confidence interval (CI) was calculated for binary data, and the mean value differences with 95% CI for continuous variables. When median and range were reported instead of mean and variance, the mean and variance were calculated based on the methods described by Hozo *et al.* (*6*). Random and fixed effects models were used to calculate the outcomes of both binary and continuous data. In cases of heterogeneity, only the results of the random effects model were reported. Heterogeneity was explored using the Chi-square test, with significance set at $p < 0.05$. Low heterogeneity was defined as $I^2 \le 33\%$. If the standard deviation was not available, it was calculated according to the guidelines of the Cochrane Collaboration. This process involved assumptions that both groups had the same variance, which may not have been true, and variance was estimated either from the range or from the p value. Forest plots were used for graphic display of the results. Quality assessment of the included studies was based on the Newcastle-Ottawa scale (*7*).

3. Results

The strategies of the literature search and the selection of studies are summarized (Figure 1). Three studies comparing ALPPS with TSH procedure met the inclusion criteria (*1,2,8*). All studies were retrospective. These three studies involved 282 patients, of whom 48 were in the ALPPS group and 234 in the TSH group. Pooled data were analyzed by combining the results of these three studies.

3.1. *Comparison of morbidity rate between ALPPS and TSH*

There was no heterogeneity among the included studies (Chi^2 = 9.97; df = 2; p = 0.007; I^2 = 80%). Morbidities were experienced in 56.3% of patients in the ALPPS group and 36.1% in the TSH group. In a random effects model, there was statistical difference (RR = 1.08; Z = 3.24; 95% CI, p = 0.001; Figure 2).

3.2. *Comparison of second surgery finish rate between ALPPS and TSH*

There was no heterogeneity among the included studies (Chi^2 = 1.54; df = 2; p = 0.46; I^2 = 72%). The staged surgeries were performed successfully in 79.1% of patients in the PVE group and 100% in the ALPPS group. In a random effects model, there was statistical difference. (Z = 2.48; 95% CI, p = 0.01; Figure 3).

3.3. *Comparison of FLR regeneration rate after first surgery between ALPPS and TSH*

There was no heterogeneity among the included studies
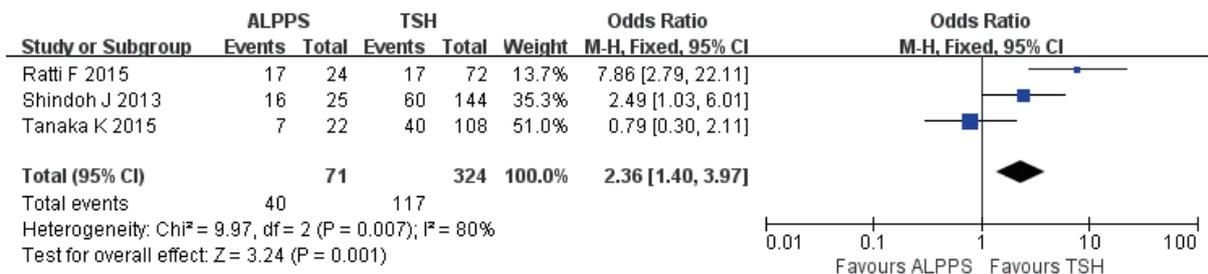
Figure 2. Comparison of morbidity rate between ALPPS and TSH. There studies were included in the analysis. Three was no heterogeneity amongst the included studies (Chi^2 = 9.97; df = 2; p = 0.007; I^2 = 80%). Morbidity was experienced in 56.3% of patients in the ALPPS group and 36.1% in the TSH group. In a random effects model, there was statistical difference (Z = 3.24; p = 0.001).
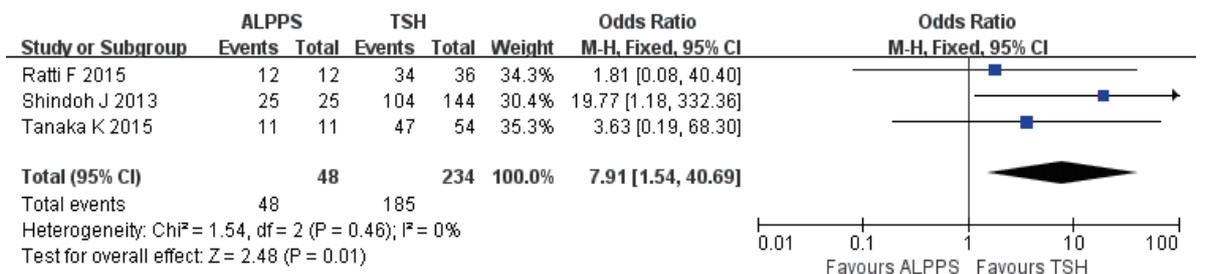
Figure 3. Comparison of second surgery finish rate between ALPPS and TSH. There studies were included in the analysis. Three was no heterogeneity among the included studies (Chi^2 = 1.54; df = 2; p = 0.46; I^2 = 0%). The secondary surgeries were performed successfully in 79.1% of patients in the PVE group and 100% in the ALPPS group. In a random effects model, there was statistical difference (Z= 2.48; 95% CI, p =0.01).
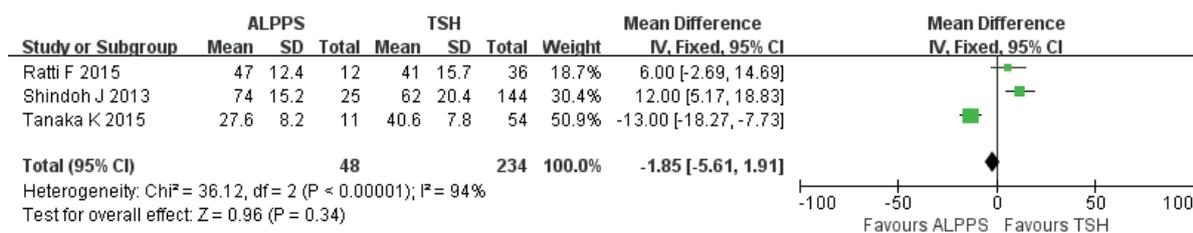
Figure 4. Comparison of FLR regeneration rate after first surgery between ALPPS and TSH. Three studies were included in the analysis. There was no heterogeneity among the included studies (Chi^2 = 36.12, df = 2; I^2 = 94%). The mean regeneration rate in FLR in the PVE group was 56.4% compared with 52.8% in the TSH group. In a fixed effects model, there was no difference in the percentage change in FLR increase between ALPPS and TSH (95% CI, p = 0.34; Figure 4).

(Chi^2 = 36.12, df = 2; I^2 = 94%). The mean regeneration rate of FLR in the PVE group was 56.4% compared with 52.8% in the TSH group. In a fixed effects model, there was no difference in the regeneration rate of FLR between ALPPS and TSH (95% CI, p = 0.34; Figure 4).

4. Discussion

This meta-analysis shows that about three years after the inaugural publication of the novel ALPPS technique (*4*), the level of evidence supporting its advantages compared with traditional TSH remains low. Studies confirm the high completion rate of 97% for ALPPS, although with the two common biases of single-center and retrospective design. Perioperative mortality rate was 11% and complications grade IIIa or higher occurred in 44% of all patients (*9*).

The reasons for the rapid hypertrophy of the FLR observed in ALPPS and the actual functional growth of the FLR are important clinical questions. Although the rapid growth of the FLR after the ALPPS procedure is very impressive, it remains not so clear that it is better compared with a right hemi-liver plus segment 4 PVE. In our meta-analysis there wasn't any statistical difference between the two types of surgeries in regeneration volume. As reported previously, the hypertrophy of the FLR is negatively correlated with the pre-PVE FLR volume (*10*). Because hepatic parenchyma transection is usually performed along the umbilical fissure (the segmental border between left lateral lobe and segment 4) in ALLPS procedure (*4,11*) while PVE is usually performed on right hemi-liver in TSH procedure (*12,13*). It is incorrect to attribute the reason for the rapid growth of the FLR to hepatic parenchyma partition (*8,11*). Therefore, more prospective studies about FLR regeneration volume comparison between ALPPS and a right hemi-liver plus segment 4 PVE should be performed.

Second, the mechanism explaining how the *in situ* splitting facilitates the regeneration of the FLR needs to be clarified. In animal models, there were no differences between TSH and ALPPS for the quantity of effective regenerative liver cells. The comparison for the quantity of effective regenerative liver cells between ALPPS and PVE was performed in rat models. DNA synthesis was assessed by bromodeoxyuridine (BrdU) and proliferating cell nuclear antigen (PCNA) immunohistochemistry staining on paraffin sections. There were no differences in BrdU$^+$ or PCNA$^+$ hepatocytes. The liver weights were assessed seven days after surgery. The weights of the remnant livers were not significantly different following PVL and ALPPS (*14*). Other research (*15*) also reported similar results that portal vein ligation and portal vein ligation combined with in situ splitting were performed in two groups of mice. The results showed no obvious differences between the two groups were observed at 24 and 48 hours after surgeries.

This systemic review was limited due to the small number of original publications about comparison of ALPPS, which is a very recently introduced technique, with TSH. The reason for this early systematic review was to support the opinion with data about the ongoing debate on the benefits and deficits of ALPPS compared with TSH. At the same time, the quality of studies published currently has not allowed the establishment of solid evidence for safety and efficacy, as shown by this systematic review. More prospective studies about comparison between ALPPS and TSH should be performed to support further assessment of feasibility, safety and oncologic efficacy.

5. Conclusion

TSH has similar remnant liver regeneration ability compared with ALPPS while the morbidity and mortality rates are relatively low. Cancer progression while waiting for the second stage hepatectomy after portal vein embolization is a major shortcoming for TSH.

Acknowledgements

References

1.   Ratti F, Schadde E, Masetti M, Massani M, Zanello M,

Serenari M, Cipriani F, Bonariol L, Bassi N, Aldrighetti L, Jovine E. Strategies to increase the resectability of patients with colorectal liver metastases: A multi-center case-match analysis of ALPPS and conventional two-stage hepatectomy. Ann Surg Oncol. 2015; 22:1933-1942.

2.   Shindoh J, Vauthey JN, Zimmitti G, Curley SA, Huang SY, Mahvash A, Gupta S, Wallace MJ, Aloia TA. Analysis of the efficacy of portal vein embolization for patients with extensive liver malignancy and very low future liver remnant volume, including a comparison with the associating liver partition with portal vein ligation for staged hepatectomy approach. J Am Coll Surg. 2013; 217:126-133.

3.   Tanaka K, Matsuo K, Murakami T, Kawaguchi D, Hiroshima Y, Koda K, Endo I, Ichikawa Y, Taguri M, Tanabe M. Associating liver partition and portal vein ligation for staged hepatectomy (ALPPS): Short-term outcome, fuctional changes in the future liver remnant, and tumor growth activity. Eur J Surg Oncol. 2015; 41:506-512.

4.   Schnitzbauer AA, Lang SA, Goessmann H, et al. Right portal vein ligation combined with *in situ* splitting induces rapid left lateral liver lobe hypertrophy enabling 2-staged extended right hepatic resection in small-for-size settings. Ann Surg. 2012; 255:405-414.

5.   Okabe H, Beppu T, Nakagawa S, et al. Percentage of future liver remnant volume before portal vein embolization influences the degree of liver regeneration after hepatectomy. J Gastrointest Surg. 2013; 17:1447-1451.

6.   Hozo SP, Djulbegovic B, Hozo I. Estimating the mean and variance from the median, range, and the size of a sample. BMC Med Res Methodol. 2005; 5:13.

7.   Martin B, Paesmans M, Berghmans T, Branle F, Ghisdal L, Mascaux C, Meert AP, Steels E, Vallot F, Verdebout JM, Lafitte JJ, Sculier JP. Role of Bcl-2 as a prognostic factor for survival in lung cancer: A systematic review of the literature with meta-analysis. Br J Cancer. 2003; 89:55-64.

8.   Takayasu K, Muramatsu Y, Shima Y, Moriyama N, Yamada T, Makuuchi M. Hepatic lobar atrophy following obstruction of the ipsilateral portal vein from hilar cholangiocarcinoma. Radiology. 1986; 160:389-393.

9.   Schadde E, Schnitzbauer AA, Tschuor C, Raptis DA, Bechstein WO, Clavien PA. Systematic review and meta-analysis of feasibility, safety, and efficacy of a novel procedure: Associating liver partition and portal vein ligation for staged hepatectomy. Ann Surg Oncol. 2015; 22:3109-3120.

10. Kokudo N, Tada K, Seki M, Ohta H, Azekura K, Ueno M, Ohta K, Yamaguchi T, Matsubara T, Takahashi T, Nakajima T, Muto T, Ikari T, Yanagisawa A, Kato Y. Proliferative activity of intrahepatic colorectal metastases after preoperative hemihepatic portal vein embolization. Hepatology. 2001; 34:267-272.

11. Nagino M, Kamiya J, Kanai M, Uesaka K, Sano T, Yamamoto H, Hayakawa N, Nimura Y. Right trisegment portal vein embolization for biliary tract carcinoma: Technique and clinical utility. Surgery. 2000; 127:155-160.

12. Jaeck D, Oussoultzoglou E, Rosso E, Greget M, Weber JC, Bachellier P. A two-stage hepatectomy procedure combined with portal vein embolization to achieve curative resection for initially unresectable multiple and bilobar colorectal liver metastases. Ann Surg. 2004; 240:1037-1049.

13. Fernandez-Ros N, Silva N, Bilbao J, Inarrairaegui M, Benito A, Avola D, Rodriguez M, Rotellar F, Pardo F, Sangro B. Partial liver volume radioembolization induces hypertrophy in the spared hemiliver and no major signs of portal hypertension. HPB (Oxford). 2014; 16:243-249.

14. Heinrich S, Jochum W, Graf R, Clavien PA. Portal vein ligation and partial hepatectomy differentially influence growth of intrahepatic metastasis and liver regeneration in mice. J Hepatol. 2006; 45:35-42.

15. Yao L, Li C, Ge X, Wang H, Xu K, Zhang A, Dong J. Establishment of a rat model of portal vein ligation combined with *in situ* splitting. PloS one. 2014; 9:e105511.

Original Article

Transarterial Y90 radioembolization versus chemoembolization for patients with hepatocellular carcinoma: A meta-analysis

Yafei Zhang[1], Yiming Li[1], Hong Ji[1], Xin Zhao[2,*], Hongwei Lu[1,*]

[1] *Department of General Surgery, Second Affiliated Hospital, School of Medicine, Xi'an Jiaotong University, Xi'an, China;*
[2] *Department of Hepatobiliary Surgery, The No. 302 Hospital of PLA, Beijing, China.*

Summary	Transarterial chemoembolization (TACE) is one of the standard locoregional treatments for intermediate stage hepatocellular carcinoma (HCC). Transarterial radioembolization (TARE) using β-emitting yttrium-90 (90Y) integral to the glass matrix of the microspheres has been developed as an alternative to TACE in recent years. Thus, we conducted a meta analysis to evaluate the safety and efficacy of TARE versus TACE for unresectable HCC. We searched PubMed, EMBASE, Web of science and the Cochrane Library for clinical trials comparing TARE with TACE for unresectable HCC. Response rate, overall survival (OS), time to progression (TTP), hospitalization time days and clinical complications were analyzed and compared. Eight studies published from 2009 to 2014, with a total of 1,499 patients, were included in this meta-analysis. The pooled results showed that TARE (90Y) is significantly better in OS (HR = 0.74; 95% CI: 0.61-0.90), 3-year OS rates (RR = 1.75; 95% CI = 1.01-3.03, p = 0.05), TTP (HR = 0.61; 95% CI: 0.41-0.89), hospitalization time days (mean difference = −2.66; 95% CI: −4.08 - −1.24) and some complications (abdominal pain [RR = 0.30, 95% CI: 0.11-0.83, p = 0.02]) for patients with HCC, but did not affect tumor response (CR [RR = 1.06; 95% CI = 0.51-2.22], PR [RR = 1.24; 95% CI = 0.79-1.94], SD [RR = 1.13; 95% CI = 0.92-1.39], PD[RR = 0.75; 95% CI = 0.37-1.51], over-all tumor control [RR = 1.16; 95 % CI = 0.94-1.44]). The current meta-analysis suggests that TARE (Y90) is significantly better in OS, 3-year OS rates, TTP, hospitalization time days and some complications for patients with HCC.

Keywords: Transarterial Y90 radioembolization, chemoembolization, hepatocellular carcinoma

1. Introduction

Hepatocellular carcinoma (HCC) is a serious cancer with high morbidity and high mortality rate (*1*). In recent years, HCC has shown a rising incidence worldwide due to increasing hepatitis C virus prevalence and other factors (*2*). Surgical resection has been considered as definitive treatment for HCC, unfortunately, most HCC patients are diagnosed at an intermediate or advanced stage in which the tumor can't be resected (*3*). Therefore, locoregional treatment for HCC patients would be

actively needed and may help to achieve longer survival.

Transarterial chemoembolization (TACE) is an increasingly locoregional treatment used for HCC, it is a chemotherapeutic agent injected at the tumor site for blocking the main feeding artery of the tumor causing tumor necrosis (*4*). TACE has been recommended as the standard therapy for intermediate stage BCLC (B) (*5,6*), but it is not suitable for all unresectable HCC patients as it may cause lots of complications: postembolization syndrome, hepatic decompensation and metastasis (*7,8*).

In recent years, transarterial radioembolization (TARE) using β-emitting yttrium-90 (90Y) integrated in glass matrix or resin microspheres has been regarded as an alternative therapy to TACE for unresected HCC (*9*). The microspheres are carried out through hepatic intra-arterial injection, treating HCC from the lobar, segmental to the sub segmental. Some studies have reported good treatment results through TARE (*10-12*). Other clinical experience reports that TARE Y-90 is able to reduce tumor burden significantly for patients

**Address correspondence to:*
Dr. Xin Zhao, Department of Hepatobiliary Surgery, The No. 302 Hospital of PLA, Beijing 100039, China.
E-mail: drzhaoxin@126.com

Dr. Hongwei Lu, Department of General Surgery, Second Affiliated Hospital, School of Medicine, Xi'an Jiaotong University, 157 Xiwu Road, Xi'an 710004, China.
E-mail: lhwdoc@163.com

with unresectable HCC which may help to downstage tumors before surgery (*13*). However, the effect of TARE with Yttrium-90 in the treatment of unresectable liver tumors still needs to be confirmed (*14,15*). Therefore, we conducted a meta analysis based on clinical trials to evaluate the efficacy and safety of TARE versus TACE for unresectable HCC.

2. Materials and Methods

2.1. *Literature search*

We searched PubMed, EMBASE, Web of science, and the Cochrane Library for clinical trials comparing TARE (90Y) with TACE for unresectable HCC. The following searching terms were used: "chemoemboli*" or "emboli*" or "TACE" or "transcatheter" or "transarterial" for identification of TACE, "90Y" or "radioemboli*" or "Yttrium-90" or "TARE" for identification of TARE, and "(liver or hepatic or hepatocellular) and (carcinom* OR cancer OR neoplasm* OR malign* OR tumor OR tumor)" or "HCC" or "hepatoma*" for identification of HCC (*16*).

The Literature was searched limited to human studies without restricting time or language. The reference lists of all articles were also manually screened for potential studies. Abstracts and citations were screened independently by two authors, and all the agreed articles needed a second screen for full-text reports.

2.2. *Review strategy*

We used endnote bibliographic software to construct an electronic library of citations identified in the literature search. All the PubMed, EMBASE, Web of science and the Cochrane Library searches were performed using Endnote; duplicates were found automatically by endnote and deleted manually. All data extraction was checked and calculated twice by two independent investigators (Yafei Zhang and Hong Ji). A standardized data extraction form was used to assist the two investigators. Data extracted from the included studies were as follows: author, year of publication, and country; patients' age and sex, study design, Child-Pugh class, treatment, pretreatment MELD score, BCLC stage, overall survival (OS), time to progression (TTP), hospitalization time days, tumor response, 1, 2, 3-year OS rate, complications and laboratory adverse events. A third reviewer (Hongwei Lu) would participate if some disagreements arose. Mean and standard deviation (SD) were preferred in some data, which will be calculated from the median and range using relevant formulae if it was not reported in the article (*17*).

2.3. *Study inclusion and exclusion criteria*

Inclusion criteria: patients were diagnosised as

unresectable HCC; compared TARE with TACE mono-therapy; compared efficacy and/or safety between TARE (Y90) and TACE. We excluded comments, editorials, systematic reviews or studies only in abstracts from our final analysis. Besides, there was no limitation for publication language.

2.4. *Quality assessment*

The quality of nocohort studies included in this meta analysis was assessed using a modified Newcastle-Ottawa scale (*18*), which graded the quality of a study from 0 to 9 points, depending on patient selection, comparability of TARE and TACE, and exposure assessment. Articles exceeding 6 points were considered as high quality.

2.5. *Statistical analysis*

All statistical analyses were performed using Review Manage (Revman, version 5.2.0, The Cochrane Collaboration, 2012) (*19*). The hazards ratio (HR) was used to evaluate the OS and TTP. Risk ratio (RR) was applied for tumor response, 1, 2, 3-year OS rates and clinical complications. Mean difference was used to evaluate the hospitalization time days. Afterward, 95% confidence intervals (CIs) were also calculated to indicate the precision of above effect measures. Pooled estimates of HR, RR or mean difference were calculated using the fixed-effects model if no substantial heterogeneity existed, otherwise, the random-effects model was used. Defined as variation between individual studies, heterogeneity was assessed with the Q-test and the I^2 statistic. Low level of heterogeneity was defined as I^2 value $\leq 50\%$ (*20*). The publication bias was evaluated using a funnel plot (*21,22*).

3. Results

3.1. *Identification of eligible studies*

The search strategy identified 2,306 related citations, and 1,543 non-duplicate references were retrieved for titles and abstracts screening. After 1,494 studies were excluded, the remaining 49 studies were examined at length. Finally, seven case control studies (*23-29*) and one cohort study (*30*) were eligible for inclusion criteria (Figure 1). A total of 1,499 patients were included among the eight studies, with 451 patients in the TARE group and 1,048 patients in TACE group.

3.2. *Characteristics of eligible studies*

The baseline characteristics of the eight studies included in our analysis are demonstrated in Table 1. The publication years of the included studies were between 2009 and 2014. Of these included studies, six
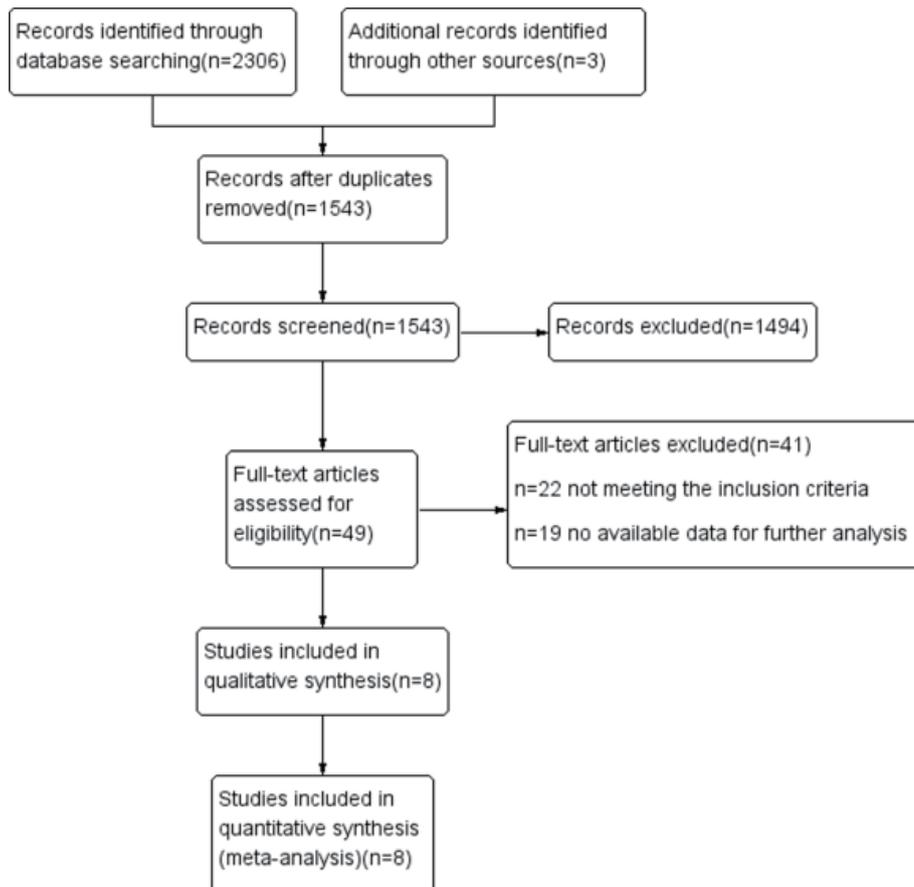
Figure 1. Flow chart of study selection.

were conducted in USA (*24-28,30*), one in China (*23*), one in Germany combined with Egypt (*29*). All the studies were published in English. The baseline liver function of most included patients was in Child-Pugh A (*23-29*). The etiology of the included patients were reported in seven studies, and most of the patients were a result from HCV and alcohol (*23-26,28-30*). Three studies reported the BCLC stage, and more than half of the patients were in BCLC-B stage (*24-26*). The median pretreatment MELD score ranged from 7.5 to 10 (*23,25,28,29*). All the included patients were definitely diagnosed to conform to the eligibility criteria.

3.3. *Quality of the included studies*

The quality of the nocohort studies was assessed by the Newcastle-Ottawa Scale (NOS), six of the result scores were 6, and another was 7, indicating that these studies have high quality according to the criteria (Table 2).

3.4. *Overall survival (OS)*

Among the eight studies included in the meta-analysis, three studies reported the results of data on OS (947 patients) (*26,28,30*). The meta-analysis showed that the OS was significantly better in the TARE with Y90 group than in the TACE group. The pooled HR for the

OS in the included studies performed using the fixed-effects was 0.74 (95% CI: 0.61-0.90; p = 0.002). This demonstrated a 26% reduction in the risk of death in patients treated with TARE. There was no evidence of heterogeneity among individual studies (p = 0.20; I^2 = 38%) (Figure 2A). Furthermore, the funnel plot revealed no publication bias.

3.5. *Time to progression (TTP)*

Two of the eight studies included in the meta-analysis reported the results of data on TTP (331 patients) (*24,26*). The meta-analysis showed that the TTP was significantly better in the TARE with Y90 group than in the TACE group. The pooled HR for the TTP in the included studies performed using the fixed-effects was 0.61 (95% CI: 0.41-0.89; p = 0.010). This demonstrated a 39% reduction in the risk of TTP in patients treated with TARE. There was no evidence of heterogeneity among individual studies (p = 0.74; I^2 = 0%) (Figure 2B). Furthermore, the funnel plot revealed no publication bias.

3.6. *Hospitalization time days*

Four of the eight studies included in the meta-analysis reported the results of data on hospitalization time days

Table 1. The baseline characteristics of the eight studies

Study	country	Study design	Treatment	n	Age	Male/female	HBV (%)	HCV (%)	Alcohol	Child-Pugh class (%) (A/B)	Pretreatment MELD score	BCLC stage (A/B/C/D)
She et al. (2014)	China	Case Control study	TARE (90Y)	16	55 (37-73)	15/1	12 (75.0)	0	NA	15/1	7.5 (6-12)	NA
			TACE	16	62.5 (48-78)	13/3	13 (81.3)	3 (27.3)	NA	14/2	8.5 (6-12)	NA
El Fouly et al. (2014)	Germany + Egypt	Case Control study	TARE (90Y)	44	66.1 ± 8.9	36/8	6 (14)	8 (18)	10 (23)	37/7	9 ± 3	NA
			TACE	42	58.3 ± 6.7	38/4	1 (2)	36 (86)	NA	33/9	10 ± 2.5	NA
Moreno-Luna et al. (2013)	USA	Case Control study	TARE (90Y)	61	64 (29-88)	49/12	NA	8 (13)	12 (20)	53/8	9 (6-18)	23/13/19
			TACE	55	66 (46-84)	43/12	NA	7 (13)	13 (24)	44/11	9 (6-19)	12/34/14
Salem et al. (2011)	USA	Case Control study	TARE (90Y)	123	66 (30-88)	87/36	13 (11)	42 (35)	20 (16)	67/54	NA	43/65/13/2
			TACE	122	61 (33-88)	102/20	12 (10)	56 (46)	21 (17)	67/53	NA	47/61/12/2
Lance et al. (2011)	USA	Case Control study	TARE (90Y)	38	63 (44-85)	33/5	NA	NA	NA	31/7	NA	NA
			TACE	35	61 (51-84)	28/7	NA	NA	NA	24/11	NA	NA
Kooby et al. (2010)	USA	Case Control study	TARE (90Y)	27	58.7 ± 10.8	23/4	NA	10 (37)	NA	13/22	10.0 ± 3.4	NA
			TACE	44	61.0 ± 9.9	36/8	NA	25 (57)	NA	14/22	10.4 ± 4.2	NA
Carr et al. (2010)	USA	Cohort study	TARE (90Y)	99	NA	70/29	9 (9)	30 (30)	37 (37)	NA	NA	NA
			TACE	691	NA	518/173	97 (14)	132 (19)	217 (31)	NA	NA	NA
Lewandowski et al. (2009)	USA	Case Control study	TARE (90Y)	43	68 (62.8-75)	38/5	2 (5)	14 (33)	9 (20)	24/19	NA	0/34/9/0
			TACE	43	65 (58.9-67.8)	36/7	6 (14)	16 (36)	10 (23)	23/18	NA	0/37/4/2

BCLC, Barcelona Clinic Liver Cancer.

Table 2. Newcastle-Ottawa Scale (NOS) for assessing the quality of nocohort studies

Author	Is the case definition adequate?	Representativeness of the cases	Selection of Controls	Definition of Controls	main factor: Child-Pugh Class	secondary factor: Aetiology	Ascertainment of exposure	Same method of ascertainment for cases and controls	Non-Response rate	Total quality score
She et al. (2014)	*	*	*	*	*	*	*	*	*	7
El Fouly et al. (2014)	*	*	*	*	*	*	*	*	*	7
Moreno-Luna et al. (2013)	*	*	*	*	*	*	*	*	*	7
Salem et al. (2011)	*	*	*	*	*		*	*	*	7
Lance et al. (2011)	*	*	*	*	*		*	*	*	6
Kooby et al. (2010)	*	*	*	*	*	*	*	*	*	7
Lewandowski et al. (2009)	*	*	*	*	*	*	*	*	*	7
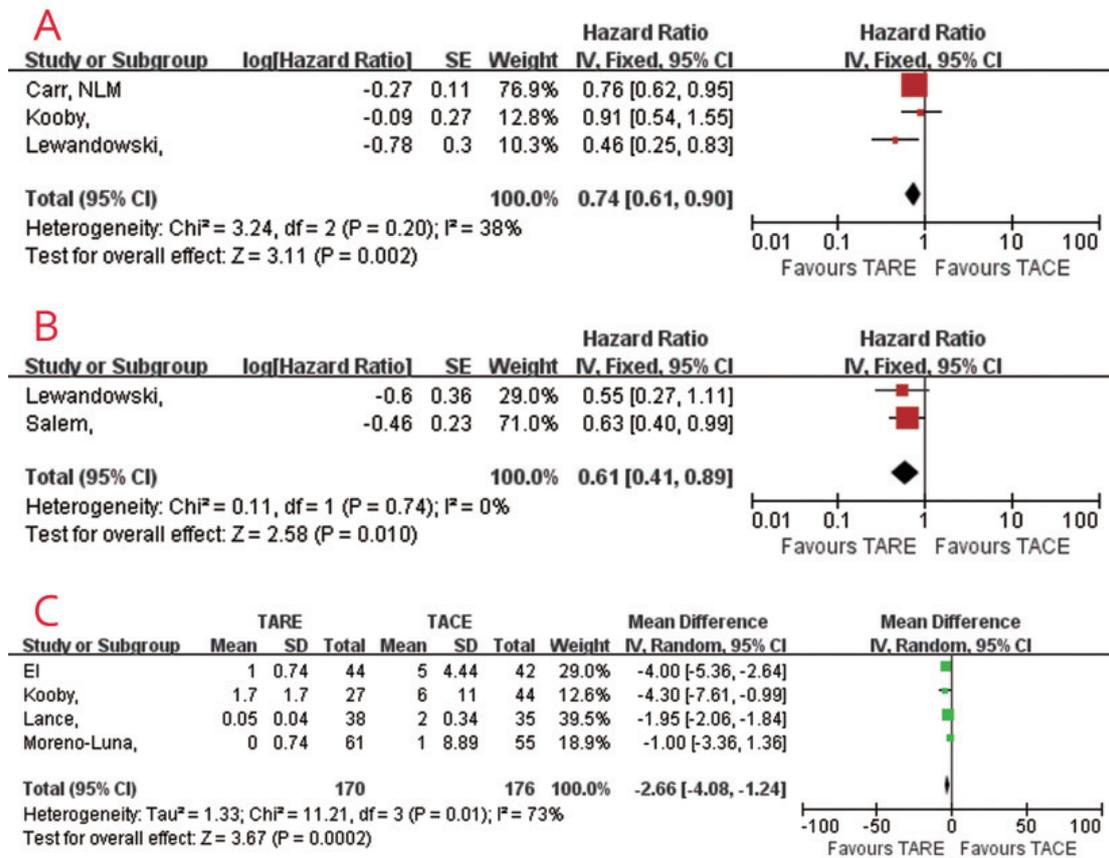
Figure 2. Forest plots of overall survival (OS) (A); time to progression (TTP) (B); hospitalization time days (C) in HCC patients that received TARE or TACE.

(346 patients) (*25,27-29*). The meta-analysis showed that the hospitalization time days was significantly shorter in the TARE with Y90 group than in the TACE group. The pooled mean difference for the hospitalization time days in the included studies performed using the random-effects was −2.66 (95% CI: −4.08 - −1.24; $p = 0.0002$). The heterogeneity among individual studies was ($p = 0.01$; $I^2 = 73\%$) (Figure 2C). Furthermore, the funnel plot revealed no publication bias.

3.7. *Tumor response*

The tumor response (involves CR [complete response], PR [partial response], SD [stable disease], PD [progressive disease], over-all tumor control [CR + PR + stable disease]) was reported in five case control studies (*23,25,26,28,29*) and one cohort study (*30*) (1,181 patients) (Table 3).

For CR, the pooled RR between TARE and TACE group was 1.92 (95% CI = 0.68-5.41; $I^2 = 0\%$) for case control study and 0.57 (95% CI = 0.18-1.80) for cohort study. The pooled RR of all six studies was (RR = 1.06; 95% CI = 0.51-2.22; $I^2 = 11\%$), and suggested that there was no statistical difference between groups (Table 3). Furthermore, the funnel plot revealed no publication bias.

For PR, the meta analysis of case control studies suggested that the patients in the TARE group had a significantly better response than those in the TACE group (RR = 1.44; 95% CI = 1.02-2.04; $I^2 = 34\%$), but the pooled RR of the cohort study favored the TACE group (RR = 0.70; 95% CI = 0.54-0.90), meta analysis of all available studies suggested that there was no statistical difference between groups (RR = 1.24; 95% CI = 0.79-1.94; $I^2 = 76\%$) (Table 3). Furthermore, the funnel plot revealed no publication bias.

For SD, the meta-analysis in the subgroup of case control studies (RR = 1.05; 95% CI = 0.79-1.40; $I^2 = 0\%$) and subgroup of cohort study (RR = 1.23; 95% CI = 0.92-1.64) suggested the patients that underwent the TARE therapy tended to have a better response to treatment than those underwent TACE treatment, though the estimates failed to achieve statistical significance. Meta analysis of all available studies suggested that there was no statistical difference between groups (RR = 1.13; 95% CI = 0.92-1.39; $I^2 = 0\%$) (Table 3). Furthermore, the funnel plot revealed no publication bias.

For PD, the meta-analysis of case control studies suggested that there was no statistical difference between groups (RR = 0.62; 95% CI = 0.37-1.04; $I^2 = 29\%$), but the pooled RR of the cohort study suggested that the patients in the TARE group had a significantly

Table 3. Tumor response compaired between the two treatments

Tumor response	Study or Subgroup	Patients (TARE/TACE)	Weight	Heterogeneity	Risk ratio (95% CI)
CR	case control study	191/200	36.40%	$p = 0.57$; $I^2 = 0\%$	1.92 (0.68-5.41)
	cohort study	99/691	63.60%	Not applicable	0.57 (0.18-1.80)
	Total	290/891	100%	$p = 0.34$; $I^2 = 11\%$	1.06 (0.51-2.22)
PR	case control study	191/200	75.30%	$p = 0.20$; $I^2 = 34\%$	1.44 (1.02-2.04)
	cohort study	99/691	24.70%	Not applicable	0.70 (0.54-0.90)
	Total	290/891	100%	$p = 0.0009$; $I^2 = 76\%$	1.24 (0.79-1.94)
SD	case control study	191/200	54.70%	$p = 0.93$; $I^2 = 0\%$	1.05 (0.79-1.40)
	cohort study	99/691	45.30%	Not applicable	1.23 (0.92-1.64)
	Total	290/891	100%	$p = 0.93$; $I^2 = 0\%$	1.13 (0.92-1.39)
PD	case control study	191/200	77.40%	$p = 0.23$; $I^2 = 29\%$	0.62 (0.37-1.04)
	cohort study	99/691	22.60%	Not applicable	2.14 (1.41-3.25)
	Total	290/891	100%	$p = 0.0007$; $I^2 = 77\%$	0.75 (0.37-1.51)
over-all	case control study	191/200	77.20%	$p = 0.73$; $I^2 = 0\%$	1.27 (1.14-1.42)
tumor control	cohort study	99/691	22.80%	Not applicable	0.86 (0.77-0.96)
	Total	290/891		$p = 0.0001$; $I^2 = 80\%$	1.16 (0.94-1.44)

Data were pooled with random-effect models. Complete response (CR), partial response (PR), stable disease (SD), progressive disease (PD) and over-all tumor control in HCC patients that received TARE or TACE.
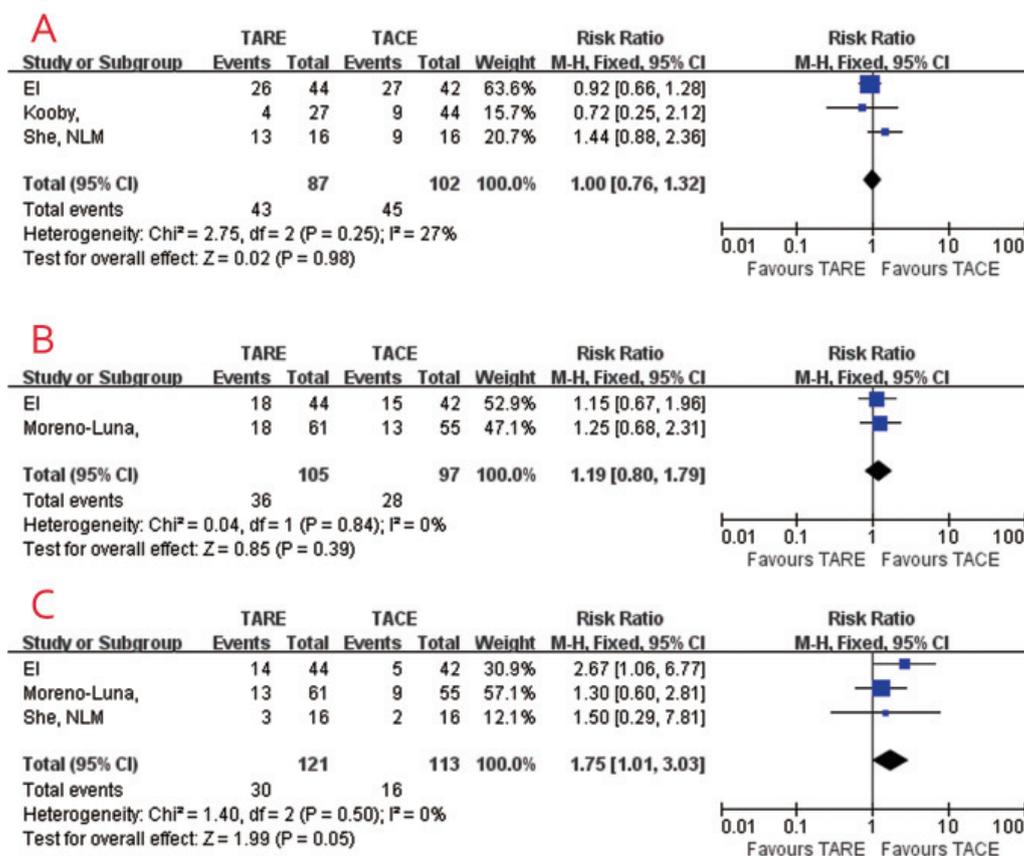
Figure 3. Forest plots of 1-year (A), 2-year (B) and 3-year (C) OS rates in HCC patients that received TARE or TACE.

better response than those in the TACE group (RR = 2.14; 95% CI = 1.41-3.25), meta analysis of all available studies suggested that there was no statistical difference between groups (RR = 0.75; 95% CI = 0.37-1.51; I^2 = 77%) (Table 3). Furthermore, the funnel plot revealed no publication bias.

For over-all tumor control, the meta analysis of case control studies suggested that the patients in the TARE group had a significantly better response than those in the TACE group (RR = 1.27; 95% CI = 1.14-1.42; I^2 = 0%), but the pooled RR of the cohort study favored the TACE group (RR = 0.86; 95% CI = 0.77-0.96), meta analysis of all available studies suggested that there was no statistical difference between groups (RR = 1.16; 95% CI = 0.94-1.44; I^2 = 80%) (Table 3). Furthermore, the funnel plot revealed no publication bias.
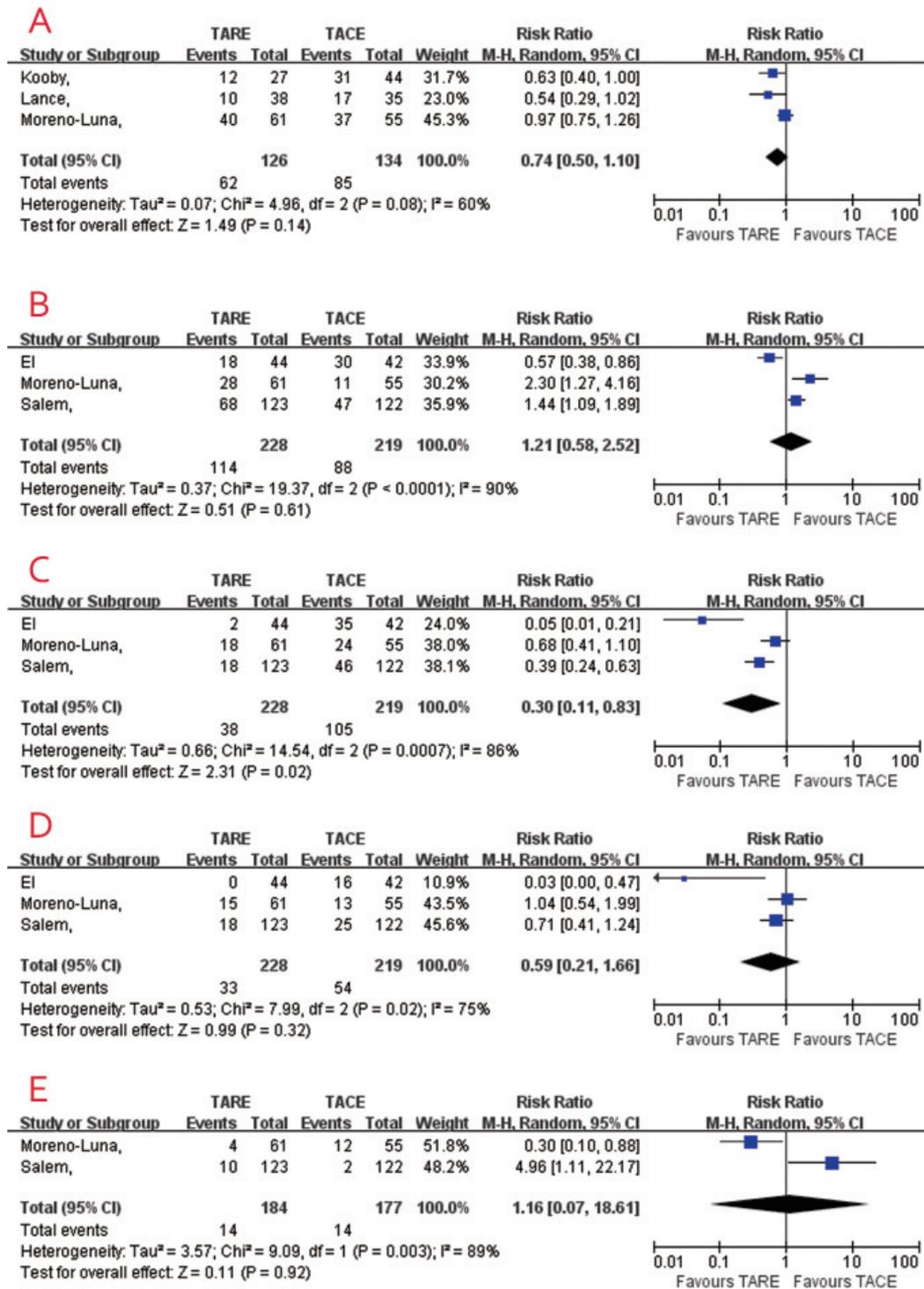
Figure 4. Forest plots of any complications (A), fatigue syndrome (B), lower abdominal pain (C), nausea/vomiting (D) and fever (E) in HCC patients that received TARE or TACE.

3.8. *1-year, 2-year, and 3-year OS rates*

A fixed-effect model was used to analyze the 1-year ($p = 0.25$, $I^2 = 27\%$), 2-year ($p = 0.84$, $I^2 = 0\%$) and 3-year ($p = 0.50$, $I^2 = 0\%$) OS rates since there was no significant heterogeneity among these studies. Three studies reported 1-year OS rates (*23,28,29*) and two studies reported 2-year OS rates (*25,29*). The meta analysis showed that there was no statistical difference

between groups on both 1-year (RR = 1.00, 95% CI 0.76-1.32, $p = 0.98$) (Figure 3A) and 2-year (RR = 1.19, 95% CI: 0.80-1.79, $p = 0.39$) (Figure 3B) OS rates. However, the pooled RR of three studies (*23,25,29*) suggested that the patients in the TARE group had a significantly higher 3-year OS rate than those in the TACE group (RR = 1.75; 95% CI = 1.01-3.03, $p = 0.05$) (Figure 3C). Furthermore, the funnel plot revealed no publication bias.

3.9. *Clinical complications*

We found that the TARE treatment lead to lower abdominal pain (*24,25,29*) (RR = 0.30, 95% CI: 0.11-0.83, *p* = 0.02) (Figure 4C) than TACE. However, the meta analysis showed that there was no statistical difference between groups on any complications (*25,27,28*) (RR = 0.74, 95% CI: 0.50-1.10, *p* = 0.14) (Figure 4A), fatigue syndrome (*24,25,29*) (RR = 1.21, 95% CI: 0.58-2.52, *p* = 0.61) (Figure 4B), nausea/vomiting (*24,25,29*) (RR = 0.59, 95% CI: 0.21-1.66, *p* = 0.32) (Figure 4D) or fever (*24,25*) (RR = 1.16, 95% CI: 0.07-18.61, *p* = 0.92) (Figure 4E). A random-effect model was used to analyze all the clinical complications for $I^2 > 50\%$ significant heterogeneity existed (Figure 4). Furthermore, the funnel plot revealed no publication bias.

4. Discussion

As modest benefit locoregional therapeutic modalities for HCC, the use of TACE had been demonstrated by two landmark trials (*31,32*), which stated that TACE was the standard therapy for intermediate HCCs. TARE with Yttrium-90, however, shows low toxicity and may provide therapeutic benefits for patients with unresectable HCC (*33*). A randomized controlled trial showed a benefit progression free survival of TARE (Y90) in patient with liver metastasis to colorectal tumors, after which, TARE (Y90) has been approved by the FDA (*34*). Presently, the safety and effectiveness of TARE (Y90) in advanced HCCs especially associated with portal vein thrombosis have been partly affirmed by many studies (*11,35-37*). Therefore, it is necessary to compare the efficacy and safety of TARE with Y90 in patients with intermediate or advanced stage HCCs.

To the best of our knowledge, this meta analysis is the first and most comprehensive to compare the efficacy and safety of TARE with Y90 in patients with an intermediate or advanced stage of HCC with TACE. Seven case control studies and one cohort study were identified and statistically analyzed in the present meta analysis, which included 451 and 1,048 patients with unresectable HCC who were treated with TARE (Y90) and TACE, respectively. With a relatively high level of evidence, the meta analysis showed that HCC patients treated with TARE (Y90) had significantly higher OS, TTP, 3-year OS rates, shorter hospitalization time days, better clinical complications and laboratory AEs than those treated with TACE. The TARE (Y90) therapy in the case control studies subgroup may also improve the PR and over-all tumor control treatment, while the total pooled estimates failed to achieve statistical significance.

Our meta analysis showed that the OS was significantly better in the TARE with Y90 group than in the TACE group (HR = 0.74; 95% CI: 0.61-0.90) (Figure 2A). This demonstrated a 26% reduction in the risk of death in patients treated with TARE. Furthermore, the meta analysis showed that there was no statistical difference between groups on both 1-year (RR = 1.00, 95% CI: 0.76-1.32, *p* = 0.98) (Figure 3A) and 2-year (RR = 1.19, 95% CI 0.80-1.79, *p* = 0.39) (Figure 3B) OS rates, however, the pooled RR of three studies suggested that the patients in the TARE group had significantly higher 3-year OS rate than those in the TACE group (RR = 1.75; 95% CI = 1.01-3.03, *p* = 0.05) (Figure 3C), suggesting that the effects of TARE (Y90) were gradually enhanced as time went by. While due to less patients included in our analysis, more studies with patients from different races are needed to further confirm this conclusion.

TTP is one of the most important indexes in treating intermediate stage HCC (*26,38*). El Fouly (*29*) reported that the TTP in TARE (Y90) patients (13.3 months) is much longer than in TACE patients (6.8 months), while the difference was not significant. In another study, TTP was significantly longer in a TARE (Y90) group than TACE (*24*). Our meta-analysis showed that the TTP was significantly better in the TARE with Y90 group than in the TACE group (HR = 0.61; 95% CI: 0.41-0.89), demonstrating a 39% reduction in the risk of TTP in patients treated with TARE (Figure 2B).

Furthermore, the meta-analysis showed that the hospitalization time days were significantly shorter in the TARE with Y90 group than in the TACE group (mean difference = −2.66; 95% CI: −4.08 - −1.24) (Figure 2C). This may be explained by the fact that most patients were accompanied by re-hospitalization to receive consecutive cycles of TACE (29).

Recently, radiological response rate was assessed according to modified RECIST (*5,39-41*). In El Fouly's study (*29*), objective response during a median time of 6 months reached disease control in 75% of TARE (Y90) patients *vs*. 50% in the TACE cohort, which reflects the higher capability of TARE (Y90) to induce tumor necrosis and ablation in vascular HCCs (*4*). For the outcome of tumor response, we used subgroup analysis to pool data from case control studies and cohort studies separately according to the study design. For CR, PR, SD, PD and over-all tumor control, meta-analysis of all available studies suggested that there was no statistical difference between groups, though the subgroup of case control studies favored the TARE for PR and over-all tumor control (Table 3). For all the six available studies, five were case control studies, only one was a cohort study, although the cohort studies can reflect the "real-world" and further support the conclusion, cohort data are of course inclined to bias because of patient selection. Thus, physicians should carefully interpret the results when applying them in clinical practice.

Lastly, we found that the TARE treatment lead to lower abdominal pain (RR = 0.30, 95% CI: 0.11-0.83, *p* = 0.02) than TACE, TARE (Y90) injects radioactive particles into a selected liver artery without causing

arterial occlusion (*42*). So, there is no overexpression of hypoxia-inducible factor 1a and vascular endothelial growth factor, which is clinically manifested as pain (*29*). However, the meta-analysis showed that there was no statistical difference between groups on any complications (RR = 0.74, 95% CI: 0.50-1.10, p = 0.14) (Figure 4A), fatigue syndrome (RR = 1.21, 95% CI: 0.58-2.52, p = 0.61), nausea or vomiting (RR = 0.59, 95% CI: 0.21-1.66, p = 0.32) and fever (RR = 1.16, 95% CI: 0.07-18.61, p = 0.92) (Figure 4). The heterogeneity of meta-analysis in clinical complications is significant. This may be due to variety in treatment schedule and complication designing criteria in the original studies. As the number of included studies is insufficient, we are unable to carry out subgroup analysis or meta-regression to explore the source of heterogeneity. The most frequent clinical complication in TARE (Y90) patients is post-embolization fatigue syndrome. While our analysis result showed that there was no statistical difference between the two groups.

There are several potential limitations in this meta-analysis. First, among the eight included studies, only one was a cohort study and the remaining seven were case control studies. While case control data are of course inclined to bias because of investigator selection. Thus, physicians should carefully interpret our results when applying them in clinical practice. Second, the characteristics of population and study designs vary considerably between the included trials, which may lead to heterogeneity and affect the results. Third, the majority of patients involved were from the USA, which limits universality of the conclusion. Hence, the results of updated clinical trials are eagerly awaited. Furthermore, because of the limited number of studies regarding the interest outcomes, caution should be taken when interpreting the results.

In conclusion, the current meta-analysis suggests that TARE (Y90) is significantly better in OS, 3-year OS rates, TTP, hospitalization time days and some complications for patients with HCC. The use of TARE (Y90) for HCC patients is promising. However, further multi-center, well-designed RCTs are needed to improve the treatment benefits for HCC patients.

References

1. Forner A, Llovet JM, Bruix J. Hepatocellular carcinoma. Lancet. 2012; 379:1245-1255.
2. El-Serag HB, Lau M, Eschbach K, Davila J, Goodwin J. Epidemiology of hepatocellular carcinoma in Hispanics in the United States. Arch Intern Med. 2007; 167:1983-1989.
3. Bruix J, Sherman M, Llovet JM, Beaugrand M, Lencioni R, Burroughs AK, Christensen E, Pagliaro L, Colombo M, Rodes J, HCC EPoEo. Clinical management of hepatocellular carcinoma. Conclusions of the Barcelona-2000 EASL conference. European Association for the Study of the Liver. J Hepatol. 2001; 35:421-430.
4. Bruix J, Sherman M. American Association for the Study

of Liver D. Management of hepatocellular carcinoma: An update. Hepatology. 2011; 53:1020-1022.
5. Llovet JM, Di Bisceglie AM, Bruix J, Kramer BS, Lencioni R, Zhu AX, Sherman M, Schwartz M, Lotze M, Talwalkar J, Gores GJ, Panel of Experts in HCCDCT. Design and endpoints of clinical trials in hepatocellular carcinoma. J Natl Cancer Inst. 2008; 100:698-711.
6. Burrel M, Reig M, Forner A, Barrufet M, de Lope CR, Tremosini S, Ayuso C, Llovet JM, Real MI, Bruix J. Survival of patients with hepatocellular carcinoma treated by transarterial chemoembolisation (TACE) using Drug Eluting Beads. Implications for clinical practice and trial design. J Hepatol. 2012; 56:1330-1335.
7. Poon RTP, Ngan H, Lo CM, Liu CL, Fan ST, Wong J. Transarterial chemoembolization for inoperable hepatocellular carcinoma and postresection intrahepatic recurrence. J Surg Oncol. 2000; 73:109-114.
8. Chan AO, Yuen MF, Hui CK, Tso WK, Lai CL. A prospective study regarding the complications of transcatheter intraarterial lipiodol chemoembolization in patients with hepatocellular carcinoma. Cancer. 2002; 94:1747-1752.
9. Moreno-Luna LE, Yang JD, Sanchez W, *et al*. Efficacy and safety of transarterial radioembolization versus chemoembolization in patients with hepatocellular carcinoma. Cardiovasc Intervent Radiol. 2013; 36:714-723.
10. Geschwind JFH, Salem R, Carr BI, Soulen MC, Thurston KG, Goin KA, Van Buskirk M, Roberts CA, Goin JE. Yttrium-90 microspheres for the treatment of hepatocellular carcinoma. Gastroenterology. 2004; 127:S194-S205.
11. Hilgard P, Hamami M, El Fouly A, Scherag A, Muller S, Ertle J, Heusner T, Cicinnati VR, Paul A, Bockisch A, Gerken G, Antoch G. Radioembolization with Yttrium-90 glass microspheres in hepatocellular carcinoma: European experience on safety and long-term survival. Hepatology. 2010; 52:1741-1749.
12. Kulik LM, Carr BI, Mulcahy MF, Lewandowski RJ, Atassi B, Ryu R, Sato KT, Benson A, Nemcek AA, Gates VL, Abecassis M, Omary RA, Salem R. Safety and efficacy of Y-90 radiotherapy for hepatocellular carcinoma with and without portal vein thrombosis. Hepatology. 2008; 47:71-81.
13. Ettorre GM, Santoro R, Puoti C, Sciuto R, Carpanese L, Antonini M, Antonucci G, Maini CL, Miglioresi L, Vennarecci G. Short-term follow-up of radioembolization with Yttrium-90 microspheres before liver transplantation: New perspectives in advanced hepatocellular carcinoma. Transplantation. 2010; 90:930-931.
14. Benson AB, Abrams TA, Ben-Josef E, *et al*. NCCN clinical practice guidelines in oncology: Hepatobiliary cancers. J Natl Compr Canc Netw. 2009; 7:350-391.
15. Jelic S, Sotiropoulos GC, Group EGW. Hepatocellular carcinoma: ESMO Clinical Practice Guidelines for diagnosis, treatment and follow-up. Ann Oncol. 2010; 21 (Suppl 5):v59-64.
16. Fu QH, Zhang Q, Bai XL, Hu QD, Su W, Chen YW, Su RG, Liang TB. Sorafenib enhances effects of transarterial chemoembolization for hepatocellular carcinoma: A systematic review and meta-analysis. J Cancer Res Clin Oncol. 2014; 140:1429-1440.
17. Hozo SP, Djulbegovic B, Hozo I. Estimating the mean and variance from the median, range, and the size of a sample. BMC Med Res Methodol. 2005; 5:13.

18. Wells GA, Shea B, O'Connell D, Peterson J, Welch V, Losos M, Tugwell P. The Newcastle-Ottawa Scale (NOS) for assessing the quality of nonrandomized studies in meta-analyses. 3rd Symposium on Systematic Reviews: Beyond the Basics. 2000;3-5.

19. Higgins JPT, Green S. Cochrane Handbook for Systematic Reviews of Interventions (Version 5.2.0). The Cochrane Colloboration. *www.cochrane-handbook.org* (updated March 2011).

20. Higgins JP, Thompson SG, Deeks JJ, Altman DG. Measuring inconsistency in meta-analyses. BMJ. 2003; 327:557-560.

21. Begg CB, Mazumdar M. Operating characteristics of a rank correlation test for publication bias. Biometrics. 1994; 50:1088-1101.

22. Egger M, Davey Smith G, Schneider M, Minder C. Bias in meta-analysis detected by a simple, graphical test. BMJ. 1997; 315:629-634.

23. She WH, Cheung TT, Yau TC, Chan AC, Chok KS, Chu FS, Liu RK, Poon RT, Chan SC, Fan ST, Lo CM. Survival analysis of transarterial radioembolization with yttrium-90 for hepatocellular carcinoma patients with HBV infection. Hepatobiliary Surg Nutr. 2014; 3:185-193.

24. Salem R, Lewandowski RJ, Kulik L, *et al.* Radioembolization results in longer time-to-progression and reduced toxicity compared with chemoembolization in patients with hepatocellular carcinoma. Gastroenterology. 2011; 140:497-507.e2.

25. Moreno-Luna LE, Yang JD, Sanchez W, *et al.* Efficacy and safety of transarterial radioembolization versus chemoembolization in patients with hepatocellular carcinoma. Cardiovasc Intervent Radiol. 2013; 36:714-723.

26. Lewandowski RJ, Kulik LM, Riaz A, Senthilnathan S, Mulcahy MF, Ryu RK, Ibrahim SM, Sato KT, Baker T, Miller FH, Omary R, Abecassis M, Salem R. A comparative analysis of transarterial downstaging for hepatocellular carcinoma: Chemoembolization versus radioembolization. Am J Transplant. 2009; 9:1920-1928.

27. Lance C, McLennan G, Obuchowski N, Cheah G, Levitin A, Sands M, Spain J, Srinivas S, Shrikanthan S, Aucejo FN, Kim R, Menon KV. Comparative analysis of the safety and efficacy of transcatheter arterial chemoembolization and Yttrium-90 radioembolization in patients with unresectable hepatocellular carcinoma. J Vasc Interv Radiol. 2011; 22:1697-1705.

28. Kooby DA, Egnatashvili V, Srinivasan S, Chamsuddin A, Delman KA, Kauh J, Staley CA, 3rd, Kim HS. Comparison of Yttrium-90 radioembolization and transcatheter arterial chemoembolization for the treatment of unresectable hepatocellular carcinoma. J Vasc Interv Radiol. 2010; 21:224-230.

29. El Fouly A, Schlaak JF, El Dorry A, Shaker MK, Dechene A, Abdella H, Ertle JM, Mueller SP, Barakat EM, Lauenstein T, Antoch G, Bockisch A, Gerken G. In intermediate stage hepatocellular carcinoma: Radioembolization with Yttrium-90 or chemoembolization? Hepatology. 2011; 54:1419a.

30. Carr BI, Kondragunta V, Buch SC, Branch RA. Therapeutic equivalence in survival for hepatic arterial chemoembolization and Yttrium 90 microsphere treatments in unresectable hepatocellular carcinoma: A

two-cohort study. Cancer. 2010; 116:1305-1314.

31. Lo CM, Ngan H, Tso WK, Liu CL, Lam CM, Poon RTP, Fan ST, Wong J. Randomized controlled trial of transarterial lipiodol chemoembolization for unresectable hepatocellular carcinoma. Hepatology. 2002; 35:1164-1171.

32. Llovet JM, Real MI, Montana X, Planas R, Coll S, Aponte J, Ayuso C, Sala M, Muchart J, Sola R, Rodes J, Bruix J, Barcelona Liver Cancer Group. Arterial embolisation or chemoembolisation versus symptomatic treatment in patients with unresectable hepatocellular carcinoma: A randomised controlled trial. Lancet. 2002; 359:1734-1739.

33. Carr BI. Hepatic arterial 90Yttrium glass microspheres (Therasphere) for unresectable hepatocellular carcinoma: Interim safety and survival data on 65 patients. Liver Transpl. 2004; 10:S107-S110.

34. Gray B, Van Hazel G, Hope M, Burton M, Moroz P, Anderson J, Gebski V. Randomised trial of SIR-Spheres plus chemotherapy *vs.* chemotherapy alone for treating patients with liver metastases from primary large bowel cancer. Ann Oncol. 2001; 12:1711-1720.

35. Sangro B, Carpanese L, Cianni R, *et al.* Survival after yttrium-90 resin microsphere radioembolization of hepatocellular carcinoma across Barcelona clinic liver cancer stages: A European evaluation. Hepatology. 2011; 54:868-878.

36. Salem R, Lewandowski RJ, Mulcahy MF, *et al.* Radioembolization for hepatocellular carcinoma using Yttrium-90 microspheres: A comprehensive report of long-term outcomes. Gastroenterology. 2010; 138:52-64.

37. Salem R, Gilbertsen M, Butt Z, *et al.* Increased quality of life among hepatocellular carcinoma patients treated with radioembolization, compared with chemoembolization. Clin Gastroenterol Hepatol. 2013; 11:1358-1365.

38. Salem R, Lewandowski RJ, Kulik L, *et al.* Radioembolization results in longer time-to-progression and reduced toxicity compared with chemoembolization in patients with hepatocellular carcinoma. Gastroenterology. 2011; 140:497-U205.

39. European Association For The Study Of The Liver; European Organisation For Research And Treatment Of Cancer. EASL-EORTC clinical practice guidelines: Management of hepatocellular carcinoma. J Hepatol. 2012; 56:908-943.

40. Riaz A, Memon K, Miller FH, *et al.* Role of the EASL, RECIST, and WHO response guidelines alone or in combination for hepatocellular carcinoma: Radiologic-pathologic correlation. J Hepatol. 2011; 54:695-704.

41. Lencioni R, Llovet JM. Modified RECIST (mRECIST) assessment for hepatocellular carcinoma. Semin Liver Dis. 2010; 30:52-60.

42. Sato K, Lewandowski RJ, Bui JT, Omary R, Hunter RD, Kulik L, Mulcahy M, Liu D, Chrisman H, Resnick S, Nemcek AA, Vogelzang R, Salem R. Treatment of unresectable primary and metastatic liver cancer with yttrium-90 microspheres (TheraSphere): Assessment of hepatic arterial embolization. Cardiovasc Intervent Radiol. 2006; 29:522-529.

Adenovirus-mediated P311 inhibits TGF-β1-induced epithelial-mesenchymal transition in NRK-52E cells *via* TGF-β1-Smad-ILK pathway

Fanghua Qi[1], Pingping Cai[1], Xiang Liu[2], Min Peng[1], Guomin Si[1,*]

[1] *Department of Traditional Chinese Medicine, Shandong Provincial Hospital affiliated to Shandong University, Ji'nan, China;*
[2] *Department of Nephrology, Shandong Provincial Hospital affiliated to Shandong University, Ji'nan, China.*

Summary	P311, a highly conserved 8-kDa intracellular protein, has been indicated as an important factor in myofibroblast transformation and in the progression of fibrosis. In the present study, we constructed a recombinant adenovirus vector of p311 (called Ad-P311) and transferred it into rat renal proximal tubular epithelial cells (NRK-52E) to explore the effect of P311 on epithelial-mesenchymal transition (EMT) of NRK-52E cells induced by TGF-β1 and to elucidate its underlying mechanism against EMT. After successfully construction of Ad-P311 and transfer into NRK-52E cells, the proliferation and growth of P311-expressing cells was detected by MTT assay. TGF-β1 was used to induce NRK-52E cells and Western blot analysis was used to examine the EMT markers (E-cadherin and α-smooth muscle actin (α-SMA)), signal transducers (p-Smad2/3 and Smad7). Integrin Linked Kinase (ILK) as a key intracellular mediator that controls TGF-β1-induced-EMT was also assayed by Western blot analysis. The results showed that P311 transfection could significantly inhibit the proliferation and growth of TGF-β1 induced NRK-52E cells. The results also showed that TGF-β1 could induce EMT in NRK-52E cells through Smad-ILK signaling pathway with an increase in α-SMA, pSmad2/3 and ILK expression, and a decrease in E-cadherin and Smad7 expression. However, P311 efficiently blocked Smad-ILK pathway activation and attenuated all these EMT changes induced by TGF-β1. These findings suggest that P311 might be involved in the pathogenesis of renal fibrosis by inhibiting the EMT process *via* TGF-β1-Smad-ILK pathway. P311 might be a novel target for the control of renal fibrosis and the progression of CKD.

Keywords: Renal fibrosis, P311, TGF-β1, epithelial-mesenchymal transition (EMT), NRK-52E cells

1. Introduction

Chronic kidney disease (CKD) has been recognized as a worldwide health issue because of its high prevalence and the accompanying increase in the risk of end-stage renal disease, cardiovascular events, and premature death (*1*). Renal fibrosis is a pivotal event in the progression of CKD, which is characterized by the deposition of extracellular matrix (ECM) (*2*).

ECM is thought to be produced by myofibroblasts. Epithelial-mesenchymal transition (EMT) of tubular epithelial cells into myofibroblasts is one of the critical pathogenic mechanisms of renal fibrosis (*3*). During the EMT process, epithelial cells lose their polarity and epithelial surface markers such as E-cadherin, and acquire mesenchymal features such as α-smooth muscle actin (α-SMA) (*4*). Preventing EMT could ameliorate renal fibrosis and delay the progression of CKD.

Increasing evidence suggests that the EMT of renal tubules is regulated by different growth factors, cytokines, hormones and extracellular signals (*5*). TGF-β1 is regarded as one of the most important cytokines which regulates the transdifferentiation of tubular epithelial cells into myofibroblasts in renal

Address correspondence to:
Dr. Guomin Si, Department of Traditional Chinese Medicine, Shandong Provincial Hospital affiliated to Shandong University, No. 324, Jingwuweiqi Road, Ji'nan 250021, Shandong, China.
E-mail: sgm977@126.com

fibrosis. It has been shown to initiate and complete the whole EMT process (*6*). Emerging data indicate that TGF-β1 induced EMT *via* Smad-dependent and Smad-independent pathways. In the Smad-dependent pathway, TGF-β signals are transduced by transmembrane serine/threonine kinase type II and type I receptors (*7*). Upon TGF-β1 binding to its receptors, Serine/Threonine kinases are activated and induce phosphorylation of Smad2/Smad3, then phosphorylate Smad2/3 partners with Smad4 translocated into the nucleus where they regulate the transcription of the target genes responsible for EMT (*8*). Integrin Linked Kinase (ILK) is an intracellular serine/threonine kinase involved in cell-matrix interactions. It is shown to be a key intracellular mediator that controls TGF-β1-induced-EMT in renal tubular epithelial cells (*9*). Although the involvement of ILK in tubular EMT has been established by several lines of evidence, intriguingly, many components of ILK signaling, including ILK and β1-integrin are induced simultaneously by TGF-β in a Smad-dependent manner (*3,10*). Therefore, it is widely accepted that TGF-β1 plays an important role in promoting tubular EMT *via* TGF-β1-Smad-ILK pathway.

P311 is a highly conserved, 8-kDa intracellular protein with a PEST domain abundantly expressed in neurons and muscles (*11*). It can bind to TGF-β latency associated protein and stimulate the translation of TGF-β (*12*). In addition, P311 is detected in myofibroblasts, at the invading edge of glioblastomas, in regenerating nerve and lung, and in hypertrophic scars (*13-17*). It has been implicated in myofibroblast transformation, cell migration, wound healing, as well as nerve and lung regeneration. Some researchers reported that P311 transfection into fibroblast cells induced phenotypic changes consistent with myofibroblast transformation, decreased TGF-β1 signaling and caused an inhibition of collagen expression. Their findings suggested that P311 might be involved in facilitating wound healing and/or minimizing scarring during wound repair *via* preventing fibrosis (*13*). A recent study indicated that P311 might be a key cytokine involved in the progression of kidneys of immunoglobulin-A nephropathy (IgAN) (*18*). However, the related reports about P311 on renal fibrosis are limited and the mechanisms of P311 in the progression of CKD remain largely unknown. Thus, in the present study, we constructed a recombinant adenovirus vector of p311 and transferred it into NRK-52E cells to explore the preventive effect and possible mechanism of P311 on TGF-β1-induced EMT, which might provide new sight for ameliorating renal fibrosis and delaying the progression of CKD.

2. Materials and Methods

2.1. Cells

Rat renal proximal tubular epithelial cells NRK-52E

and human embryonic kidney cells HEK293A were purchased from the Institute of Biochemistry and Cell Biology (Shanghai, China) and cultured in DMEM (Gibco, CA, USA) with 10% fetal bovine serum (FBS) (Gibco, CA, USA) in an atmosphere of 5% CO_2 at 37°C.

2.2. Construction and identification of plasmid

P311 gene adenovirus plasmid was constructed according to previous studies (*19*). First, according to the sequence of GeneBank, the target gene P311-His_tag was designed and synthesized with His_tag sequence and SpeI added at the 3' end and EcoRI added at the 5' end of the P311 gene. Second, both target gene P311-His_tag and shuttle vector pDown-MCS-IRES/eGFP were digested by EcoRI and SpeI and recovered by agarose gel electrophoresis. Third, the digested products were purified and ligated with T4 DNA ligase and then co-transformed into *E. coli* stbl3 cells (Gibco, CA, USA). Thus, the fragment of P311-His_tag gene was cloned into the shuttle plasmid pDown-MCS-IRES/eGFP (Invitrogen, NY, USA), and the recombinant adenoviral plasmid was generated. Following amplification, the plasmid was extracted and cloned.

2.3. Packaging and amplification of the recombinant adenovirus

To package the adenovirus, HEK293A cells were cultured and were inoculated on 6-well plates. The recombinant adenovirus plasmid was digested with PacI and linearized, and was then purified by gel recycling. The linearized plasmid DNA was then transfected into HEK293A cells using Lipofectamine 2000 (Invitrogen, NY, USA) and incubated for 7 days at 37°C as described in the manual. The cells were scraped off the plates and the virus was collected by three consecutive freezing/thawing cycles. To amplify the adenovirus, 1/3 of the obtained virus was used for infection of HEK293A cells, and cells were collected after 48 h. Amplification was repeated as such for a total of four times, all cells were collected, and were then frozen and thawed repeatedly to obtain the recombinant adenovirus. The titer of recombinant adenovirus (called Ad-P311) was detected by TCID50. The control Ad-CMV-eGFP was constructed in the same way. The Ad-P311 and Ad-CMV-eGFP were stored at -80°C for use.

2.4. Determination of infection efficiency in NRK-52E cells infected by Ad-P311 in vitro and the most optimal MOI

The adenovirus Ad-CMV-eGFP was used as a control and the efficiency of infection was determined by the rate of GFP expression according to standard procedure

and improved according to previous studies (*20*). Briefly, reconstructed adenovirus (stored at -80 °C) was serially diluted in DMEM without serum and pre-incubated with Lipofectamine 2000 at a final concentration of 1%. The virus-lipid mixture was incubated at 37 °C for 30 min before adding to the NRK-52E cells. NRK-52E cells within three generations were digested with trypsin and mixed, then transferred into 12-well plates at a density of 1×10^5 cells/per well with routine culture until firm adherence. Different volumes (2 μL, 4 μL, 6 μL, 8 μL, 10 μL, and 15 μL) of Ad-P311 and Ad-CMV-eGFP were respectively transferred into NRK-52E cells. Following incubation for 8 h (being rocked every 30 min) at 37°C, CO_2, the cells were routinely cultured for 48 h with complete medium and then observed under the inversion fluorescence microscope. The best multiplicity of infection (MOI) was worked out according to a formula (MOI) = (virus titer) × (virus liquid volume)/(cell number for transfection). The largest MOI not causing a marked cytopathic effect (CPE) was considered as the best MOI. The virus liquid was transferred into NRK-52E cells at its best MOI value in the following experiments.

2.5. *P311 mRNA expression in NRK-52E Cells infected by Ad-P311*

Firstly, NRK-52E cells were infected with Ad-P311 (as described above) for 48h, and then infected NRK-52E cells were collected. The mRNA expression of P311 was detected by quantitative real-time RT-PCR assay (*21*). The primers for the P311 and GAPDH are shown as follows: P311: forward 5'-AACAAGGACATGGAGGGAAGG-3' and reverse 5'-TAACTGATTCTTGGGGAGCGG-3'; GAPDH: forward 5'-GGCTCATGACCACAGTCCAT-3' and reverse 5'-TCAGCTCTGGGATGACCTTG-3'. First, total RNA was prepared from the cells using TRIzol (Grand Island, NY, USA) reagent according to the manufacturer's instructions. Then, total RNA was reverse transcribed into cDNA using the SuperScript II First Strand Synthesis System (Grand Island, NY, USA) according to the manufacturer's directions. Afterwards, according to the protocol of SYBR Premix Ex Taq™ kit (TaKaRa Bio Inc., Dalian, China), amplification of target gene and GAPDH were conducted using ABI Prism 7500 Detection System (Applied Biosystems, Inc., USA). The analysis of relative gene expression was performed by comparative $2^{-\Delta\Delta CT}$ method.

2.6. *Cell treatment*

After infection with adenovirus, cells were treated and divided into six groups as follows: NRK-52E group, NRK-52E/GFP group (infected by Ad-CMV-eGFP), NRK-52E/P311 (infected by Ad-P311), and TGF-β1 (5 ng/mL) induced groups: NRK-52E (TGF-β1) group,

NRK-52E/GFP (TGF-β1) group, and NRK-52E/P311 (TGF-β1) group. NRK-52E group was control group and the other five groups were treatment groups. At the indicated time points, cells were harvested and processed for the following experiments.

2.7. *Cell proliferation assay*

A MTT (3-[4, 5-dimethylthiazol-2-yl]-2,5-diphenyl-tetrazolium bromide) assay was used to detect cell viability as previously described (*22*). The cells were cultured at a density of 6×10^3 cells/well in triplicate in 96-well plates with TGF-β1 (5 ng/mL) for 7 days and exposed to fresh media and TGF-β1 every other day. MTT assay was performed every day up to the 7th day. Briefly, 20 μL of 5 mg/mL MTT (Sigma, St. Louis, MO, USA) was added to each well; plates were incubated at 37°C for 4 h. The generated formazan was dissolved in 150 μl dimethyl sulfoxide (DMSO) and measured with a microplate reader (BioRad, Hercules, CA) at an optical density (OD) at 570 nm for determining cell viability. Cell proliferation rate was calculated according to a formula as follows: Cell proliferation rate (%) = OD value of treatment group/ OD value of control group × 100%.

2.8. *Western blot analysis*

After culturing with TGF-β1 (5 ng/mL) for 48h, total cell lysates and cytosolic fractions were prepared as previously described (*21*). Thirty micrograms of total cellular proteins were resolved using sodium dodecyl sulfate polyacrylamide gel electrophoresis (SDS PAGE) and transferred onto polyvinylidene fluoride (PVDF) transfer membranes for Western blotting. The results were quantified using Image J (National Institutes of Health, Bethesda, MD, USA). The following antibodies were used: Smad2/3, Smad7, α-SMA, E-cadherin, ILK, and GAPDH (Santa Cruz Biotechnology, Santa Cruz, CA, USA).

2.9. *Statistical analysis*

Statistical analysis was performed using SPSS software, version 17.0 (SPSS Inc., USA). The data are expressed as the mean ± standard deviation (SD). The statistical significance differences were calculated using the t-test and one-way analysis of variance (ANOVA), and $p < 0.05$ was considered statistically significant.

3. Results

3.1. *Construction of pAd-P311*

The sequence of P311-His_tag was confirmed to be correct by restriction endonuclease reaction (Figure
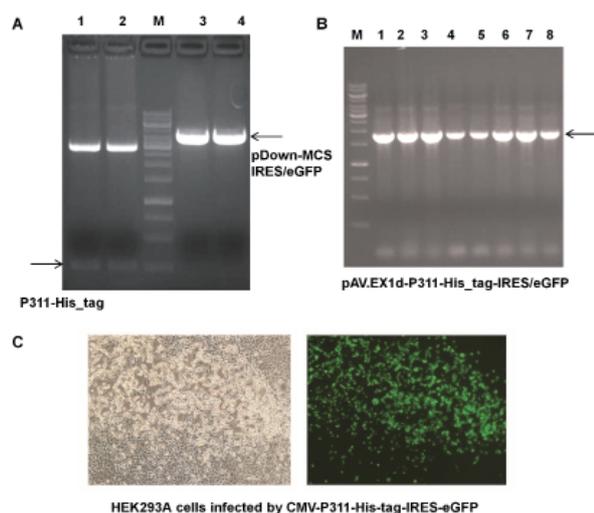
Figure 1. The construction and identification of Ad P311. (A) P311-His_tag (lane 1 and 2) and shuttle vector pDown-MCS-IRES/eGFP (lane 3 and 4) were digested by EcoRI and SpeI (P311-His_tag fragment about 248 bp, and shuttle vector pDown-MCS-IRES/eGFP about 3.8 kb). Lane M: 1-10 kbp DNA Ladder marker. **(B)** pAV.EX1d-P311-His_tag-IRES/eGFP was produced in *E. coli* stbl3 cells ((lane 1-8, about 1740 bp). **(C)** HEK293A cells infected by CMV-P311-His-tag-IRES-eGFP. After 8 days infection, the white light and fluorescence were seen (×100).

1A). Then P311-His_tag was cloned into shuttle vector pDown-MCS-IRES/eGFP carrying the GFP gene to generate a recombinant plasmid pDown-P311-His_tag-IRES/eGFP and confirmed to be correct by direct sequencing once again and restriction endonuclease reaction. The pDown-P311-His_tag-IRES/eGFP and pAV.Des1d were linearized and simultaneouly electroporated into host bacteria *E. coli* stbl3 cells to generate homologous recombination. The positive clone was identified by sequencing and restriction endonuclease digestion (Figure 1B). The recombinant pAd CMV-P311-His-tag-IRES-eGFP was transferred into HEK293A cells for packaging. When CMV-P311-His_tag-IRES/eGFP was completely transfected into HEK293A cells for 10 days, the vast majority of cells showed CPE. As shown in Figure 1C, fluorescence and cell change effects were seen after 10 days of post-transfection under the fluorescence microscope. The recombinant pAd CMV-P311-His-tag-IRES-eGFP adenovirus was amplified in HEK293A cells, collected and named Ad-P311. The virus titer of Ad-P311 and Ad-CMV-eGFP was determined to be 3.675×10^{10} TU/mL and 1.570×10^{10} TU/mL, respectively.

3.2. The efficiency of infection in NRK-52E cells by recombinant Ad-P311

When different volumes (2 μL, 4 μL, 6 μL, 8 μL, 10 μL, and 15 μL) of Ad-P311 and Ad-CMV-eGFP were respectively transferred into NRK-52E cells for 48h, the efficiency of infection was detected using the inverted fluorescence microscope. After infection by Ad-P311
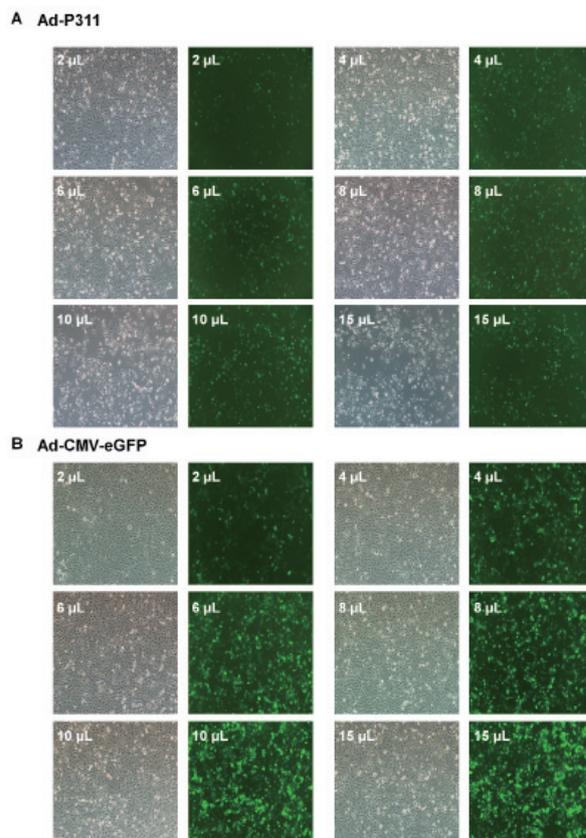
Figure 2. The efficiency of infection in NRK-52E cells by recombinant Ad-P311. Different volumes (2 μL, 4 μL, 6 μL, 8 μL, 10 μL, and 15 μL) of Ad-P311 and Ad-CMV-eGFP were respectively transferred into NRK-52E cells for 48h, and the efficiency of infection was detected using the inverted fluorescence microscope (×100). After infection by Ad-P311 at a volume of 6μL or higher **(A)**, or infection by Ad-CMV-eGFP at a volume of 4 μL or higher **(B)**, the transfection rate of NRK-52E cells could reach more than 90%.

at a volume of 6μL or higher, the transfection rate of NRK-52E cells could reach more than 90% (Figure 2A), and the best MOI was 2205. After infection by Ad-CMV-eGFP at a volume of 4 μL or higher, the transfection rate of NRK-52E cells also could reach more than 90% (Figure 2B), and the best MOI was 628. These results indicated that the adenovirus-mediated transfection had a high efficiency in NRK-52E cells.

3.3. P311 mRNA expression in NRK-52E cells infected by recombinant Ad-P311

After determination of optimal MOI as described above, we then infected NRK-52E cells with Ad-P311 (MOI = 2205). The mRNA expression of P311 in NRK-52E cells infected by recombinant Ad-P311 was detected by quantitative real-time RT-PCR assay. As shown in Figure 3, compared to the NRK-52E group and NRK-52E/GFP group, the mRNA expression of P311 in the NRK-52E/P311 group increased significantly. Furthermore, there is no significant difference between NRK-52E group and NRK-52E/GFP group on mRNA expression of P311. These results showed that P311 was expressed stably in
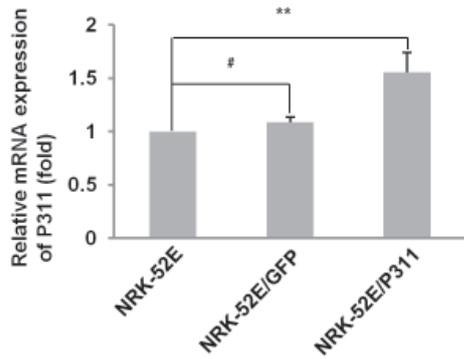
Figure 3. P311 mRNA expression in NRK-52E cells infected by recombinant Ad-P311. P311 was expressed stably in NRK-52E cells after being infected with Ad-p311. Compared to the NRK-52E group and NRK-52E/GFP group, the mRNA expression of P311 in the NRK-52E/P311 group increased significantly (**$p < 0.01$). There is no significant difference between NRK-52E group and NRK-52E/GFP group on the mRNA expression of P311 (#$p > 0.05$).
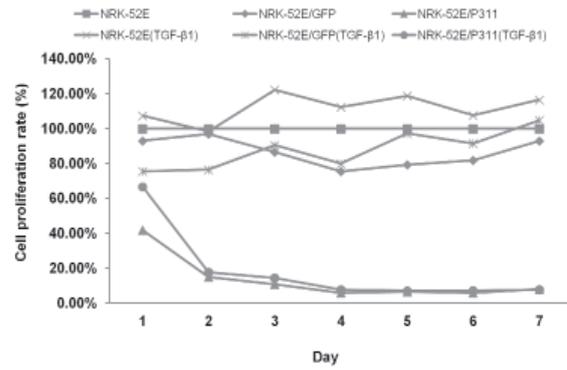
Figure 4. Growth curve of TGF-β1-induced NRK-52E cells infected by Ad-P311. P311 had a significant growth-inhibiting effect on NRK-52E cells. Compared to the NRK-52E (TGF-β1) group, the cell proliferation rate in the NRK-52E/P311 (TGF-β1) was decreased significantly.
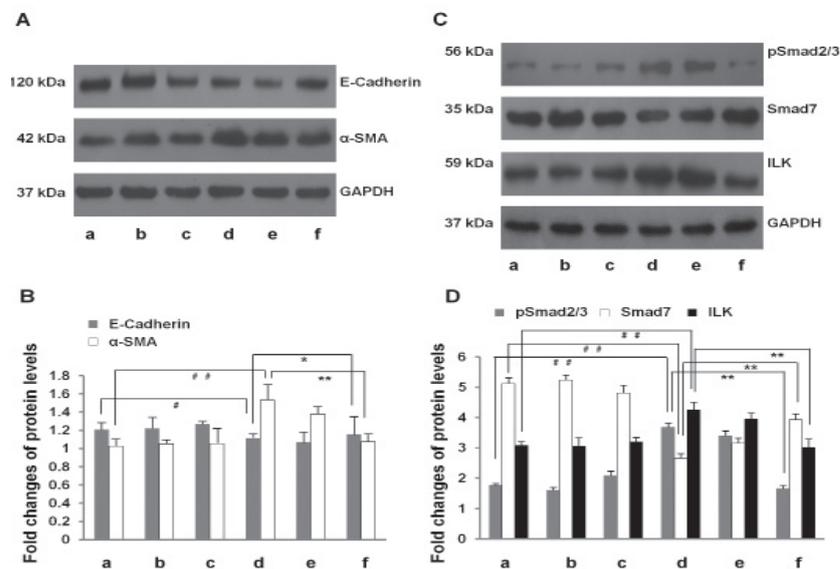
Figure 5. EMT related proteins expression in TGF-β1-induced NRK-52E cells infected by Ad-P311. (A) Expression of E-cadherin and α-SMA at the protein level were determined with GAPDH used as an internal control. **(B)** The expression level of E-cadherin and α-SMA was quantitatively analyzed with Image J software. **(C)** Expression of pSmad2/3, Smad7, and ILK at the protein level were determined with GAPDH used as an internal control. **(D)** The expression level of pSmad2/3, Smad7, and ILK was quantitatively analyzed with Image J software. The data show mean ± SD. #$p < 0.05$, ##$p < 0.01$, and ###$p < 0.005$ versus control (NRK-52E group). *$p < 0.05$, **$p < 0.01$, and ***$p < 0.005$ versus control (NRK-52E (TGF-β1) group). (**a**: NRK-52E group; **b**: NRK-52E/GFP group; **c**: NRK-52E/P311 group; **d**: NRK-52E(TGF-β1) group; **e**: NRK-52E/GFP(TGF-β1) group; **f**: NRK-52E/P311(TGF-β1) group).

NRK-52E cells after being infected with Ad-p311.

3.4. *Growth curve of TGF-β1-induced NRK-52E cells infected by Ad-P311*

MTT assays were performed to investigate the effects of P311 on the proliferation of TGF-β1-induced NRK-52E cells, and a growth curve was drawn according to the results. As shown in Figure 4, after incubation with Ad-P311 for 7 days, P311 had a significant growth-inhibiting effect on the TGF-β1-induced NRK-52E cells. The cell proliferation rate was higher in the NRK-52E (TGF-β1) group than in the NRK-52E group, which indicated that TGF-β1 had the effect of inducing

NRK-52E cell proliferation. Compared to the NRK-52E (TGF-β1) group, the cell proliferation rate in the NRK-52E/P311 (TGF-β1) was decreased significantly, which indicated that P311 could inhibit the proliferation of TGF-β1-induced NRK-52E cells. These results showed that P311 had a significant growth-inhibiting effect on NRK-52E cells.

3.5. *EMT related proteins expression in TGF-β1-induced NRK-52E cells infected by Ad-P311*

To explore the effect of P311 on TGF-β1-induced EMT in NRK-52E cells, the expression of the epithelial marker E-cadherin, and the mesenchymal marker

α-SMA were examined by Western blot analysis. As shown in Figure 5A and 5B, exposure of cells to TGF-β1 resulted in a significant reduction in E-cadherin and an increase in α-SMA, compared with control. P311 significantly prevented TGF-β1 stimulated changes of E-cadherin and α-SMA expression. These results suggest that P311 prevents the loss of the epithelial marker Ecadherin and the de novo expression of myofibroblast marker α-SMA in renal epithelial cells stimulated by TGF-β1.

To explore the possible mechanism of P311 on TGF-β1-induced EMT in NRK-52E cells, the protein expression of EMT related proteins Smad2/3, Smad7, and ILK were measured by Western blot analysis. As shown in Figure 5C and 5D, exposure to TGF-β1 resulted in a significant increase in Smad2/3 phosphorylation and ILK expression, and a significant reduction in Smad7 expression compared with control. Ad-P311 transfection significantly decreased the phosphorylation of Smad2/3 and the expression of ILK in NRK-52E cells compared with TGF-β1-treated group. These results suggest that P311 inhibits TGF-β1-induced EMT in NRK-52E cells *via* regulating the expression of Smad2/3, Smad7 and ILK.

4. Discussion

Although previous work has suggested P311 might be an important factor in myofibroblast transformation and in the progression of fibrosis, the related reports about P311 on renal fibrosis are limited and the mechanism of P311 in the progression of CKD remains largely unknown. EMT plays important roles in accelerating renal fibrosis and promoting the progression of CKD. TGF-β1 is a well-known profibrotic cytokine in several renal diseases and plays a critical role in the renal EMT process. Thus, in the current study, we constructed a recombinant adenovirus vector of p311 and transferred it into NRK-52E cells to explore the preventive effect and possible mechanism of P311 on TGF-β1-induced EMT.

We first successfully constructed recombinant adenovirus vector of P311 (called Ad-P311) and transferred it into rat renal tubular epithelial cells NRK-52E (Figure 1). Then we investigated the effects of Ad-P311 transfection on the biological characteristics of NRK-52E cells. Transfection efficiency of Ad-P311 in NRK-52E cells was evaluated by expression of GFP under the fluorescence microscope (Figure 2). After infection by Ad-P311 at a volume of 6μL or higher, the transfection rate of NRK-52E cells could reach more than 90% and the best MOI was 2205, which indicated that the adenovirus-mediated transfection (Ad-P311) had a high efficiency in NRK-52E cells. To investigate the expression of P311 in NRK-52E cells after transfection, the quantitative real-time RT-PCR assay was performed. Results showed that mRNA expression of P311 was specifically expressed in NRK-52E/P311

cells rather than in NRK-52E cells or NRK-52E/GFP cells (Figure 3). All these findings demonstrate that the P311 gene can be highly and stably transfected into NRK-52E cells wih adenovirus mediation.

We investigated the proliferation and growth of P311-expressing cells by MTT assay (Figure 4). From the growth curve of NRK-52E cells, we could see that TGF-β1 had a significant effect on inducing NRK-52E cell proliferation. The cell proliferation rate was higher in the NRK-52E (TGF-β1) group than that in the NRK-52E group. We also could see that P311 had a significant growth-inhibiting effect on the TGF-β1-induced NRK-52E cells. Compared to the NRK-52E (TGF-β1) group, the cell proliferation rate in the NRK-52E/P311 (TGF-β1) group was decreased significantly. All these findings demonstrate that P311 transfection can significantly inhibit the proliferation and growth of TGF-β1 induced NRK-52E cells.

To investigate the possible mechanism by which the P311 gene inhibits cell proliferation and TGF-β1 induced EMT in NRK-52E cells, Western blot analysis was performed to detect the expression of EMT-related proteins and signal pathways. EMT is well known as an important process in the pathogenesis of tubulointerstitial fibrosis and involves a loss of epithelial cell characteristics (loss of E-cadherin) and an increase of mesenchymal cell markers (*e.g.*, α-SMA). TGF-β1 is identified as the most potent mediator and convergent pathway in inducing EMT and renal fibrosis (*23*). Here we found that exposure to TGF-β1 for 48 h in NRK-52E cells, E-cadherin expression was decreased and α-SMA expression was increased significantly (Figure 5A and 5B). However, P311 significantly reverses all of above changes *in vitro* (Figure 5A and 5B). These results suggest that P311 prevents TGF-β1-mediated renal EMT *in vitro*.

TGF-β1/Smads signal pathway has been shown to play a critical role in the process of inducing EMT (*7*). The Smad family has 8 members forming three subfamilies: the R-Smads (receptor regulated Smads), the Co-Smads (common Smad mediators), and the I-Smads (inhibitory Smads), which are the main TGF-β signaling transducers, mediating signaling from cell surface receptors to nuclear target genes (*24*). Homologous proteins Smad2 and Smad3 belong to the R-Smads, which are highly activated in the fibrotic kidney. It has been demonstrated that activation of TGF-β1 signaling triggers a dramatic induction of Smad2/3 phosphorylation (*25*). Smad7, as an inhibitory regulator in the TGF-β/Smad signaling pathway, can be induced by TGF-β1 to block the overactivation of TGF-β signals *via* its negative feedback loop. TGF-β not only induces Smad7 transcription, but also promotes the degradation of Smad7 *via* the Smad3-dependent Smurfs/arkadia-mediated ubiquitin-proteasome degradation pathway (*26*). In this study, we investigated the effects of P311 on the TGF-β1/
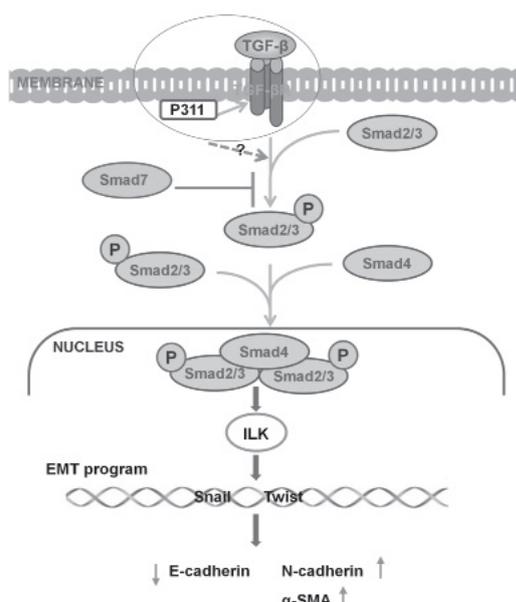
Figure 6. The possible mechanisms of P311 involved in the TGF-β1-induced EMT process in renal fibrosis via TGF-β1-Smad-ILK pathway.

Smads signal pathway in NRK-52E cells. Here we found that exposure to TGF-β1 for 48 h in NRK-52E cells, p-Smad2/3 expression was increased and Smad7 expression was decreased significantly (Figure 5C and 5D). However, P311 significantly reverses all of the above changes *in vitro* (Figure 5C and 5D). Our results showed that P311 inhibited p-Smad2/3 activation and promoted Smad7 activation induced by TGF-β1 in NRK-52E cells. We also further studied the effects of P311 on ILK expression, which was the important downstream mediator of TGF-β1/Smads signaling pathway. ILK has shown to be a key intracellular mediator that controls TGF-β1-induced-EMT in renal tubular epithelial cells (*9*). Here we found that exposure to TGF-β1 for 48 h in NRK-52E cells, ILK expression was increased significantly (Figure 5C and 5D), however, P311 significantly reverses the above changes *in vitro* (Figure 5C and 5D). These results showed that infection of P311 in NRK-52E cells attenuated TGF-β1-induced upregulation of ILK expression.

In conclusion, our data present that P311 could block TGF-β1-induced EMT probably by inhibiting the activation of p-Smad2/3 and ILK and promoting the activation of Smad7 in NRK-52E cells. These findings suggest that P311 might be involved in the pathogenesis of renal fibrosis by inhibiting the EMT process *via* the TGF-β1-Smad-ILK pathway (Figure 6). P311 might be a novel target for control of renal fibrosis and progression of CKD.

Acknowledgements

References

1. Tonelli M, Wiebe N, Culleton B, House A, Rabbat C, Fok M, McAlister F, Garg AX. Chronic kidney disease and mortality risk: A systematic review. J Am Soc Nephrol. 2006; 17:2034-2047.
2. Boor P, Ostendorf T, Floege J. Renal fibrosis: Novel insights into mechanisms and therapeutic targets. Nat Rev Nephrol. 2010; 6:643-656.
3. Liu Y. New insights into epithelial-mesenchymal transition in kidney fibrosis. J Am Soc Nephrol. 2010; 21:212-222.
4. Kriz W, Kaissling B, Le Hir M. Epithelial-mesenchymal transition (EMT) in kidney fibrosis: Fact or fantasy? J Clin Invest. 2011; 121:468-474.
5. Guo Y, Li Z, Ding R, Li H, Zhang L, Yuan W, Wang Y. Parathyroid hormone induces epithelial-to-mesenchymal transition *via* the Wnt/β-catenin signaling pathway in human renal proximal tubular cells. Int J Clin Exp Pathol. 2014; 7:5978-5987.
6. Wang Q, Wang Y, Huang X, Liang W, Xiong Z, Xiong Z. Integrin β4 in EMT: An implication of renal diseases. Int J Clin Exp Med. 2015; 8:6967-6976.
7. Sun S, Sun W, Xia L, Liu L, Du R, He L, Li R, Wang H, Huang C. The T-box transcription factor Brachyury promotes renal interstitial fibrosis by repressing E-cadherin expression. Cell Commun Signal. 2014; 12:76.
8. Jia L, Ma X, Gui B, Ge H, Wang L, Ou Y, Tian L, Chen Z, Duan Z, Han J, Fu R. Sorafenib ameliorates renal fibrosis through inhibition of TGF-β-induced epithelial-mesenchymal transition. PLoS One. 2015; 10:e0117757.
9. Kim MK, Maeng YI, Sung WJ, Oh HK, Park JB, Yoon GS, Cho CH, Park KK. The differential expression of TGF-β1, ILK and wnt signaling inducing epithelial to mesenchymal transition in human renal fibrogenesis: An immunohistochemical study. Int J Clin Exp Pathol. 2013; 6:1747-1758.
10. Li Y, Yang J, Dai C, Wu C, Liu Y. Role for integrin-linked kinase in mediating tubular epithelial to mesenchymal transition and renal interstitial fibrogenesis. J Clin Invest. 2003; 112:503-516.
11. Penn JW, Grobbelaar AO, Rolfe KJ. The role of the TGF-β family in wound healing, burns and scarring: A review. Int J Burns Trauma. 2012; 2:18-28.
12. Paliwal S, Shi J, Dhru U, Zhou Y, Schuger L. P311 binds to the latency associated protein and downregulates the expression of TGF-beta1 and TGF-beta2. Biochem Biophys Res Commun. 2004; 315:1104-1109.
13. Pan D, Zhe X, Jakkaraju S, Taylor GA, Schuger L. P311 induces a TGF-beta1-independent, nonfibrogenic myofibroblast phenotype. J Clin Invest. 2002; 110:1349-1358.
14. Mariani L, McDonough WS, Hoelzinger DB, Beaudry C, Kaczmarek E, Coons SW, Giese A, Moghaddam M, Seiler RW, Berens ME. Identification and validation of P311 as a glioblastoma invasion gene using laser capture microdissection. Cancer Res. 2001; 61:4190-4196.
15. Fujitani M, Yamagishi S, Che YH, Hata K, Kubo T, Ino H, Tohyama M, Yamashita T. P311 accelerates nerve regeneration of the axotomized facial nerve. J

Neurochem. 2004; 91:737-744.

16. Zhao L, Leung JK, Yamamoto H, Goswami S, Kheradmand F, Vu TH. Identification of P311 as a potential gene regulating alveolar generation. Am J Respir Cell Mol Biol. 2006; 35:48-54.

17. Tan J, Peng X, Luo G, Ma B, Cao C, He W, Yuan S, Li S, Wilkins JA, Wu J. Investigating the role of P311 in the hypertrophic scar. PLoS One. 2010; 5:e9995.

18. Wang F, Xie X, Fan J, Wang L, Guo D, Yang L, Ma X, Zhang L, Li Z. Expression of P311, a transforming growth factor beta latency-associated protein-binding protein, in human kidneys with IgA nephropathy. Int Urol Nephrol. 2010; 42:811-819.

19. Liu D, Hu L, Zhang Z, Li QY, Wang G. Construction of human BMP2-IRES-HIF1αmu adenovirus expression vector and its expression in mesenchymal stem cells. Mol Med Rep. 2013; 7:659-663.

20. Zhao YN, Li Q. Adenovirus mediated BIMS transfer induces growth supression and apoptosis in Raji lymphoma cells. Biomed Environ Sci. 2014; 27:655-664.

21. Yin Y, Qi F, Song Z, Zhang B, Teng J. Ferulic acid combined with astragaloside IV protects against vascular endothelial dysfunction in diabetic rats. Biosci Trends. 2014; 8:217-226.

22. Cui XY, Inagaki Y, Wang DL, Gao JJ, Qi FH, Gao B, Kokudo N, Fang DZ, Tang W. The supercritical CO_2 extract from the skin of Bufo bufo gargarizans Cantor blocks hepatitis B virus antigen secretion in HepG2.2.15 cells. BioScience Trends. 2014; 8:38-44.

23. Lamouille S, Xu J, Derynck R. Molecular mechanisms of epithelial-mesenchymal transition. Nat Rev Mol Cell Biol. 2014; 15:178-196.

24. Tirado-Rodriguez B, Ortega E, Segura-Medina P, Huerta-Yepez S. TGF-β: An important mediator of allergic disease and a molecule with dual activity in cancer development. J Immunol Res. 2014; 2014:318481.

25. Meng XM, Chung AC, Lan HY. Role of the TGF-β/BMP-7/Smad pathways in renal diseases. Clin Sci (Lond). 2013; 124:243-254.

26. Meng XM, Tang PM, Li J, Lan HY. TGF-β/Smad signaling in renal fibrosis. Front Physiol. 2015; 6:82.

DHEA promotes osteoblast differentiation by regulating the expression of osteoblast-related genes and Foxp3^{+} regulatory T cells

Xuemin Qiu[1,2], Yuyan Gui[1,2], Yingping Xu[1,2], Dajin Li[1,*], Ling Wang[1,2,*]

[1] *Obstetrics and Gynecology Hospital, Fudan University, Shanghai, China;*
[2] *Shanghai Key Laboratory of Female Reproductive and Endocrine-related Disorders, Shanghai, China.*

Summary Several studies have reported that dehydroepiandrosterone (DHEA) promotes osteoblast proliferation and inhibits osteoblast apoptosis and that DHEA inhibits osteoclast maturation. However, whether DHEA regulates osteoblast differentiation remains unclear. The present study first examined the effect of DHEA on bone morphology *in vivo*. DHEA was found to increase bone volume (BV), bone mineral density (BMD), and the number of trabeculae in bone (Th.N) and it was found to decrease trabecular spacing in bone (Th.sp) in ovariectomized (OVX) mice. Next, the effect of DHEA on osteoblast differentiation was examined *in vitro* and osteoblastogenesis-related marker genes, such as *Runx2*, *Osterix*, *Collagen1*, and *Osteocalcin*, were also detected. DHEA increased osteoblast production in mesenchymal stem cells (MSCs) cultured in osteoblastogenic medium, and DHEA increased the expression of Runx2 and osterix, thereby increasing the expression of osteocalcin and collagen1. Immune cells and bone interact, so changes in immune cells were detected *in vivo*. DHEA increased the number of Foxp3^{+} regulatory T cells (Tregs) in the spleen but it did not affect CTLA-4 or IL-10. When MSCs were treated with DHEA in the presence of Tregs, alkaline phosphatase (ALP) activity increased. Osteoblasts and adipocytes are both generated by MSCs. If osteoblast differentiation increases, adipocyte differentiation will decrease, and the reverse also holds true. DHEA was found to increase the number of adipocytes in osteoblastogenic medium but it had no effect on the number of adipocytes and expression of PPARγ mRNA in adipogenic medium. This finding suggests that osteoblasts may be involved in adipocyte production. In conclusion, the current results suggest that DHEA can improve postmenopausal osteoporosis (PMO) by up-regulating osteoblast differentiation *via* the up-regulation of the expression of osteoblastogenesis-related genes and *via* an increase in Foxp3^{+} Tregs.

Keywords: DHEA, postmenopausal osteoporosis, MSCs, osteoblast, adipocyte, regulatory T cells

1. Introduction

The level of dehydroepiandrosterone (DHEA) in postmenopausal women is lower than that in fertile women, which suggests the potential clinical benefit of DHEA as treatment for postmenopausal osteoporosis (PMO) (*1*). Treatment of postmenopausal osteoporosis is mainly hormone replacement therapy, but this therapy is often accompanied by adverse reactions, limiting its use (*2,3*). The pressing task is to identify a new way to treat PMO that can prevent osteoporosis without causing adverse reactions.

Mesenchymal stem cells (MSCs) are able to differentiate into multiple types of cells. Under certain conditions, MSCs can be induced to differentiate into osteoblasts, adipocytes, cartilage cells, and other types of cells (*4,5*). Inducing MSCs to differentiate into osteoblasts and inhibiting MSCs from differentiating into adipocytes is crucial to preventing PMO.

DHEA begins to increase when the adrenal cortex

**Address correspondence to:*
Dr. Dajin Li, Laboratory for Reproductive Immunology, Hospital and Institute of Obstetrics and Gynecology, Fudan University Shanghai Medical College, No.413, Zhaozhou Road, Shanghai 200011, China
E-mail: djli@shmu.edu.cn

Dr. Ling Wang, Obstetrics & Gynecology Hospital, Fudan University Shanghai Medical College, 413 Zhaozhou Road, Shanghai 200011, China.
E-mail: dr.wangling@vip.163.com

begins to function and it gradually decreases after puberty. Along with other endocrine hormones, DHEA in the blood decreases with the onset of menopause. DHEA can prevent diabetes, cancer, and heart disease and it can enhance immune function, suggesting that DHEA can prolong survival and improve the quality of life.

DHEA has a positive effect on bone metabolism (*6-8*). DHEA can promote the growth and proliferation of osteoblasts, and mitogen-activated protein kinase signaling pathways are required for expression of osteoblast-specific genes. DHEA can promote a shift in the Th1/Th2 ratio towards Th2, thus improving immunity in a model of PMO.

Immune cells and bone interact (*9-11*). Regulatory T cells (Tregs) are important immunosuppressive cells that regulate the functioning of osteoblasts and osteoclasts (*12,13*). Whether DHEA affects immune cells and then affects bone metabolism is unclear. Whether DHEA affects the differentiation of MSCs into osteoblasts or adipocytes and the means by which it does so are still unknown. The present study will explore the mechanisms by which DHEA affects the differentiation of MSCs.

2. Materials and Methods

2.1. *Mice and reagents*

C57BL/6 mice (6-8 weeks of age) were provided by the Laboratory Animal Facility of the Chinese Academy of Sciences (Shanghai, China) and were housed and handled in accordance with the guidelines of the Chinese Council for Animal Care. Sham-operated mice were used as controls, and ovariectomized (OVX) mice were used as a model of PMO. Mice were divided into 3 groups and then treated with different drugs, *i.e.* estrogen, DHEA, or saline. MEM, estrogen, DHEA, PBS and saline, and ALP solution/alizarin red solution were purchased from Sigma-Aldrich Co (Saint Louis, MO, USA). Flow cytometry antibodies CD4-FITC, CD25-APC, CTLA-4-PE, IL-10-PE, Foxp3-PE were purchased from eBioscience (San Diego, CA, USA).

2.2. *Experimental protocols in vivo*

Animals were anesthetized with 10% chloral hydrate. Mice in the sham-operated group underwent surgery but were not OVX. Mice in the treatment groups underwent a bilateral ovariectomy and were divided into 3 groups (OVX, OVX + DHEA, and OVX + E2). One week later, the sham-operated group was treated with saline (containing 0.1% ethanol), and OVX mice group in the treatment groups were given saline, DHEA (5 mg/kg per day orally), or estrogen (100 μg/kg per day orally) (*6*). The four groups received equal quantities of fluids at the same time during treatment. All mice

were sacrificed after 3 months of treatment. Blood was collected from the heart and serum was stored at -80°C for use in cell culture, the spleen was collected for analysis of Tregs, and femurs were stored for micro-CT analysis (*14*).

2.3. *Flow cytometry (FCM)*

The spleen was harvested from mice in every group and mechanically disrupted in 10 mL of PBS. The cell suspension was then filtered through nylon mesh with a pore size of 110 μm and treated with NH4Cl/Tris buffer to remove RBC. The cells were then washed three times and transferred into tubes (100 μL per tube) for immunolabeling. The cells were fixed, permeabilized, and stained for Foxp3, IL-10, CTLA-4 using PE-labeled antibodies after cells were labeled with CD4 (FITC) and CD25 (APC). The cells were then washed twice and resuspended in PBS for FCM with a flow cytometer (Becton Dickinson, Palo Alto, CA, USA). PE-conjugated isotypes were used as controls. Statistical analysis was done using isotype-matched controls.

2.4. *MSC culture*

MSCs were cultured as previously described (*15*). Mice were anesthetized with 10% chloral hydrate and immersed in 75% ethanol for 10 min. Under aseptic conditions, the femur was removed and rinsed three times with PBS. The epiphyseal end of the femur was removed, revealing the marrow cavity. Bone marrow was removed, placed in L-DMEM with penicillin and streptomycin, and repeatedly sieved to obtain a single cell suspension. The suspension was centrifuged at 1,000 r/min for 5 min and the supernatant was discarded. The concentrated cells were placed in culture bottles at a concentration of 1×10^9 L^{-1} cells. Cells were cultured at 37°C in a 5% CO_2 environment with saturated humidity.

Medium was supplemented after 48 h. Medium was completely replaced with fresh medium every 3 d. Cells covering the bottom of the culture bottle formed a 70-80% confluent monolayer. After digestion with 0.25% trypsin, cells were subcultured at a ratio of 1:2.

2.5. *MSC-derived osteoblasts*

MSCs were seeded as previously reported (*16*) in order to induce differentiation into osteoblasts. Twenty-four hours after seeding, the growth medium was replaced with osteoblastogenic medium (OM) and 10% FCS was replaced with solvent alone (control), 10^{-7} M DHEA, or 10^{-9} M E2. Medium was changed every 2-3 days. After 14-21 days of osteogenic differentiation, cells were fixed with 70% ethanol for 1 h, washed three times with demineralized water, and then stained with an ALP

solution/alizarin red solution for 10 min. Finally, cells were washed three times with PBS.

ALP precipitates were solubilized to quantify ALP activity. Briefly, stained samples were incubated with 800 mL acetic acid (10%) for 30 min, the supernatant was transferred into a 1.5 mL tube and boiled for 10 min at 85°C, and then the supernatant was placed on ice for 5 min. After centrifugation (15,000/g, 15 min), 500 μL of the supernatant was transferred into another 1.5-mL tube and mixed with 200 μL of 10% ammonium hydroxide. Samples were transferred into a 96-well microtiter plate and optical density was measured at 405 nm using a standard ELISA reader. *P* was calculated with a student's *t*-test (*n* = 3) to detect statistically relevant differences.

2.6. *MSC-derived adipocytes*

Adipogenic culture of MSCs as reported (*17*) was performed to induce differentiation into adipocytes. Briefly, MSCs in the second or third passage were induced to form adipocytes in an adipogenic medium (a-MEM and 10% FBS) for up to 12 days as determined by peak adipogenesis. At that point, the medium was changed to an adipocyte-sustaining medium consisting of high-glucose DMEM with 10 μg/mL insulin and 10% FBS to promote adipocyte maturity. Cultures were analyzed prior to adipogenesis on day 0 and at specific points in time over a period of 25 days.

2.7. *Oil Red O staining*

Cells were fixed with 4% paraformaldehyde for 20 min at 4°C. Cells were rinsed and washed and then stained with Oil Red O solution for 15 min to stain lipid droplets/ vacuoles. Cells in random fields were manually counted and the number in 5 high power fields was averaged.

2.8. *Real-time PCR*

RNA treated with DNase was isolated from MSC-derived osteoblasts and adipocytes, enriched adipofibroblasts, and lipid-laden adipocyte cultures at specific time-points using an RNeasy Mini Kit in accordance with the manufacturer's instructions (Qiagen). Cells were lysed on plates in buffer containing GITC (Buffer RLT). Reverse Transcription was performed immediately after RNA isolation using a Transcriptor First Strand cDNA synthesis kit and oligo-dT primers (Roche, Branchburg, NJ). Real-time PCR was performed using SybrGreen and Taqman technology. Briefly, 10 mL of SybrGreen Master Mix (Applied Biosystems, Darmstadt, Germany) was mixed with 1 mL (10 pg) of forward primer, 1 mL (10 pg) of reverse primer, 6.8 mL of water, and 1.2 mL (60 ng) of template. Levels of expression of the beta-actin gene were used to normalize mRNA expression for real-time PCR. Reactions were performed using the following

conditions: 95°C for 10 min and cycles of 95°C for 15 sec, 55-60°C for 30 sec, and 72°C for 30 sec for 40 cycles. The primers used for each gene were as follows: Runx2: Forward GACAGTCCCAACTTCCTGTG, Reverse GCGGAGTAGTTCTCATCATTC; Osterix: Forward GCTCGTAGATTTCTATCCTC, Reverse CTTAGTGACTGCCTAACAGA; Collagen1: Forward TGACTGGAAGAGCGGAGAGTA, Reverse GACGGCTGAGTAGGGAACAC; Osteocalcin: Forward TGCCTGGCTGGAGATTCTG, Reverse GCTGCTGTGACATCCATACTT; PPARγ: Forward GGAATTAGATGACAGTGACTTGGC, Reverse ATCTTCTGGAGCACCTTGGC; β-actin: Forward CCTCTATGCCAACACAGT, Reverse AGCCACCAATCCACACAG.

2.9. *Statistical analysis*

All values are expressed as the mean ± SEM. Data were analyzed with the aid of SPSS database, and variance was evaluated with one-way ANOVA. Differences were considered significant at *p* < 0.05.

3. Results

3.1. *The effects of DHEA on bone morphology*

Bone volume (BV), bone mineral density (BMD), and the number of trabecules in bone (Tb.N) were lower in the OVX group than in the sham-operated group (*p* < 0.05). Trabecular spacing (Tb.sp) was wider in the OVX group than in the sham-operated group (*p* < 0.05), suggesting that a mouse model of PMO was successfully established. Compared to the OVX group that was treated with saline, the OVX + DHEA and OVX + E2 groups had a higher BV, BMD, and Tb.N and a smaller Tb.sp, suggesting that DHEA and E2 improved bone morphology in mice with osteoporosis (Figure 1).

3.2. *DHEA increases osteoblastogenesis by up-regulating the expression of osteoblastogenesis-related genes*

In osteoblastogenic medium, DHEA promoted MSCs to differentiate into osteoblasts. The ALP activity of osteoblasts was higher in groups treated with DHEA or E2 than that in the control group (*p* < 0.05) (Figure 2A). The number of bone nodules also increased in the groups treated with DHEA or E2 compared to the control group (*p* < 0.05) (Figures 2B and 2C). The expression of mRNA by osteogenesis-related genes was examined using real-time PCR in order to explore the mechanisms by which DHEA regulates MSC differentiation. Compared to the control treatment, DHEA and E2 promoted expression of *collagen I*, *osteocalcin*, *Runx2*, *and osterix*. However, there was no difference in levels of expression in the two groups (Figure 2D).
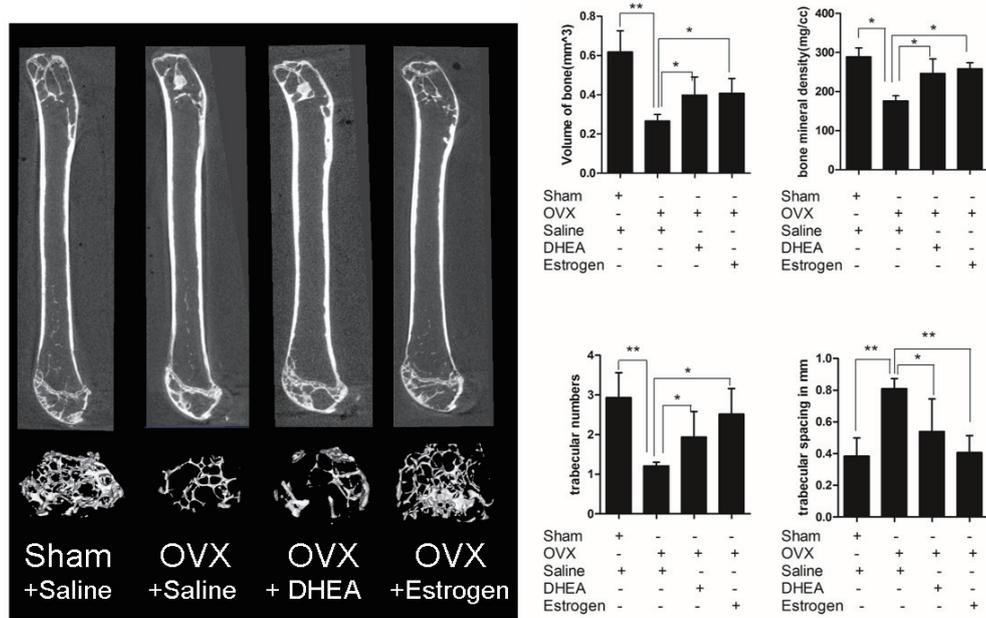
Figure 1. Effects of DHEA on bone morphology in OVX mice. Sham mice underwent mock surgery and received saline. Ovariectomized (OVX) mice underwent bilateral oophorectomy and were randomly divided into three groups: OVX (treated with saline), OVX + DHEA (treated daily with 5 mL of mixed raw herbs [BSNXD] per kg body weight), and OVX + E2 (treated daily with 5 mL of DHEA per kg body weight). Femur samples were harvested after 12 weeks of treatment. Micro-CT was performed to determine the bone morphology in femurs. Bone volume, bone mineral density, the number of trabecules in bone, and trabecular spacing were measured at the original magnification (200×). Data are presented as the mean ± SEM. ($n = 6$). $^{*}p <$ 0.05, $^{**}p < 0.01$ compared to the OVX group.
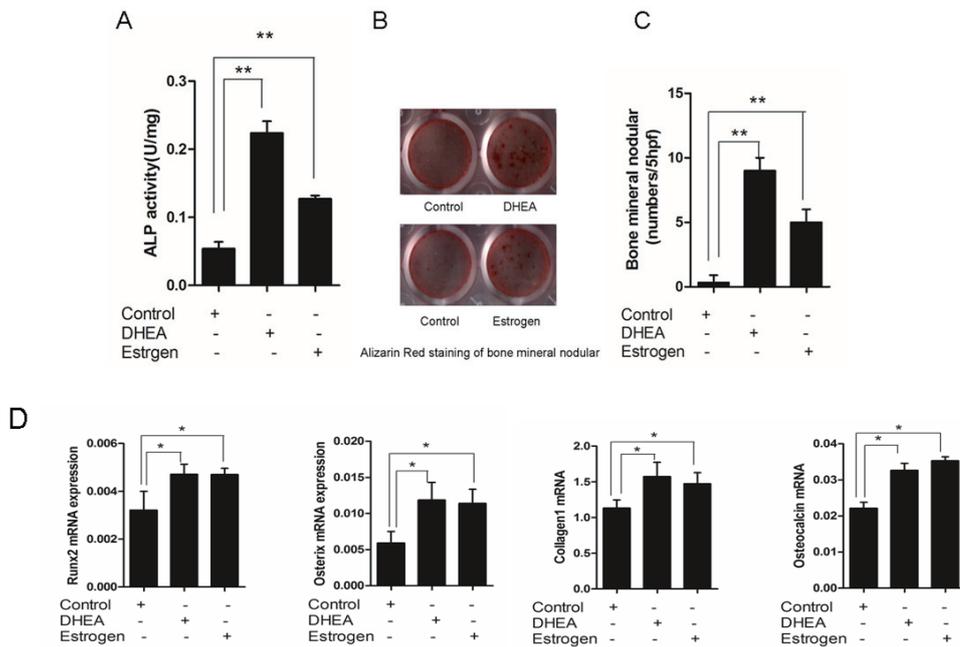
Figure 2. DHEA increased ALP activity and expression of mRNA by osteoblastogenesis-related genes. Primary MSCs were exposed to control serum, 10^{-7} M DHEA, or 10^{-9} M E2 for 48 h under osteoblastogenic conditions. The ALP activity of osteoblasts was determined with a kit to analyze ALP activity after 7 days of culturing (**2A**), alizarin red staining was performed after 21 days of culturing (**2B**), and the number of mineralized bone nodules was counted (**2C**). *Runx2*, *osterix*, *collagen I*, and *osteocalcin* mRNA were analyzed (**2D**). Data are presented as the mean ± SEM. ($n = 6$). $^{*}p < 0.05$, $^{**}p < 0.01$ compared to the control group.

3.3. *DHEA increases the proportion of Foxp3^{+} Tregs in the spleen and enhances osteoblastogenesis*

Immune cells can influence bone metabolism, so this

study determined whether immune cells were affected after DHEA treatment. Changes in spleen-derived immune cells after DHEA treatment were examined first. Compared to the sham-operated group, the OVX
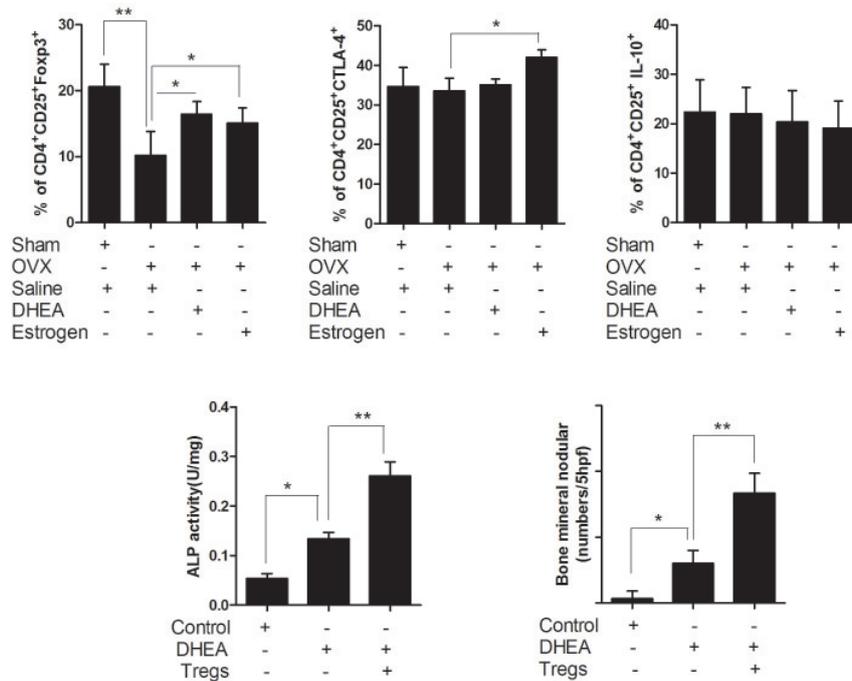
Figure 3. DHEA increased the number of Foxp3$^+$ Tregs, and Tregs enhanced the effects of DHEA on osteoblast differentiation. Sham mice underwent mock surgery and received saline. OVX mice underwent bilateral oophorectomy and were randomly divided into three groups: OVX (treated with saline), OVX + DHEA (treated daily with 5 mL of E2 per kg body weight), and OVX + E2 (treated daily with 5 mL of E2 per kg body weight). Spleen samples were harvested after 12 weeks. Flow cytometry was performed to ascertain immune cells in the spleen. Data are presented as the mean ± SEM. ($n = 6$). * $p < 0.05$, ** $p < 0.01$ compared to the OVX group. Primary MSCs were exposed to control serum, 10^{-7} M DHEA, or 10^{-9} M E2 for 48 h under osteoblastogenic conditions in the presence or absence of Tregs. ALP activity of osteoblasts was determined using a kit to analyze ALP activity. The number of bone nodules was assessed using alizarin red staining. Data are presented as the mean ± SEM. ($n = 6$). * $p < 0.05$, ** $p < 0.01$.

group had fewer Foxp3-positive Tregs. DHEA treatment increased the percentage of Foxp3$^+$ Tregs ($p < 0.05$) while E2 did not. Conversely, E2 treatment increased the percentage of CTLA-4$^+$ Tregs but DHEA did not significantly influence the number of Tregs (Figure 3). MSCs were cultured in the presence or absence of Tregs in order to determine the effects of Tregs on DHEA-mediated differentiation of MSCs. In the presence of Tregs, ALP activity was higher and bone nodular production increased, suggesting that Tregs can enhance the effect of DHEA on differentiation of MSCs (Figure 3).

3.4. *DHEA does not directly affect adipocyte differentiation*

MSCs can differentiate into osteoblasts and adipocytes. Increased numbers of adipocytes indicate a significant risk of PMO developing. MSCs cultured in osteoblastogenic medium and treated with DHEA had increased numbers of adipocytes. However, MSCs cultured in adipogenic medium and treated with DHEA or E2 did not produce different numbers of adipocytes. The transcription factor PPARγ regulates adipogenesis. Expression of this gene was assessed using real-time PCR, and the levels of expression in the group treated with DHEA did not differ from those in the control

group and the group treated with E2 (Figure 4).

4. Discussion

Mature OVX mice were previously used to model postmenopausal bone loss (*18*). Analysis of bone morphology has revealed that OVX mice have significantly reduced bone mass, bone density, and fewer trabeculae in bone as well as significantly wider trabecular spacing compared to sham-operated mice (*19*). These findings were evident in the present study, suggesting that a model of PMO was successfully established.

After treatment with DHEA, the OVX mice had significantly increased bone mass, bone density, and more trabeculae in bone as well as significantly smaller trabecular spacing, suggesting that DHEA significantly improves bone morphology. An improvement in bone morphology can increase the mechanical strength and integrity of bone and affect bone growth, suggesting that DHEA has clinical significance in the prevention and treatment of PMO.

Runx2 and osterix are transcription factors associated with osteoblastogenesis while collagen1 and osteocalcin are genes expressed in osteoblasts; all four of these genes are markers of different stages of bone

MSCs culture in osteoblast induction medium
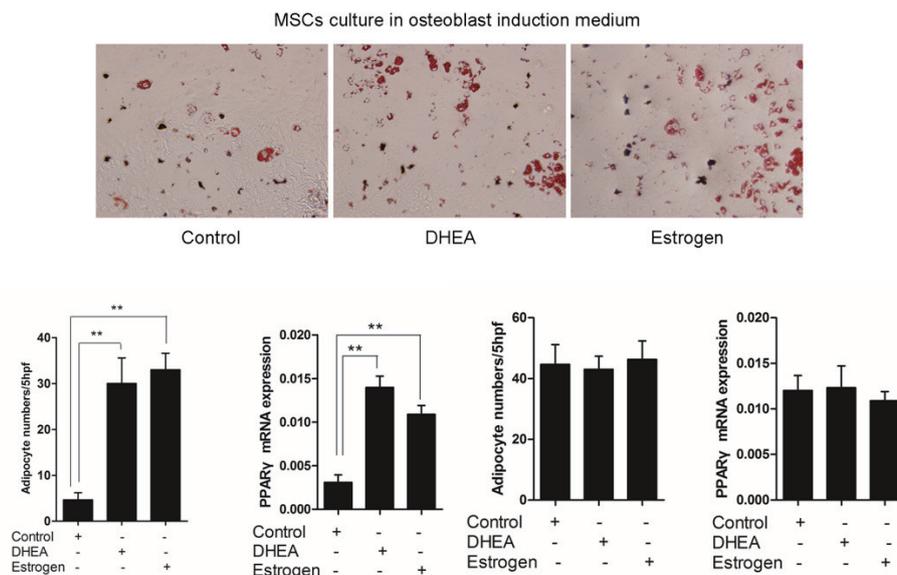
Figure 4. DHEA affected adipocyte differentiation *via* osteoblast production. Primary MSCs were exposed to control serum, 10^{-7} M DHEA, or 10^{-9} M E2 for 48 h under adipogenic conditions. The number of adipocytes was assessed using oil red O staining. Expression of *PPARγ* mRNA was assessed using real-time PCR. Data are presented as the mean ± SEM. ($n = 6$). $*$ $p < 0.05$, $**$ $p < 0.01$ compared to the OVX group.

development (*20-22*). PPARγ is a transcriptional factor that regulates adipogenesis (*23*). Although DHEA increases the number of adipocytes in osteoblastogenic medium, it produces no changes in the number of adipocytes in adipogenic medium (*24-30*).

Tregs affect bone metabolism, and this action is directly regulated by Foxp3 and CTLA-4 or it is indirectly regulated by TGF-β and IL-10 (*31-36*). DHEA can markedly increase the proportion of Foxp3^{+} Tregs and encourage osteoblast differentiation to prevent PMO. DHEA does not affect the ratio of CTLA 4[+] or IL-10^{+} Tregs, suggesting that DHEA plays a role on osteoblast differentiation *via* Foxp3.

In a previous study, the current authors found that DHEA significantly promoted proliferation and inhibited apoptosis of osteoblast *via* mitogen-activated protein kinase signaling pathways independent of either androgen receptors or estrogen receptors, suggesting that it may play a direct role *via* a DHEA-specific receptor instead of *via* conversion to androgens or estrogens (*6*).

Results of *in vivo* and *ex vivo* experiments revealed that DHEA can directly promote differentiation of MSCs into osteoblasts. DHEA increased the expression of Runx2, Collagen1, Osterix, and Osteocalcin mRNA, increasing the ALP activity of osteoblasts and the number of mineralized bone nodules. DHEA increases the number of Foxp3^{+} Tregs, increasing osteoblast differentiation. Therefore, DHEA is likely to be an ideal solution to prevent and treat PMO.

Acknowledgements

References

1. Wang L, Hao Q, Wang YD, Wang WJ, Li DJ. Protective effects of dehydroepiandrosterone on atherosclerosis in ovariectomized rabbits *via* alleviating inflammatory injury in endothelial cells. Atherosclerosis. 2011; 214:47-57.
2. El Maghraoui A, Rezqi A, El Mrahi S, Sadni S, Ghozlani I, Mounach A. Osteoporosis, vertebral fractures and metabolic syndrome in postmenopausal women. BMC Endocr Disord. 2014; 14:93.
3. Caputo EL, Costa MZ. Influence of physical activity

on quality of life in postmenopausal women with osteoporosis. Rev Bras Reumatol. 2014; 54:467-473.
4. Hoshiba T, Kawazoe N, Chen G. The balance of osteogenic and adipogenic differentiation in human mesenchymal stem cells by matrices that mimic stepwise tissue development. Biomaterials. 2012; 33:2025-2031.
5. Hwang NS, Varghese S, Elisseeff J. Controlled differentiation of stem cells. Adv Drug Deliv Rev. 2008; 60:199-214.
6. Wang L, Wang YD, Wang WJ, Li DJ. Differential regulation of dehydroepiandrosterone and estrogen on bone and uterus in ovariectomized mice. Osteoporos Int. 2009; 20:79-92.
7. Wang L, Wang YD, Wang WJ, Zhu Y, Li DJ. Dehydroepiandrosterone improves murine osteoblast growth and bone tissue morphometry *via* mitogen-activated protein kinase signaling pathway independent of either androgen receptor or estrogen receptor. J Mol Endocrinol. 2007; 38:467-79.
8. Wang YD, Wang L, Li DJ, Wang WJ. Dehydroepiandrosterone inhibited the bone resorption through the upregulation of OPG/RANKL. Cell Mol Immunol. 2006; 3:41-46.
9. Faienza MF, Ventura A, Marzano F, Cavallo L. Postmenopausal osteoporosis: The role of immune system cells. Clin Dev Immunol. 2013; 2013:575936.
10. Danks L, Takayanagi H. Immunology and bone. J Biochem. 2013; 154:29-39.
11. Dziak R. Osteoimmunology: Cross-talk between bone and immune cells. Immunol Invest. 2013; 42:657-660.
12. Yin G, Wen FQ. Immune mediated inflammatory pathogenesis and assessment of disease activity in rheumatoid arthritis. Sichuan Da Xue Xue Bao Yi Xue Ban. 2015; 46:267-271.
13. Yuan FL, Li X, Lu WG, Xu RS, Zhao YQ, Li CW, Li JP, Chen FH. Regulatory T cells as a potent target for controlling bone loss. Biochem Biophys Res Commun. 2010; 402:173-176.
14. Cuijpers VM, Alghamdi HS, Van Dijk NW, Jaroszewicz J, Walboomers XF, Jansen JA. Osteogenesis around CaP-coated titanium implants visualized using 3D histology and micro-computed tomography. J Biomed Mater Res A. 2015; 103:3463-3473.
15. Costa-Pinto AR, Correlo VM, Sol PC, Bhattacharya M, Charbord P, Delorme B, Reis RL, Neves NM. Osteogenic differentiation of human bone marrow mesenchymal stem cells seeded on melt based chitosan scaffolds for bone tissue engineering applications. Biomacromolecules. 2009; 10:2067-2073.
16. Vater C, Kasten P, Stiehler M. Culture media for the differentiation of mesenchymal stromal cells. Acta Biomater. 2011; 7:463-477.
17. Nuttall ME, Gimble JM. Controlling the balance between osteoblastogenesis and adipogenesis and the consequent therapeutic implications. Curr Opin Pharmacol. 2004; 4:290-294.
18. Hempel E, Günther P, Neumann G, Müller B. Experimental studies on the castration osteoporosis in the rat. II. Behavior of bone minerals. Zentralbl Gynakol. 1978; 100:1391-1398.
19. Tuomikoski P, Ylikorkala O, Mikkola TS. Postmenopausal hot flushes and bone mineral density: A longitudinal study. Acta Obstet Gynecol Scand. 2015; 2:198-203.
20. Kahler RA, Yingst SM, Hoeppner LH, Jensen ED, Krawczak D, Oxford JT, Westendorf JJ. Collagen 11a1

is indirectly activated by lymphocyte enhancer-binding factor 1 (Lef1) and negatively regulates osteoblast maturation. Matrix Biol. 2008; 27:330-338.
21. Lu X, Gilbert L, He X, Rubin J, Nanes MS. Transcriptional regulation of the osterix (Osx, Sp7) promoter by tumor necrosis factor identifies disparate effects of mitogen-activated protein kinase and NF kappa B pathways. J Biol Chem. 2006; 281:6297-6306.
22. Viereck V, Siggelkow H, Tauber S, Raddatz D, Schutze N, Hüfner M. Differential regulation of Cbfa1/Runx2 and osteocalcin gene expression by vitamin-D3, dexamethasone, and local growth factors in primary human osteoblasts. J Cell Biochem. 2002; 86:348-356.
23. Duque G. Will reducing adopogenesis in bone increase bone mass?: PPARgamma2 as a key target in the treatment of age-related bone loss. Drug News Perspect. 2003; 16:341-346.
24. Cao JJ. Effects of obesity on bone metabolism. J Orthop Surg Res. 2011; 6:30.
25. Colaianni G, Brunetti G, Faienza MF, Colucci S, Grano M. Osteoporosis and obesity: Role of Wnt pathway in human and murine models. World J Orthop. 2014; 5:242-246.
26. Rosen CJ, Bouxsein ML. Mechanisms of disease: Is osteoporosis the obesity of bone? Nat Clin Pract Rheumatol. 2006; 2:35-43.
27. Foresta C, Strapazzon G, De Toni L, Gianesello L, Calcagno A, Pilon C, Plebani M, Vettor R. Evidence for osteocalcin production by adipose tissue and its role in human metabolism. J Clin Endocrinol Metab. 2010; 95:3502-3506.
28. Maurin AC, Chavassieux PM, Frappart L, Delmas PD, Serre CM, Meunier PJ. Influence of mature adipocytes on osteoblast proliferation in human primary cocultures. Bone. 2000; 26:485-489.
29. Ali AT, Penny CB, Paiker JE, van Niekerk C, Smit A, Ferris WF, Crowther NJ. Alkaline phosphatase is involved in the control of adipogenesis in the murine preadipocyte cell line, 3T3-L1. Clin Chim Acta. 2005; 354:101-109.
30. Ikeda K, Takeshita S. Factors and mechanisms involved in the coupling from bone resorption to formation: How osteoclasts talk to osteoblasts. J Bone Metab. 2014; 21:163-167.
31. Zhang Y, Khan D, Delling J, Tobiasch E. Mechanisms underlying the osteo- and adipo-differentiation of human mesenchymal stem cells. Scientific World Journal. 2012; 2012:793823.
32. Luo C, Wang L, Sun C, Li Dj. Estrogen enhances the functions of CD4^{+}CD25^{+}Foxp3^{+} regulatory T cells that suppress osteoclast differentiation and bone resorption *in vitro*. Cell Mol Immunol. 2010; 1:50-8.
33. Churlaud G, Pitoiset F, Jebbawi F, Lorenzon R, Bellier B, Rosenzwajg M, Klatzmann D. Human and mouse CD8^{+}CD25^{+}FOXP3^{+} regulatory T cells at steady state and during interleukin-2 therapy. Front Immunol. 2015; 6:171.
34. Ligeiro de Oliveira AP, Peron JP, Santos Franco AL, Golega BA, Paula Vieira R, Ibanez OC, Ribeiro OG, Cabrera WH, De Franco M, Oliveira-Filho RM, Rizzo LV, Vargaftig BB, de Lima WT. Ovariectomized OVA-sensitized mice display increased frequency of CD4^{+} Foxp3^{+} T regulatory cells in the periphery. PLoS One. 2013; 8:e65674.
35. Liu JC, Zhou CH, Zhang X, Chen Y, Xu BL, Cui L, Xu DH. Effect of 1,25-dihydroxyvitamin D-3 on regulatory

T cells in ovariectomized mice. Biomedical and Environmental Sciences. 2014; 27:779-785.

36. Zaiss MM, Frey B, Hess A, Zwerina J, Luther J, Nimmerjahn F, Engelke K, Kollias G, Hünig T, Schett G, David JP. Regulatory T cells protect from local and systemic bone destruction in arthritis. J Immunol. 2010; 184:7238-7246.

315

Original Article

Protective effect of oleanolic acid on oxidized-low density lipoprotein induced endothelial cell apoptosis

Jianhua Cao[1], Guanghui Li[1], Meizhi Wang[2], Hui Li[1], Zhiwu Han[2,*]

[1] *Department of Pharmacy, the Third People's Hospital of Qingdao, Qingdao, China;*
[2] *Department of Pharmacology, the Affiliated Hospital of Medical College, Qingdao University, Qingdao, China.*

Summary	Oleanolic acid (3β-hydroxyolean-12-en-28-oic acid, OA) is a naturally-occurring triterpenoid with various promising pharmacological properties. The present study was conducted to determine the protective effects of OA against oxidized low-density lipoprotein (ox-LDL) induced endothelial cell apoptosis and the possible underlying mechanisms. Our results showed that ox-LDL significantly decreased cell viability and induced apoptosis in human umbilical vein endothelial cells (HUVECs). OA in the co-treatment showed a protective effect against ox-LDL induced loss in cell viability and an increase in apoptosis, which was associated with the modulating effect of OA on ox-LDL induced hypoxia-inducible factor 1α (HIF-1α) expression. Moreover, our results showed that the modulating effect of OA against ox-LDL induced HIF-1α expression was obtained via inhibition of lipoprotein receptor 1 (LOX-1)/reactive oxygen species (ROS) signaling. Collectively, we suggested that the protective effect of OA against ox-LDL induced HUVEC apoptosis might, at least in part, be obtained via inhibition of the LOX-1/ROS/HIF-1α signaling pathway.

Keywords: Hypoxia-inducible factor 1α (HIF-1α), lipoprotein receptor 1 (LOX-1), reactive oxygen species (ROS)

1. Introduction

Dysfunction of vascular endothelial cells (EC) is now believed to play an important role in the pathogenesis of atherosclerosis (AS) (*1*). A number of studies have showed that EC apoptosis functions as an initiating step for AS by inducing atherosclerotic lesion formation and plaque shedding (*2,3*). Oxidized low-density lipoprotein (ox-LDL), an essential atherosclerotic risk factor, has been found to play a crucial role in multiple functional alternations occurring during the pathogenesis of AS, including enhancing EC apoptosis (*4,5*). Therefore, inhibition of ox-LDL induced EC apoptosis may have therapeutic significance in the prevention and treatment of AS.

The mechanism of ox-LDL induced apoptosis was thought to be related to ox-LDL elicited reactive oxygen species (ROS) release through lipoprotein receptor (LOX), which in turn up-regulates the transcription factor hypoxia-inducible factor 1 (HIF-1) (*6,7*). In recent years, oleanolic acid (3β-hydroxyolean-12-en-28-oic acid), a naturally-occurring triterpenoid with widespread distribution in many fruits and plants like apple, grape, date, pomegranate and olive oil, is attracting much attention for its various pharmacological properties, such as hepatoprotective, vasorelaxant, antiproliferative, anti-inflammatory and apoptosis-inducing effects in various cancerous tissues (*8,9*). Notably, a synthetic triterpenoid analog of oleanolic acid has been shown to have a potent antioxidative effect by inducing NADH-quinone oxidoreductase and heme oxygenase 1 (*10*). However, the effect of OA against ox-LDL induced apoptosis in EC remains largely unknown.

In this study, we used human umbilical vein endothelial cells (HUVECs) to investigate the effects of OA on ox-LDL induced cytotoxicity in HUVECs and the relevant underlying mechanisms.

*Address correspondence to:
Dr. Zhiwu Han, Department of Pharmacology, the Affiliated Hospital of Medical College, Qingdao University, Qingdao 266003, China.
E-mail: drzhiwuhan@163.com

2. Materials and Methods

2.1. *Cell culture*

HUVEC cells were purchased from ATCC (Manassas, VA, USA) and cultured in F-12K medium (ATCC, VA, USA) containing 10% fetal bovine serum (FBS, Gibco BRL Co.Ltd., Grand Island, NY, USA), 1% antibiotic-antimycotic solution (Gibco BRL Co.Ltd., Grand Island, NY, USA), 0.1 mg/mL heparin(Sigma. St. Lious, MO, USA), and 0.03 mg/mL endothelial cell growth supplement (Sigma. St. Lious, MO, USA) under an atmosphere of 5% CO_2 at 37°C. The cells were subcultured and split 1:4 every 4 days.

2.2. *Cytotoxicity assay*

A viability assay was performed using a trypan blue exclusion method described previously (*11*). Briefly, HUVEC (2×10^5 cells) were cultured in 24-well tissue culture plates (Corning-Costar, Cambridge, MA, USA). After drug administration, cells were trypsinized with 0.1% trypsin-EDTA (Gibco-BRL, Grand Island, NY, USA). Following centrifugation and washing, HUVECs were suspended in PBS and stained with trypan blue dye (Sigma, St Louis, MO, USA). Fractions of dead cells with a blue signal were visualized and counted using a reverse phase microscope (Nikon, Tokyo, Japan).

2.3. *Analysis of apoptotic cells*

Apoptotic cells were determined according to the method of Tai *et al.* (*12*). After drug treatment, HUVECs were harvested and fixed in cold 80% ethanol. Following a process of centrifugation and washing, fixed cells were stained with propidium iodide (Sigma. St. Lious, MO, USA) and analyzed using a FACS flow cytometer (Beckman Coulter Inc., Brea, CA, USA) on the basis of a 560-nm dichromic mirror and a 600-nm bandpass filter.

2.4. *Immunoblotting*

HUVEC cells in logarithmic growth phase were used and plated in 60 mm dishes at a density of 2×10^5 cells/well and were cultured overnight at 37°C under 5% CO_2. The cells were treated, harvested and lysed as described previously. Briefly, the cells were washed twice with ice-cold PBS and lysed in lysis buffer (25 mmol/L Tris/HCl pH 7.5, 25 mmol/L NaCl, 0.5 mmol/L EGTA, 10 mmol/L NaF, 20 mmol/L h-glycerophosphate, 1 mmol/L Na_3VO_4, 1 mmol/L PMSF, and 10 mg/mL aprotinin) (Sigma. St. Lious, MO, USA) at 4°C. After sonication and centrifugation at 15,000 rpm, the supernatant was used for immunoblotting. The lysate (20 μg protein per lane) was separated on 12% SDS-polyacrylamide gel (Sigma. St. Lious, MO, USA), electroblotted onto nitrocellulose membrane (Millipore, Billerica, MA, USA) and incubated with specific primary antibodies (Cell Signaling Technology, Inc., Boston, MA. USA). The antibodies were probed with a horseradish peroxidase-linked secondary antibody (Cell Signaling Technology, Inc, Boston, MA. USA) using an enhanced chemiluminescence system (Amersham Pharmacia Biotech, Shinjuku-ku, Tokyo). Densitometric analysis was performed using an image scanner and analyzing software. The rabbit polyclonal antibody to β-actin (Cell Signaling Technology, Inc, Boston, MA. USA) was used as a gel loading control.

2.5. *Silencing HIF-1α with shRNA and overexpression of HIF-1α*

For silencing HIF-1α, the HIF-1α-targeting shRNA (Sense sequence: GATCCCGCACAGTTACAGTA TTCCATCAAGAGTGGAATACTGTGCTTTTTT; Antisense sequence: CTAGAAAAAAGCACAGTT ACAGTATTCCACTCTTGATGGAATACTGTAAC TGTGCGG) was inserted into pGE-1 plasmid (pGE-1 PredigestedCloning Kit, Agilent Technologies Inc., Shanghai, China) after cutting with restriction enzymes BamH I and Xba I. Scrambled shRNA was used as a negative control. Transfection of the cells with shRNA was performed following the standard protocol. Briefly, the cells were plated at a density of 5×10^3 cells/well in a 6-well culture plate and incubated to allow 70-80% confluence (about 24 h). The cells were then starved in serum-free culture for 1 h. The transfection mixture containing HIF-1α-targeting shRNA and Lipofectamine 2000 reagent (Invitrogen, Carlsbad, CA, USA) was incubated for 20 min at room temperature. The cells were then incubated with the above mixture for 5 h at 37°C in a humidified atmosphere containing 5% CO_2. Subsequently, the cells were washed with PBS and maintained in DMEM containing 10% FBS for 48 h. The expression of HIF-1α was detected by Western blot analysis.

Based on the human HIF-1α sequence, primers (Sense primer: GCGGATCCAACGTCGAAAAGAAA AGTCTCG; Antisense primer: GCTCTAGAAAGTTTG TGCAGTATTGTAGCC) were designed to obtain the HIF-1α sequence. Then the PCR product was cut with restriction enzymes BamH I and Xba I before cloning into pEGFP-N1 vector (Takara Biomedical Technology Co., Ltd., Beijing, China). For HIF-1α overexrepression, the HUVECs were grown to sub-confluent densities and transfected with pEGFP-N1 empty or pEGFP-N1-HIF-1α vector (Takara Biomedical Technology Co., Ltd., Beijing, China) constructs using the transfection reagent TransIT-LT-1 and following manufacturer's instructions (Mirus Bio Corp., Madison, WI, USA). Overexpression of HIF-1α was confirmed by Western blots.

2.6. *LOX-1 knockdown and LOX-1 overexpression*

LOX-1 knockdown was performed using an RNA interference (RNAi) synthesized based on a previously published sequence (Sense: CCCTTCAGGTACCTGTGCATATATA) following a siRNA transfection protocol provided by Santa Cruz Biotechnology (Santa Cruz, CA, USA) (*13*). Briefly, after culturing HUVECs in antibiotic free Dulbecco's modified Eagle's medium at 37°C in a humidified atmosphere of 5% CO_2 for 24 h, the siRNA duplex solution was added to HUVECs. After transfection for 24 h, the medium was replaced with normal Dulbecco's modified Eagle's medium (Sigma, St. Lious, MO, USA), and HUVECs were treated with OA, ox-LDL, or a combination of OA and ox-LDL.

To generate LOX-1 overexpression vectors, CDS region of LOX-1-coding sequences were obtained by RT-PCR and cloned into pEGFP-N1 vector (Takara Biomedical Technology Co., Ltd., Beijing, China). The resulting plasmid was named pEGFP-N1- LOX-1. HUVECs were transfected with pEGFP-N1-LOX-1 vector to induce excessive LOX-1 expression or pEGFP-N1 vector to generate stable clones expressing LOX-1 constitutively as control.

2.7. *Quantitative RT-PCR (qRT-PCR)*

Total RNA was extract from cells using RNA simple Total RNA Kit (TIANGEN Co., Beijing, China) and 3 μg of RNA was converted into cDNA using the High Capacity cDNA Archive Kit (Applied Biosystems, Foster City, CA, USA). For detection of LOX-1 mRNA the primers used were: upstream 5'-CTGCCAGCCTGAAGTCCATT-3' and downstream 5'-TCTGTCTGTCTGTCCGTAAGTG-3', with an amplified fragment of 340 bp. The synthesis of the primers used for HIF-1α was based on the published sequence (*14*). For each PCR reaction, a master mix that including SYBR GREEN mastermix (Solarbio Co., Beijing, China), forward primer, reverse primer, and 10 ng template cDNA was prepared. The PCR conditions were 5 min at 95°C followed by 40 cycles of 95°C for 30 s, 60°C for 30 s, and 72°C for 30 s. Data were analyzed using the comparative ΔCt method (ABPrism software, Applied Biosystems, Foster City, CA) using GAPDH as an internal normalization control.

2.8. *Detection of intracellular ROS detection*

Intracellular ROS level was measured by oxidation-sensitive fluorescent dye 2,7-dichlorodihydrofluorescein diacetate (DCF-DA) (Invitrogen, Carlsbad, CA, USA) method. Briefly, after washing once with PBS, treated cells were incubated with 20 μM DCF-DA in serum-free DMEM at 37°C for 30 min before analysis.

2.9. *Statistical analysis*

All statistical analysis was performed using PASW Statistical software (version 18.0 for Windows). Values are presented as the mean ± S.D. Statistical comparisons were performed by one-way ANOVA. Tukey's post hoc test was used for multiple group comparisons and Student's *t*-test was used for single comparisons. $p < 0.05$ was considered to be statistically significant.

3. Results

3.1. *Effects of OA on ox-LDL induced cytotoxicity in HUVECs*

We first examined the cytotoxicity of OA (Melone Biotech, Ltd., Dalian, China, Purity ≥ 98%) on HUVECs. Our results showed that incremental doses of OA treatment for 24 h did not affect HUVECs cell viability until 25 μM ($p < 0.05$ *vs.* control) (Figure 1A). Meanwhile, ox-LDL treatment for 24 h resulted in a dose-dependent decrease in cell viability, 100 μg/mL ox-LDL led to 49% reduction (Figure 1B). Therefore 100 μg/mL ox-LDL was chosen for the following experiments. Then the effect of ox-LDL and OA co-treatment was examined. We found OA at 1, 5, and 10 μM lowered the ox-LDL-caused decrease in viability of HUVECs by 5%, 12%, and 29%, respectively (Figure 1C).

3.2. *Effect of OA on ox-LDL induced apoptosis in HUVECs*

Apoptosis of HUVECs was analyzed by flow cytometry. As shown in Figure 2A, treatment of HUVECs with 100 μg/mL ox-LDL for 24 h increased the apoptotic cell population up to 31% while OA at 1, 5, and 10 μM significantly lowered the ox-LDL-induced apoptosis of HUVECs by 5%, 12%, and 21%, respectively (Figure 2A). In addition, activation of caspase-3 and PARP was also examined in HUVECs following treatments, which also showed OA treatment at 10 μM significantly attenuated the ox-LDL-induced apoptosis (Figure 2B).

3.3. *Effect of OA on ox-LDL induced HIF-1α*

It has been shown that HIF-1α is involved in regulatory pathways that leads to the activation of several transcription factors and to the release of cytokines and growth factors from endothelial cells (*6*). Therefore, we postulated that the protective effect of OA on ox-LDL induced apoptosis in HUVECs may be through modulating the HIF-1α related pathway. To confirm our postulation, the expression of HIF-1α was examined by Western blot. As shown in Figure 3A, ox-LDL treatment resulted in a dose-dependent increase of HIF-1α expression in HUVECs, while co-treatment
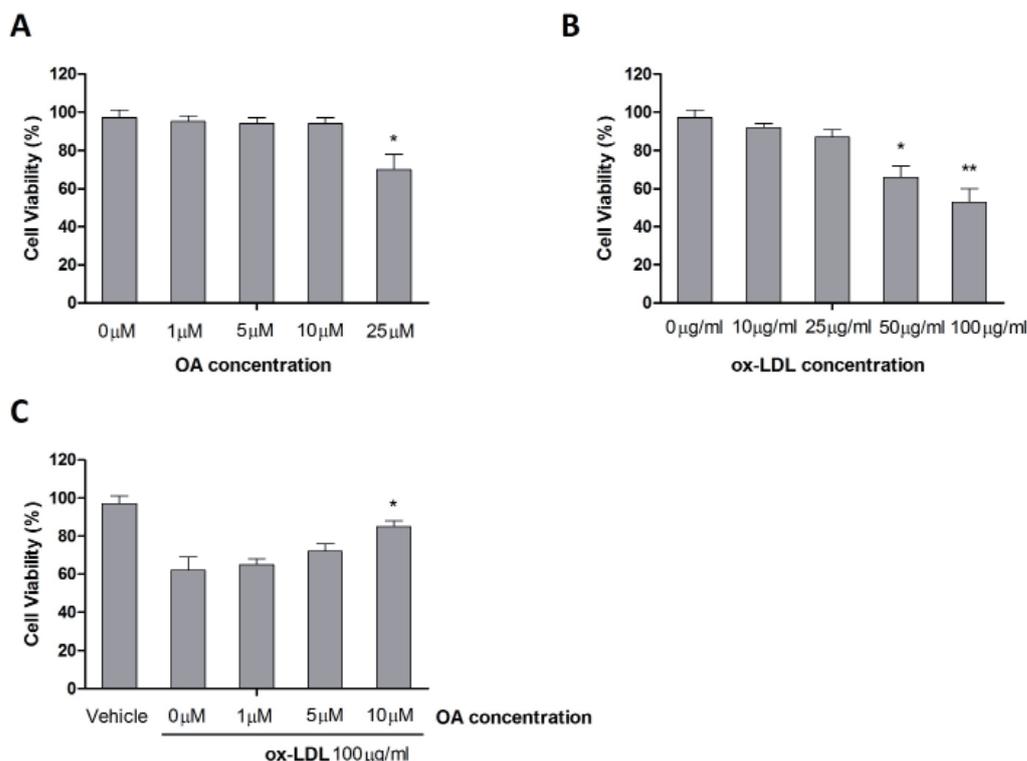
Figure 1. OA suppresses ox-LDL-induced loss of cell viability in HUVECs. (A), Effect of OA on cell viability of HUVECs. **(B)**, Effect of ox-LDL on cell viability of HUVECs. **(C)**, Suppressive effect of OA on ox-LDL-induced loss of cell viability in HUVECs. * $p < 0.05$ *vs.* control, ** $p < 0.01$ *vs.* control.
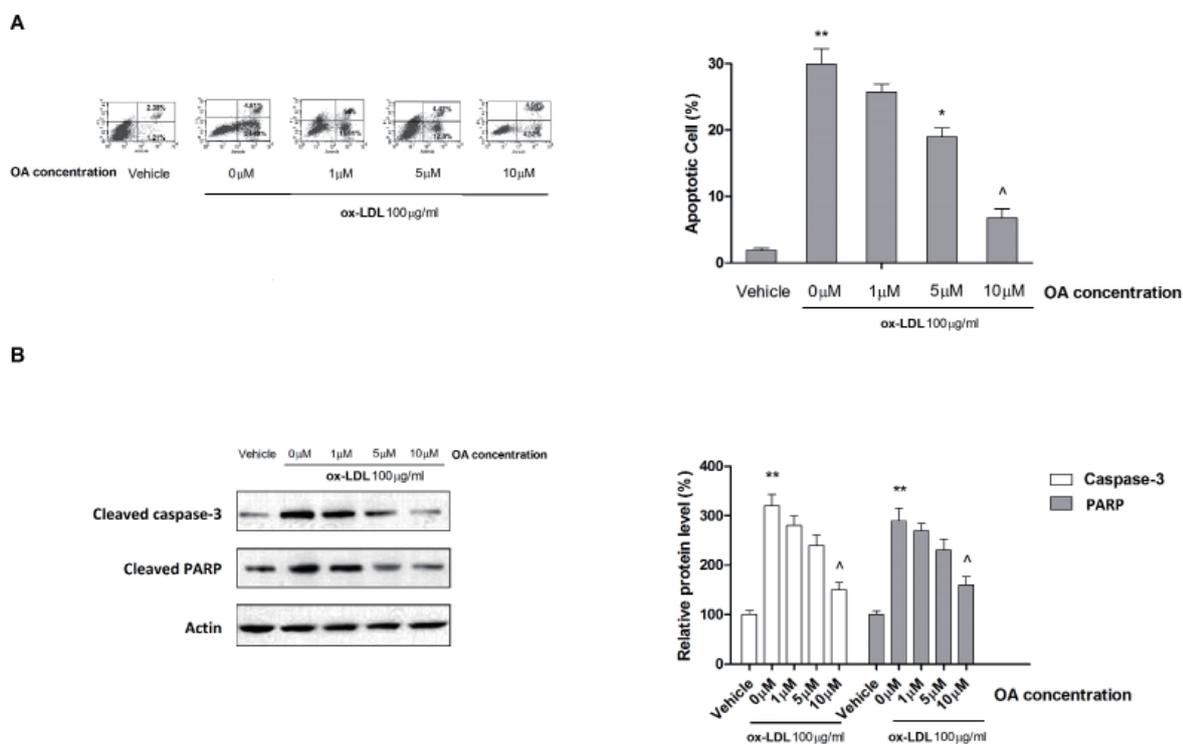
Figure 2. OA protects ox-LDL-induced apoptosis in HUVECs. (A), Suppressive effect of OA on ox-LDL-induced apoptosis in HUVECs. **(B)**, Suppressive effect of OA on ox-LDL-induced activation of caspase-3 and PARP in HUVECs. * $p < 0.05$ *vs.* control, ** $p < 0.01$ *vs.* control, ^ $p < 0.05$ *vs.* ox-LDL.

with OA caused a dose-dependent decrease of HIF-1α expression, suggesting that OA attenuates ox-LDL induced enhancement in HIF-1α expression (Figure

3B). To further demonstrate the association between HIF-1α expression and ox-LDL-induced apoptosis, the expression of HIF-1α was manipulated with siRNA and
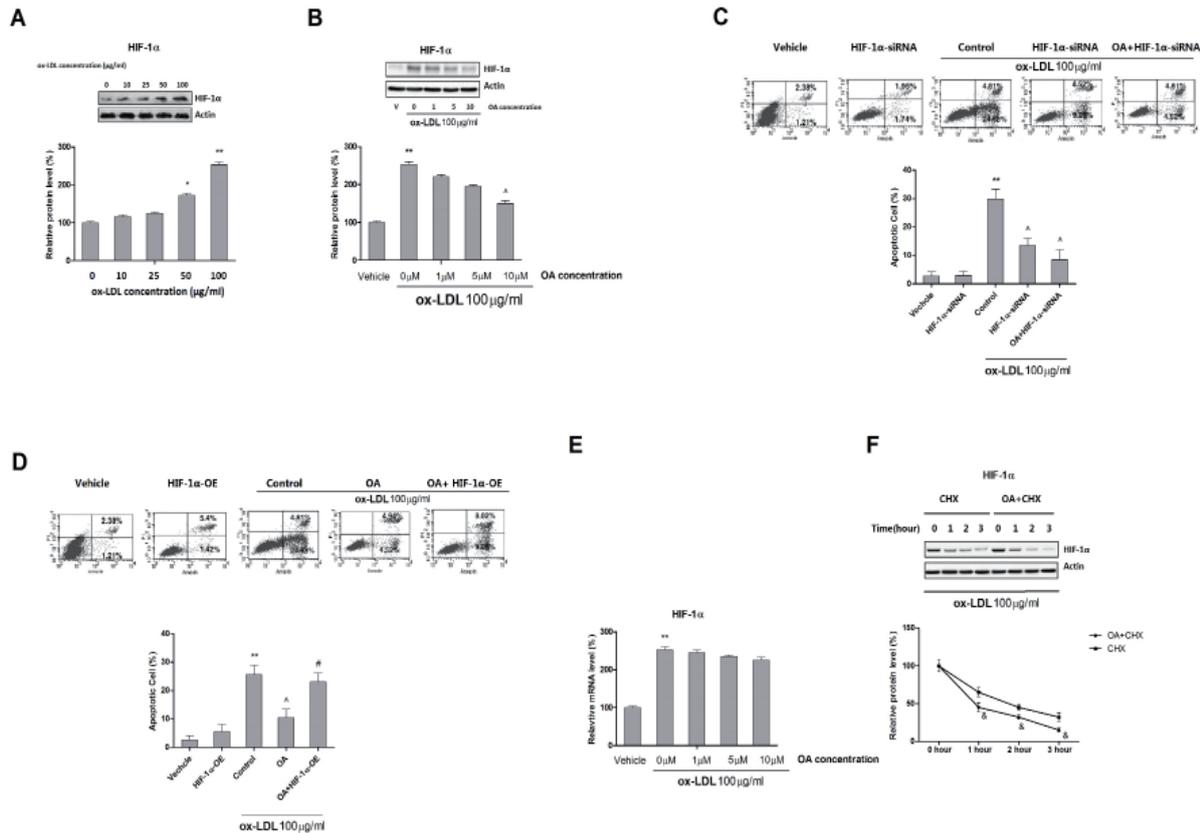
Figure 3. Protection of OA against ox-LDL-induced apoptosis is mediated by downregulation of HIF-1α. (A), Effect of ox-LDL on HIF-1α expression in HUVECs. **(B)**, Effect of OA on ox-LDL-induced HIF-1α expression. **(C)**, Effect of HIF-1α knockdown on ox-LDL-induced apoptosis and the protection of OA against ox-LDL-induced apoptosis. **(D)**, Effect of HIF-1α overexpression on ox-LDL-induced apoptosis and the protection of OA against ox-LDL-induced apoptosis. **(E)**, Effect of OA on ox-LDL-induced HIF-1α mRNA expression. **(F)**, Effect of OA on HIF-1α degradation. * $p < 0.05$ *vs.* control, ** $p < 0.01$ *vs.* control, ^ $p < 0.05$ *vs.* ox-LDL, # $p < 0.05$ *vs.* ox-LDL+OA, & $p < 0.05$ *vs.* CHX.

overexpressing plasmid. As shown in Figure 3C, siRNA targeting HIF-1α alone did not cause significant change in apoptotic cells while it significantly attenuated ox-LDL-induced HUVEC apoptosis and co-treatment with OA and HIF-1α siRNA synergistically reduced ox-LDL caused cell apoptosis. In comparison, overexpression of HIF-1α alone in HUVECs slightly affected cell apoptosis but almost completely attenuated OA-involved protection against ox-LDL induced apoptotic insults (Figure 3D).

We further examined the expression level of HIF-1α mRNA during co-treatment and found that, contrary to the protein expression pattern, which was suppressed in a dose-dependent manner by OA, the expression of HIF-1α mRNA remained unchanged even with the highest concentration of OA (Figure 3E). We then examined the involvement of the proteasomal degradation of HIF-1α in HUVECs treated by using cycloheximide (CHX, a translational inhibitor). Following incubation with ox-LDL for 24 hours, HUVECs cells were challenged with CHX alone or in combination with OA for 0, 1, 2, and 3 h. As shown in Figure 3F, our results revealed that HIF-1α protein degradation rate was significantly increased in cells treated with both OA and CHX, which indicated that OA interfered with the stabilization of HIF-1α in

HUVECs. Collectively, our results showed that OA modulated ox-LDL induced HIF-1α expression by both suppressing translation and promoting degradation.

3.4. Involvement of ROS in the modulating effect of OA on ox-LDL-induced HIF-1α

Recent evidence has showed that HIF-1α can be induced by free radicals, especially ROS, and a number of studies have established that ROS generation was closely associated with ox-LDL induced endothelial cell apoptosis (*15-17*). Based on these previous studies, we explored the effect of OA on ox-LDL-induced ROS generation and the association between ROS and HIF-1α expression. Our results showed that OA alone did not cause significant change in ROS level in HUVECs while ox-LDL treatment resulted in ROS generation in a dose-dependent manner (Figure 4A). When ox-LDL (100 µg/mL) and OA (10 µM) were used in combination, OA was able to significantly attenuate ox-LDL induced ROS generation (Figure 4B). To further demonstrate the association between ROS generation and HIF-1α, ROS inducer ($CoCl_2$) and inhibitor NAC were employed. We found that NAC, serving as a positive control, was able to significantly downregulate
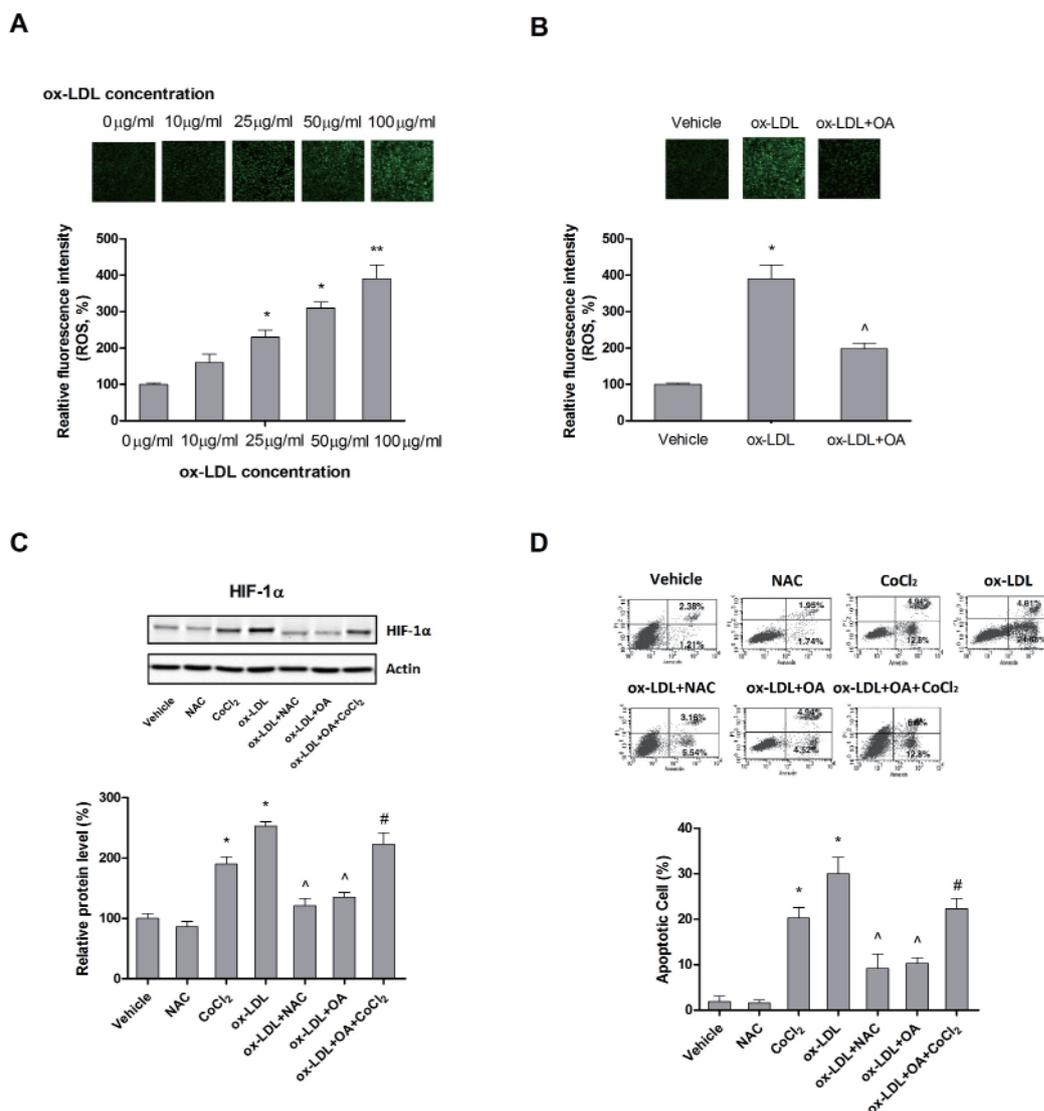
Figure 4. ox-LDL enhances HIF-1α expression by accumulating intracellular ROS. (A), Effect of ox-LDL on intracellular ROS in HUVECs. **(B)**, Effect of OA on ox-LDL-induced ROS accumulation. **(C)**, Effect of ROS inducer ($CoCl_2$) and inhibitor (NAC) on ox-LDL-induced HIF-1α expression and the attenuating role of OA in ox-LDL-induced HIF-1α expression. **(D)**, Effect of ROS inducer ($CoCl_2$) and inhibitor (NAC) on ox-LDL-induced apoptosis and the protection of OA against ox-LDL-induced apoptosis. * $p < 0.05$ *vs.* control, ** $p < 0.01$ *vs.* control, ^ $p < 0.05$ *vs.* ox-LDL, # $p < 0.05$ *vs.* ox-LDL+OA.

ox-LDL induced HIF-1α expression. In contrast, $CoCl_2$ was able to significantly elevate the level of HIF-1α and the combination of OA and $CoCl_2$ significantly abolished the attenuating effect of OA on ox-LDL-induced HIF-1α expression. Moreover, the effect of both NAC and $CoCl_2$ on ox-LDL-induced apoptosis was also examined. Our results showed that NAC, similar to OA, significantly attenuated ox-LDL-induced HUVEC apoptosis while $CoCl_2$ significantly abrogated the protective effect of OA against ox-LDL-induced HUVEC apoptosis.

3.5. *Modulation of OA on LOX-1 mRNA and protein expression*

LOX-1 is expressed in endothelial cells and activation of LOX-1 promotes intracellular ROS accumulation

(18,19). Given the fact that OA can modulate ox-LDL-induced intracellular ROS generation, we investigated the effect of OA on ox-LDL-induced LOX-1 expression. As shown in Figure 5A, after administration of ox-LDL, the expression of Lox-1 mRNA was enhanced by approximately 3-fold whereas OA decreased ox-LDL-induced Lox-1 mRNA production in a dose-dependent manner. Similar results were obtained when the effect of OA on LOX-1 protein level was analyzed (Figure 5B). The involvement of LOX-1 in the modulation of ROS and protective effect of OA against ox-LDL-induced apoptosis was further investigated by LOX-1 targeting siRNA and LOX-1 overexpressing plasmid. In the HUVECs with LOX-1 knockdown, siRNA targeting LOX-1 by itself did not affect apoptosis or ROS accumulation in HUVECs (Figure 5C and 5D). However, LOX-1 siRNA significantly decreased the
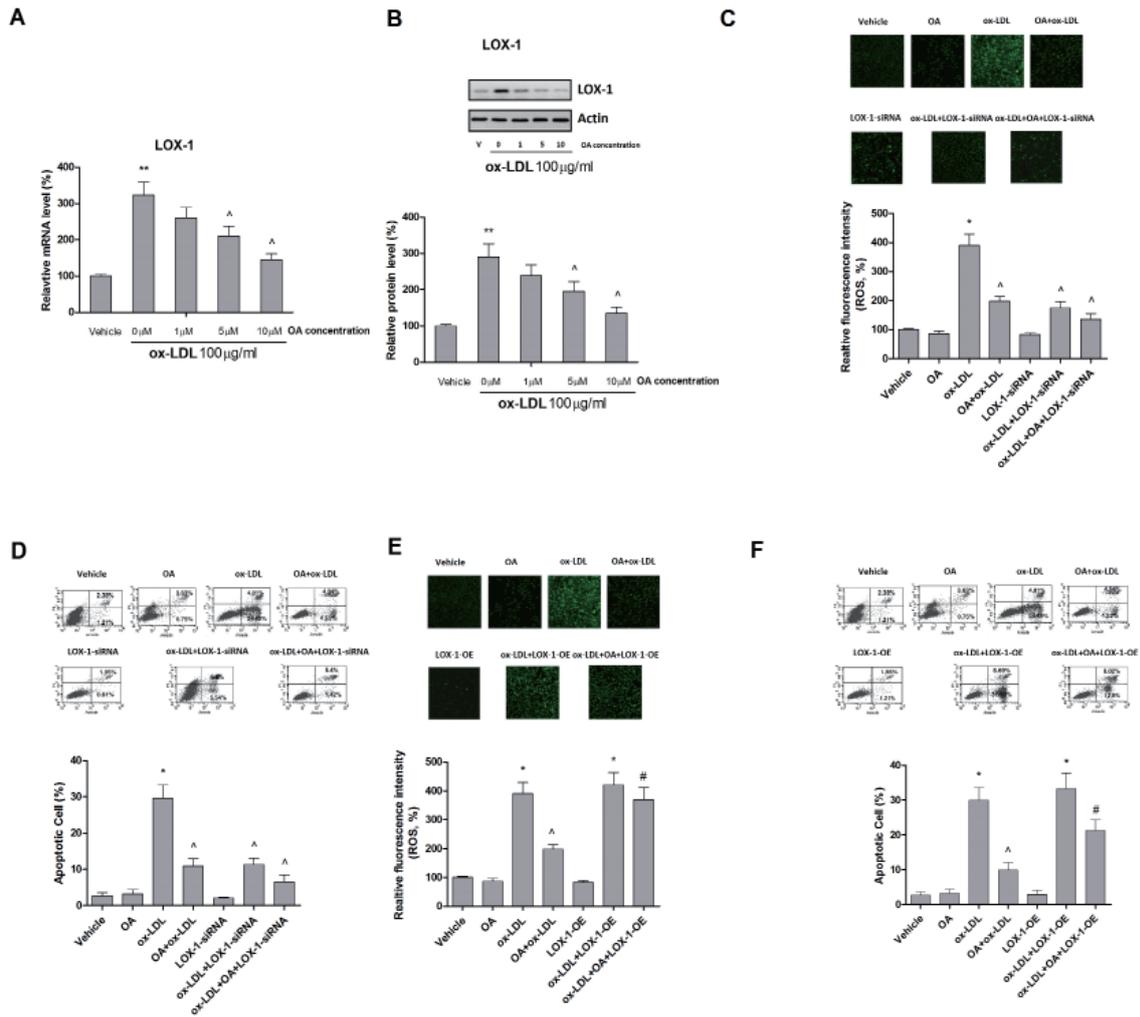
Figure 5. OA attenuates ox-LDL-induced ROS generation by modulating LOX-1 expression. (A), Effect of OA on ox-LDL-induced LOX-1 mRNA expression. **(B)**, Effect of OA on ox-LDL-induced LOX-1 protein expression. **(C)**, Effect of LOX-1 knockdown on ox-LDL-induced ROS generation and the protection of OA against ox-LDL-induced ROS generation. **(D)**, Effect of LOX-1 knockdown on ox-LDL-induced apoptosis and the protection of OA against ox-LDL-induced apoptosis. **(E)**, Effect of LOX-1 overexpression on ox-LDL-induced ROS generation and the protection of OA against ox-LDL-induced ROS generation. **(F)**, Effect of LOX-1 overexpression on ox-LDL-induced apoptosis and the protection of OA against ox-LDL-induced apoptosis. $^*p < 0.05$ *vs.* control, $^{**}p < 0.01$ *vs.* control, $^\wedge p < 0.05$ *vs.* ox-LDL, $^\#p < 0.05$ *vs.* ox-LDL+OA.

capability of ox-LDL to induce apoptosis as well as ROS accumulation in HUVECs. Cotreatment with OA and LOX-1 siRNA synergistically reduced oxLDL-caused cell apoptosis and ROS generation by 64.7%. Although overexpression of LOX-1 alone in HUVECs did not affect cell apoptosis or ROS generation, enhanced expression of LOX-1 markedly potentiated the capability of ox-LDL to induce ROS accumulation and apoptosis. However, overexpression of LOX-1 significantly attenuated OA involved protection against oxLDL-induced apoptosis and ROS generation in HUVECs (Figures 5E and 5F). Taken together, our results showed that the protective effect of OA against ox-LDL induced HUVEC apoptosis might, at least in part, be obtained *via* inhibition of LOX-1/ROS/HIF-1α signaling.

4. Discussion

A growing body of evidence suggests that ox-LDL induced endothelial cell apoptosis plays key roles in the pathogenesis of atherosclerosis by promoting a reduction of vascular integrity, deposition of lipids, invasion of vascular smooth muscle cells, migration of monocytes, and formation of atherosclerotic plaque (*20,21*). Therefore, suppressing ox-LDL-induced endothelial cell apoptosis may provide a new therapeutic option for prevention and treatment of atherogenesis. In this study, we employed human umbilical vein endothelial cells (HUVECs) which have high relevancy to actual human cardiovascular system cells as an *in vitro* model to investigate the protective effects of OA protected against ox-LDL induced apoptosis in endothelial cells. Our results demonstrated that (*i*) OA protected HUVECs from ox-LDL-induced loss in cell viability and apoptosis in a concentration-dependent manner; (*ii*) the modulating effect of OA on HIF-1α participated in the anti-apoptotic effects of OA; (*iii*) the anti- apoptosis effects of OA were obtained

via suppressing the signaling cascade of LOX-1/ROS/HIF-1α. To our knowledge, this is the first study that elucidates the role of HIF-1α in ox-LDL induced apoptosis in endothelial cells.

The involvement of HIF-1α in the pathogenesis of atherosclerosis has been shown in a variety of cell types (*6*). A few studies have shown that HIF-1α played an essential role in the function of macrophages when challenged by ox-LDL and promoted the transformation of macrophages to foam cells (*22,23*). In leucocytes, which function as a key factor in the development and progression of atherosclerotic lesions, HIF-1α has been reported to have a direct effect on the cytokine profile (*24*). Jeong *et al.* also reported that activation of HIF-1α in mast cells could stimulate the expression of VEGF, leading to direct and indirect attraction of inflammatory cells into the intima in various stages of atherogenesis (*25,26*). Moreover, a number of studies have established the crucial role of HIF-1α in vascular smooth muscle cells proliferation exposed to hypoxic stimulus (*27*). However, the role of HIF-1α in endothelial cells has never been studied. In this study, we found that the ox-LDL was able to induce expression of HIF-1α. Then we manipulated the expression of HIF-1α level in HUVECs with HIF-1α-targeted siRNA and HIF-1α overexpressing plasmid, both did not show any marked effect on HUVECs apoptosis alone. However, HIF-1α-targeted siRNA significantly attenuated ox-LDL-induced apoptosis in HUVECs, suggesting that ox-LDL induced apoptosis, at least partly, was mediated *via* HIF-1α signaling. Interestingly, we found that OA was able to modulate the expression of HIF-1α, which led to its protective effect against ox-LDL induced apoptosis in HUVECs, as demonstrated by the effect of OA on ox-LDL induced apoptosis in HIF-1α knockdown or HIF-1α overexpressing HUVECs. Based on our results, we suggest that HIF-1α might serve as a novel target in the prevention and treatment of AS.

It is known that intracellular ROS positively correlated with HIF-1α level in a variety cells (*28*) and OA has been identified as a free radical scavenger (*29*). Consistent with previous studies, our results also confirmed the role of OA as a free radical scavenger in endothelial cells by demonstrating that OA treatment was able to reduce ox-LDL-induced ROS in a dose-dependent manner. Moreover, a combined use of OA with ROS inducer CoCl₂ or ROS inhibitor NAC showed that the modulating effect of OA on HIF-1α level in HUVECs was mediated by regulating the intracellular ROS levels. It was suggested that ROS may be involved in stabilizing HIF-1α, leading to elevated levels of HIF-1α (*30*). Therefore, interfering with the ROS level will affect the degradation of HIF-1α. Our experiments showed that OA decreased the level of HIF-1α in part by promoting HIF-1α degradation, supporting our argument that OA modulated HIF-1α level *via* eliminating intracellular ROS. However, it is

to be noted that the regulatory effect of OA on HIF-1α level also involved its effect on translational level (our results showed that OA had no effect on HIF-1α mRNA but a dose-dependent effect on HIF-1α protein level in HUVECs), which indicated that OA might modulate HIF-1α level *via* more than a single pathway. Meanwhile, we also noticed that OA does not always work as a free radical scavenger. A recent study by Lin *et al* reported that activation of ROS/ASK1/p38 MAPK pathways is responsible for the apoptosis stimulated by OA in cancer cells (*31*), which suggests that the effect of OA on ROS might be cell specific.

First identified as an endothelial-specific scavenger receptor by Sawmura in 1997 (*18*), LOX-1 has been found to be expressed in endothelial cells, macrophages, vascular smooth muscle and platelets and can be upregulated by many factors such as ox-LDL, Ang II, shear stress, and advanced glycation (*32-34*). A number of studies implicated that the apoptosis of endothelial cells induced by ox-LDL was predominantly mediated by LOX-1 whose expression is strongly induced by exposure to ox-LDL (*16,34*). More importantly, ox-LDL induces apoptosis in endothelial cells, which can be suppressed by agents that are able to downregulate LOX-1 expression (*16,35*). As shown in the present study, an approximately 3-fold expression of LOX-1 protein/mRNA was observed in ox-LDL treated HUVECs, compared to the control group while OA significantly decreased the induced expression of LOX-1 by ox-LDL in a dose-dependent manner. We also found that OA decreased the intracellular ROS level by downregulating LOX-1, which probably resulted from compromised ox-LDL intake by HUVECs due to less available LOX-1 (*18*). Moreover, by applying LOX-1-targeted siRNA and LOX-1 overexpressing plasmid in HUVECs, we were able to prove the contribution of downregulating LOX-1 in the anti-apoptotic effect of OA against ox-LDL induced apoptosis in HUVECs. Collectively, our results suggest that the LOX-1/ROS/HIF-1α signaling pathway might, at least partly, be involved in the anti-apoptotic effects of OA.

5. Conclusions

In summary, the present study on HUVECs provides evidence that OA protected ox-LDL induced cell apoptosis by suppressing sequential events cause by ox-LDL treatment including LOX-1 up-regulation, ROS overproduction, and HIF-1α overexpression. Our work provides new insights into therapeutic potential of OA in the treatment of AS.

Acknowledgements

References

1. Libby P. Inflammation in atherosclerosis. Nature 2002; 420:868-874.
2. Durand E, Scoazec A, Lafont A, Boddaert J, Al Hajzen A, Addad F, Mirshahi M, Desnos M, Tedgui A, Mallat Z. *In vivo* induction of endothelial apoptosis leads to vessel thrombosis and endothelial denudation: A clue to the understanding of the mechanisms of thrombotic plaque erosion. Circulation. 2004; 109:2503-2506.
3. Wang N, Han Y, Tao J, Huang M, You Y, Zhang H, Liu S, Zhang X, Yan C. Overexpression of CREG attenuates atherosclerotic endothelium apoptosis *via* VEGF/PI3K/AKT pathway. Atherosclerosis. 2011; 218:543-551.
4. Chang HC, Chen TG, Tai YT, Chen TL, Chiu WT, Chen RM. Resveratrol attenuates oxidized LDL-evoked Lox-1 signaling and consequently protects against apoptotic insults to cerebrovascular endothelial cells. J Cereb Blood Flow Metab. 2011; 31:842-854.
5. Mitra S, Deshmukh A, Sachdeva R, Lu J, Mehta JL. Oxidized low-density lipoprotein and atherosclerosis implications in antioxidant therapy. Am J Med Sci. 2011; 342:135-142.
6. Gao L, Chen Q, Zhou X, Fan L. The role of hypoxia-inducible factor 1 in atherosclerosis. J Clin Pathol. 2012; 65:872-876.
7. Zhang L, Zhou G, Song W, Tan X, Guo Y, Zhou B, Jing H, Zhao S, Chen L. Pterostilbene protects vascular endothelial cells against oxidized low-density lipoprotein-induced apoptosis *in vitro* and *in vivo*. Apoptosis. 2012;17:25-36.
8. Pollier J, Goossens A. Oleanolic acid. Phytochemistry. 2012; 77:10-15.
9. Liu J. Pharmacology of oleanolic acid and ursolic acid. J Ethnopharmacol. 1995; 49:57-68.
10. Dinkova-Kostova AT, Liby KT, Stephenson KK, Holtzclaw WD, Gao X, Suh N, Williams C, Risingsong R, Honda T, Gribble GW, Sporn MB, Talalay P. Extremely potent triterpenoid inducers of the phase 2 response: Correlations of protection against oxidant and inflammatory stress. Proc Natl Acad Sci U S A. 2005;102:4584-4589.
11. Ho WP, Chan WP, Hsieh MS, Chen RM. Runx2-mediated bcl-2 gene expression contributes to nitric oxide protection against hydrogen peroxide-induced osteoblast apoptosis. J Cell Biochem. 2009; 108:1084-1093.
12. Tai YT, Cherng YG, Chang CC, Hwang YP, Chen JT, Chen RM. Pretreatment with low nitric oxide protects osteoblasts from high nitric oxide-induced apoptotic insults through regulation of c-Jun N-terminal kinase/ c-Jun-mediated Bcl-2 gene expression and protein translocation. J Orthop Res. 2007; 25:625-635.
13. Feng Y, Cai ZR, Tang Y, Hu G, Lu J, He D, Wang S. TLR4/NF-κB signaling pathway-mediated and oxLDL-induced up-regulation of LOX-1, MCP-1, and VCAM-1 expressions in human umbilical vein endothelial cells. Genet Mol Res. 2014; 13:680-695.
14. Hsu CC, Wang CH, Wu LC, Hsia CY, Chi CW, Yin PH, Chang CJ, Sung MT, Wei YH, Lu SH, Lee HC. Mitochondrial dysfunction represses HIF-1α protein synthesis through AMPK activation in human hepatoma HepG2 cells. Biochim Biophys Acta. 2013; 1830:4743-4751.
15. Yu W, Ying H, Tong F, Zhang C, Quan Y, Zhang Y. Protective effect of the silkworm protein 30Kc6 on human vascular endothelial cells damaged by oxidized low density lipoprotein (Ox-LDL). PLoS One. 2013; 8:e68746.
16. Bao MH, Zhang YW, Zhou HH. Paeonol suppresses oxidized low-density lipoprotein induced endothelial cell apoptosis *via* activation of LOX-1/p38MAPK/NF-κB pathway. J Ethnopharmacol. 2013; 146:543-551.
17. Yen CH, Hsieh CC, Chou SY, Lau YT. 17Beta-estradiol inhibits oxidized low density lipoprotein-induced generation of reactive oxygen species in endothelial cells. Life Sci. 2001; 70:403-413.
18. Sawamura T, Kume N, Aoyama T, Moriwaki H, Hoshikawa H, Aiba Y, Tanaka T, Miwa S, Katsura Y, Kita T, Masaki T. An endothelial receptor for oxidized low-density lipoprotein. Nature. 1997; 386:73-77.
19. Mitra S, Goyal T, Mehta JL. Oxidized LDL, LOX-1 and atherosclerosis. Cardiovasc Drugs Ther. 2011; 25:419-429.
20. Bao MH, Zhang YW, Lou XY, Cheng Y, Zhou HH. Protective effects of let-7a and let-7b on oxidized low-density lipoprotein induced endothelial cell injuries. PLoS One. 2014; 9:e106540.
21. Choy JC, Granville DJ, Hunt DW, McManus BM. Endothelial cell apoptosis: Biochemical characteristics and potential implications for atherosclerosis. J Mol Cell Cardiol. 2001; 33:1673-1690.
22. Hutter R, Speidl WS, Valdiviezo C, Sauter B, Corti R, Fuster V, Badimon JJ. Macrophages transmit potent proangiogenic effects of oxLDL *in vitro* and *in vivo* involving HIF-1α activation: A novel aspect of angiogenesis in atherosclerosis. J Cardiovasc Transl Res. 2013; 6:558-569.
23. Lee SJ, Thien Quach CH, Jung KH, Paik JY, Lee JH, Park JW, Lee KH. Oxidized low-density lipoprotein stimulates macrophage 18F-FDG uptake *via* hypoxia-inducible factor-1α activation through Nox2-dependent reactive oxygen species generation. J Nucl Med. 2014; 55:1699-1705.
24. Ben-Shoshan J, Afek A, Maysel-Auslender S, Barzelay A, Rubinstein A, Keren G, George J. HIF-1α overexpression and experimental murine atherosclerosis. Arterioscler Thromb Vasc Biol. 2009; 29:665-670.
25. Jeong HJ, Chung HS, Lee BR, Kim SJ, Yoo SJ, Hong SH, Kim HM. Expression of proinflammatory cytokines *via* HIF-1α and NF-κB activation on desferrioxamine-stimulated HMC-1 cells. Biochem Biophys Res Commun. 2003; 306:805-811.
26. Lee KS, Kim SR, Park SJ, Min KH, Lee KY, Choe YH, Park SY, Chai OH, Zhang X, Song CH, Lee YC. Mast cells can mediate vascular permeability through regulation of the PI3K-HIF-1α-VEGF axis. Am J Respir Crit Care Med. 2008; 178:787-797.
27. Schultz K, Murthy V, Tatro JB, Beasley D. Prolyl hydroxylase 2 deficiency limits proliferation of vascular smooth muscle cells by hypoxia-inducible factor-1α-dependent mechanisms. Am J Physiol Lung Cell Mol Physiol. 2009; 296:L921-927.
28. Hielscher A, Gerecht S. Hypoxia and free radicals: Role in tumor progression and the use of engineering-based platforms to address these relationships. Free Radic Biol Med. 2015; 79:281-291.
29. Sultana N, Ata A. Oleanolic acid and related derivatives as medicinally important compounds. J Enzyme Inhib Med Chem. 2008; 23:739-756.

30. Chandel NS, Schumacker PT. Cellular oxygen sensing by mitochondria: Old questions, new insight. J Appl Physiol (1985). 2000; 88:1880-1889.

31. Liu J, Wu N, Ma LN, Zhong JT, Liu G, Zheng LH, Lin XK. p38 MAPK signaling mediates mitochondrial apoptosis in cancer cells induced by oleanolic acid. Asian Pac J Cancer Prev. 2014; 15:4519-4525.

32. Kataoka H, Kume N, Miyamoto S, Minami M, Moriwaki H, Murase T, Sawamura T, Masaki T, Hashimoto N, Kita T. Expression of lectinlike oxidized low-density lipoprotein receptor-1 in human atherosclerotic lesions. Circulation. 1999; 99:3110-3117.

33. Yoshida H, Kondratenko N, Green S, Steinberg D, Quehenberger O. Identification of the lectin-like receptor for oxidized low-density lipoprotein in human macrophages and its potential role as a scavenger receptor. Biochem J 1998; 334 (Pt 1):9-13.

34. Yoshimoto R, Fujita Y, Kakino A, Iwamoto S, Takaya T, Sawamura T. The discovery of LOX-1, its ligands and clinical significance. Cardiovasc Drugs Ther. 2011; 25:379-391.

35. Liu YX, Han GZ, Wu T, Liu P, Zhou Q, Liu KX, Sun HJ. Protective effect of α-lipoic acid on oxidized low density lipoprotein-induced human umbilical vein endothelial cell injury. Pharmacol Rep. 2011; 63:1180-1188.

Decrease of ZEB1 expression inhibits the B16F10 cancer stem-like properties

Fengshu Zhao[1,*], Xiangfeng He[2,*], Yaqing Wang[1,*], Fangfang Shi[1], Di Wu[1], Meng Pan[1], Miao Li[1], Songyan Wu[1], Xiaoying Wang[1], Jun Dou[1,]**

[1] *Department of Pathogenic Biology and Immunology, School of Medicine, Southeast University, Nanjing, China;*
[2] *Department of Medical Oncology, Affiliated Tumor Hospital of Nantong University, Nantong, China.*

Summary	Increasing evidence supports that cancer stem cells (CSCs) are responsible for driving tumor initiation and maintenance. Zinc-finger E-box binding homeobox 1 (ZEB1) is a transcription factor for regulating tumor progression, and contributes to maintenance of CSC-like properties. The goal of the present study is to investigate the effect of decreasing ZEB1 expression on the B16F10 CSC-like properties. The recombinant shRNA targeting ZEB1 were transfected into melanoma B16F10 cells, and shZEB1-CD133$^+$CD44$^+$ CSCs were isolated from the stable transfected cells using the magnetic-associated cell sorting method. The shZEB1-CD133$^+$CD44$^+$ CSC-like properties were systematically analyzed. The results show the B16F10 shZEB1-CD133$^+$CD44$^+$ CSCs significantly decreased the ability of clonogenicity, cellular proliferation, migration, and invasion. Importantly, tumorigenicity and tumor lung metastasis was significantly inhibited in B16F10 shZEB1-CD133$^+$CD44$^+$ CSCs compared with B16F10 scramble-CD133$^+$CD44$^+$ CSCs. The decrease of ZEB1 expression markedly resulted in down-regulation of vimentin and N-cadherin expression as well as up-regulation of E-cadherin expression in tumor tissues from the mice injected with B16F10 shZEB1-CD44$^+$CD133$^+$ CSCs. These findings contribute to understanding the maintenance of B16F10 CD133$^+$CD44$^+$ CSC-like properties that was closely associated with ZEB1 expression. ZEB1 may serve as a new therapeutic target for treatment of malignant melanoma.

Keywords: Melanoma, cancer stem cells, stem-like properties, RNA interference, zinc finger E-box-binding protein 1

1. Introduction

Human malignant melanoma is a highly aggressive and drug-resistant skin cancer that contains cancer cell subsets with self-renewing cancer stem-like cells (CSCs). Those cells are considered responsible for tumor resistance to therapies. The frequency of these cells in the tumor, however, is still a topic of debate (*1-3*). Although increasing study reports were published during the past decade, which have contributed to the advance of knowledge in this field, the complex biological properties of melanoma CSCs and how to regulate the properties are still insufficiently understood (*4,5*).

Accumulating evidence supports the concept that the epithelial-to-mesenchymal transition (EMT) finishes the typical phenotype changes of cellular epithelial (epithelium) and interstitial (mesenchyma) state conversion in the process of epithelial originated tumor cells, including breast, prostate, ovarian, colorectal, pancreatic cancer cells, *etc*. (*6-8*). Though melanoma is not an epithelial originated tumor, it possesses epithelial-like properties through interactions between cancer cells and tumor microenvironment to bear phenotype switching (*9-11*). Moreover, melanoma cells are characterized by their "stem-like" properties and their more differentiated progeny, which should be eradicated to achieve a durable cure for melanoma patients (*12*).

Recent discoveries have shown that breast epithelial cells can gain CSC-like properties through an EMT

---

*These authors contributed equally to this works.
**Address correspondence to:*
Dr. Jun Dou, Department of Pathogenic Biology and Immunology, School of Medicine, Southeast University, Dingjiaqiao 87#, Nanjing 210009, Jiangsu, China.
E-mail: njdoujun@seu.edu.cn

program, and residual breast cancer cells following chemotherapy are enriched in EMT and CSC-like properties, which allows metastatic CSC colonization in distant organs (*13,14*). Zinc-finger E-box binding homeobox 1 (ZEB1), a transcription factor, is essential for the physiological processes of differentiation, cell growth, and cell death (*15,16*), and plays a key function in regulating EMT processes of melanoma cells together with miR-200c feedback loop (*5,6,17,18*). Thus, ZEB1 function is closely associated with the melanoma CSC-like property maintenance. For this reason, we investigated whether decreasing ZEB1 expression would inhibit the B16F10 CD133$^+$CD44$^+$ CSC-like properties by altering cellular biological behavior including the tumorigenicity and metastatic potential. The data from this study showed that down-regulating ZEB1 expression in B16F10 CD133$^+$CD44$^+$ CSCs resulted in reduced cellular self-renewing, tumorigenicity, and metastatic potential in a mouse model, suggesting that inhibition of the B16F10 CD133$^+$CD44$^+$ CSC-like properties by suppression of EMT processes i*n vitro* and *in vivo*.

2. Materials and Methods

2.1. *Cell line and mice*

B16F10 murine melanoma cell line is syngeneic in C57BL/6 mice, ordered from the Cellular Institute of China in Shanghai. Cells were cultured at 37ºC in 5% CO$_2$ atmosphere in RPMI 1640 supplemented with 10% fetal bovine serum that contained 100 U/mL penicillin G sodium and 100 mg/L streptomycin sulfate. C57BL/6 mice 5-6 weeks old were obtained from Yangzhou University of China. All mice were housed under pathogen-free conditions and the experiments were performed in compliance with the guidelines of the Animal Research Ethics Board of Southeast University.

2.2. *Short hairpin RNA sequence design*

Short hairpin RNA sequences of mouse ZEB1 were designed based on the ZEB1 DNA sequence (GenBank NO.NM_011546.3) using siDESIGN software (Dharmacon, *http://www.thermoscientificbio.com/ design-center/*) and BLAST (*http://www.ncbi.nlm.nih. gov/BLAST*) as well as Block-iTTM RNAi Designer (Invitrogen, Grand island, NY, USA) and were performed as described previously (*17,19*).

2.3. *Construction of recombinant containing shRNA1 targeting the ZEB1 gene*

A pSUPER-EGFP1 (enhanced green fluorescent protein 1) vector was used to construct recombinants. The recombinant pSUPER-EGFP1-ZEB1-shRNA (shZEB1) was developed as previously described (*19,20*). The target sequence for ZEB1 shRNA includes base pairs of

3,458-3,476 bp of the ZEB1 cDNA sequence. shRNA sequences are as follows: ZEB1-siRNA: sense, 5′-GA TCCCCAGGAAGAGGAGGAGGATAATTCAAGA GATTATCCTCCTCCTCTTCCTTTTTTGGAAA-3′; antisense, 5′-AGCTTTTCCAAAAAAGGAAGAGG AGGAGGATAATCTCTTGAATTATCCTCCTCCTC TT CCTGGG-3′; A pSUPER-EGFP1-scrambled shRNA (scramble) was used as a negative control. Scramble-siRNA: sense, 5′-GATCCCCTTCTCCGAACGTGTCA CGTTTCAAGAGAACGTGACACGTTCGGAGAATT TTTGGAAA-3′; antisense, 5′-AGCTTTCCAAAAATT CTCCGAACGTGTCACGTTCTCTTGAAACGTGAC ACGTTCGGAGAAGGG-3′. The nucleotide sequences underlined contain the restriction endonuclease Bgl II and Hind III sites, respectively. These recombinants were verified by analysis of endonuclease digestion and sequencing.

2.4. *Clonal selection, identification and isolation of CD133$^+$CD44$^+$ cells*

The constructed recombinant plasmid shZEB1 were transfected into B16F10 cells by using Lipofectamine^{TM} 2000 reagent (Invitrogen, USA) according to the manufacturer's protocol. The stably transfected clones were selected from RPMI containing 800 μg/mL G418 (Clontech, CA, USA), and cloned into the cell line by limiting dilution assay. B16F10 shZEB1-CD133$^+$CD44$^+$cells or B16F10 scramble-CD133$^+$CD44$^+$ cells were isolated from the B16F10-shZEB1 cells or the B16F10 scramble-cells with the magnetic activated cell sorting (MACS, Miltenyi Biotec, Gladbach, Germany) method that was performed as described previously (*2,21*). The isolated B16F10 shZEB1-CD133$^+$CD44$^+$ cells were named for B16F10-shZEB1 CD133$^+$CD44$^+$ CSCs while B16F10 scrambled-CD133$^+$CD44$^+$ cells were named for B16F10-Scramble-CD133$^+$CD44$^+$ CSCs.

2.5. *Colony forming assay*

We investigated the colony formation capability of B16F10-shZEB1 CD44$^+$CD133$^+$ CSCs. A colony with a diameter larger than 75 μm or having more than 50 cells was counted as 1 positive colony according to our previous report (*2*). The plate clone formation efficiency was calculated as (number of colony/number of cells inoculated) × 100%. As control, B16F10 scramble-CD133$^+$CD44$^+$ cells, and B16F10 CD44$^+$CD133$^+$ CSCs were used in this experiment.

2.6. *Proliferative assay*

Cell proliferation was measured using a 3-(4,5-dimethylthiaxol-2-yl)-2,5- diphenyltetrazolium bromide (MTT) assay (St. Louis, Mo, CA, USA). B16F10-shZEB1 CD133$^+$CD44$^+$ CSCs, B16F10

scramble-CD133⁺CD44⁺ cells, and B16F10 CD44⁺CD133⁺ CSC suspension were respectively seeded onto a 96-microwell plate (1×10^5/well). The subsequent steps were performed as described in the previous report (22).

2.7. Resistance to chemotherapeutic agents in cells

1×10^4 B16F10-shZEB1 CD133⁺CD44⁺ CSCs or B16F10 Scramble-CD133⁺CD44⁺ cells or B16F10 CD133⁺CD44⁺ CSC suspensions were seeded into a 96-well plate with 10 μg/mL epirubicin in each well for 48h (Baiyunshang Company, Guangdong, China). Cellular resistance to chemotherapeutic agents was calculated according to the previous report (23).

2.8. Cell migration assay

To determine the role of down-regulating ZEB1 expression on cellular migration, B16F10-shZEB1 CD133⁺CD44⁺ CSCs, B16F10 scramble-CD133⁺CD44⁺ cells, and B16F10 CD133⁺CD44⁺ were used in the wound healing assay. Briefly, 5×10^5 cells per well were respectively plated in 6-well plates to form a monolayer one day before the assay; non-adherent cells were removed by PBS washing. On the following day, a uniform scratch was made down the center of the well using a sterile micropipette tip. The distance traveled by the cells was measured between the two boundaries of the cellular area at 0, 12, and 24 h after incubation. Each experiment was performed in triplicate (24,25).

2.9. Cell invasion assay

Briefly, the transwell inserts with 8 μm pores was coated with Matrigel (20 μg/well; Becton Dickinson, Waltham, MA, USA); the different cancer cells were seeded in the upper chamber in RPMI1640 medium supplemented with 10% fetal bovine serum. After incubation at 37ºC, the cells that invaded the lower surface of the Matrigel-coated membranes were fixed with 70% ethanol and stained with trypan blue; cells from five randomly selected fields were then counted under a light microscope (24,25).

2.10. In vivo tumorigenicity experiments

The C57BL/6 mice (female, weight: 16-18 g and age between 5 and 6 weeks) were randomly divided into three groups of equal size (three per group): the B16F10-shZEB1 CD133⁺CD44⁺ CSC group, the B16F10 scrambled-CD133⁺CD44⁺ CSC group, and the B16F10 CD133⁺CD44⁺ CSC group. The back of the mice were subcutaneously (*s.c.*) injected with 5×10^5 of the above cells, respectively. Except for observation of mouse general conditions each day, such as overall behavior, feeding, body weight and appearance

of fur, tumor formation and growth in the groups were monitored every two days by 2-dimensional measurements of individual tumors from each mouse. The endpoint for this study was one diameter of tumor ≥ 15 mm, at which point mice were euthanized. The tumorigenicity experiment was repeated twice (22,26).

2.11. Tissue histopathology

To evaluate tumor metastases to the lung, lung tissues were removed from the mice; after the metastatic tumor nodes were counted the lung tissues were fixed in 10% formalin and then embedded in paraffin. Tissue sections of 4 μm thin were cut and mounted on SuperFrost Plus glass slides; the lung tissue sections were fixed in methanol and stained in hematoxylin and eosin (HE). The slides were viewed under a Zeiss Axioplan light microscope at a magnification of ×100 or 400. Arrows represent the metastatic melanoma cells (22,27).

2.12. Immunohistochemistry

Immunohistochemistry was performed as reported previously (27,28). Briefly, 4 μm-thin formalin fixed and paraffin-embedded tumor slides were incubated with the rabbit anti-mouse/human ZEB1, vimentin, and E-cadherin, respectively, overnight at 4°C. The antibody concentration was 1:500. The samples were then labeled with horseradish peroxidase-conjugated streptavidin (Invitrogen, CA, USA), and the chromogenic reaction was developed by using Liquid DAB Substrate Pack according to the manufacturer's instructions. The stained cells from random and non-overlapping fields were counted under a magnification of ×200.

2.13. Western blot

Approximately 1×10^6 tumor tissue cells were collected and lysed in the protein extraction buffer (Novagen, Madison, WI, USA) by following the manufacturer's protocol. Protein (15 μg/lane) was separated by SDS/PAGE (12% gels) and transferred onto a nitrocellulose membrane. The membrane was blocked with saturating buffer for 1 h at 25ºC, followed by specific antibodies: the rabbit anti-mouse/human ZEB1, vimentin, and E-cadherin (Bioworld Technology, USA), respectively, overnight at 4ºC. The membrane was rinsed for 5 min with an antibody wash solution 3 times before adding to it the goat anti-rabbit fluorescence secondary antibody. Immunoreactive bands were detected by an Odyssey scanning instrument (LI-COR Odyssey Imaging System, USA). Protein semi-quantitation was calculated using Image Lab software developed by Bio-Rad (6,28).

2.14. Statistical analysis

Values of interest were presented as the mean plus or

minus standard deviation. Statistical comparisons were performed using the Student's *t*-test method. Bonferroni correction was used where multiple comparisons were made. A *p* value of < 0.05 was considered statistically significant.

3. Results

3.1. *Decrease of ZEB1 expression in CD133⁺CD44⁺ CSCs reduces its ability for colony formation, proliferation, drug resistance, migration, and invasion*

To understand the B16F10 CD133$^+$CD44$^+$ CSC-like properties, we first decreased cellular ZEB1 expression with the RNA interference technique, and then observed the biological behavior that exhibits stem-like properties. The results in Figures 1A and 1B show that B16F10 shZEB1-CD133$^+$CD44$^+$ CSCs significantly decreased the colony forming rates in common plate medium compared with B16F10 CD133$^+$CD44$^+$ CSCs (19% *vs.* 53%, *p* < 0.0005), and B16F10 scramble-CD133$^+$CD44$^+$ CSCs (19% *vs.* 48%, *p* = 0.0043), respectively; in soft agar medium, the colony forming rates of B16F10 shZEB1-CD133$^+$ CD44$^+$ CSCs was also significantly decreased compared with B16F10 CD133$^+$CD44$^+$ CSCs (8.5% *vs.* 41.5%, *p* < 0.0001), and B16F10 scramble-CD133$^+$CD44$^+$ CSCs (8.5% *vs.* 31.9%, *p* < 0.0003), respectively. Figure 1C shows

that the proliferative activity of B16F10 shZEB1-CD133$^+$CD44$^+$ CSCs dynamically every 24 h as measured by the OD value was markedly reduced when compared with B16F10 CD133$^+$CD44$^+$ CSCs (*p* < 0.01) or B16F10 scramble-CD133$^+$CD44$^+$ CSCs (*p* < 0.05). Figure 1D shows that drug resistance to epirubicin in B16F10 shZEB1-CD133$^+$CD44$^+$ CSCs was decreased, which was statistically significant compared with B16F10 CD133$^+$CD44$^+$ CSCs (41.24% *vs.* 61.46%, *p* = 0.0130) or B16F10 scramble-CD133$^+$CD44$^+$ CSCs (41.24% *vs.* 59.45%, *p* = 0.0248).

In addition, the ability of migration and invasion in B16F10 CD133$^+$CD44$^+$ CSCs with down-regulated ZEB1 expression was significantly inhibited as compared to control cells. We found in Figures 2A and 2B that the results at 24 h showed a statistically significant reduction in wound closures in B16F10 shZEB1-B16F10 CD133$^+$CD44$^+$ CSCs compared with B16F10 CD133$^+$CD44$^+$ CSCs (*p* = 0.0033) or B16F10 scramble-CD133$^+$CD44$^+$ CSCs (*p* = 0.0074). Consistently, the effect of down- regulated ZEB1 expression on B16F10 CD133$^+$CD44$^+$ CSC invasive ability was also inhibited, which was done using the transwell invasive assay. The representative photos in Figure 2C show the cell invasive ability was statistically significantly decreased in B16F10 shZEB1-CD133$^+$CD44$^+$ CSCs compared with B16F10 CD133$^+$CD44$^+$ CSCs (*p* < 0.0001) or B16F10 scramble-
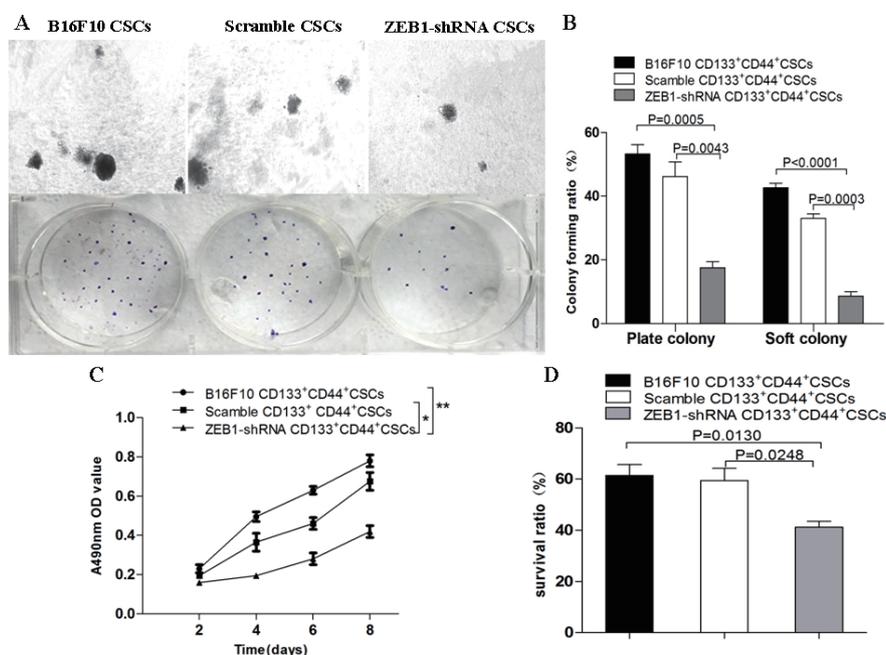
Figure 1. Short hairpin ZEB1-B16F10 CD133$^+$CD44$^+$ CSCs decreases the ability of colony forming, cell proliferation as well as drug resistance *in vitro*. (A) The colony forming ratios of B16F10 ZEB1-shRNA-CD133$^+$CD44$^+$ CSCs in plate and soft agar medium was significantly decreased compared with the ratio in B16F10 CD133$^+$CD44$^+$ CSCs and B16F10 scramble-CD133$^+$CD44$^+$ CSCs. **(B)** Between-group differences of colony-forming ratios in the plate medium and the soft agar medium; all the differences were statistically significant. **(C)** The cell proliferation ability *in vitro* was detected by MTT assay. At day 8, the proliferation of B16F10 ZEB1- shRNA-CD133$^+$CD44$^+$ CSCs was significantly inhibited compared with B16F10 CD133$^+$CD44$^+$ CSCs and B16F10 scramble-CD133$^+$CD44$^+$ CSCs. **(D)** Drug resistance to epirubicin (10 μg/mL) in B16F10 ZEB1-shRNA-CD133$^+$CD44$^+$ CSCs was significantly reduced compared with B16F10 CD133$^+$CD44$^+$ CSCs and B16F10 scramble-CD133$^+$CD44$^+$ CSCs; refer to the statistically significant differences as indicated.
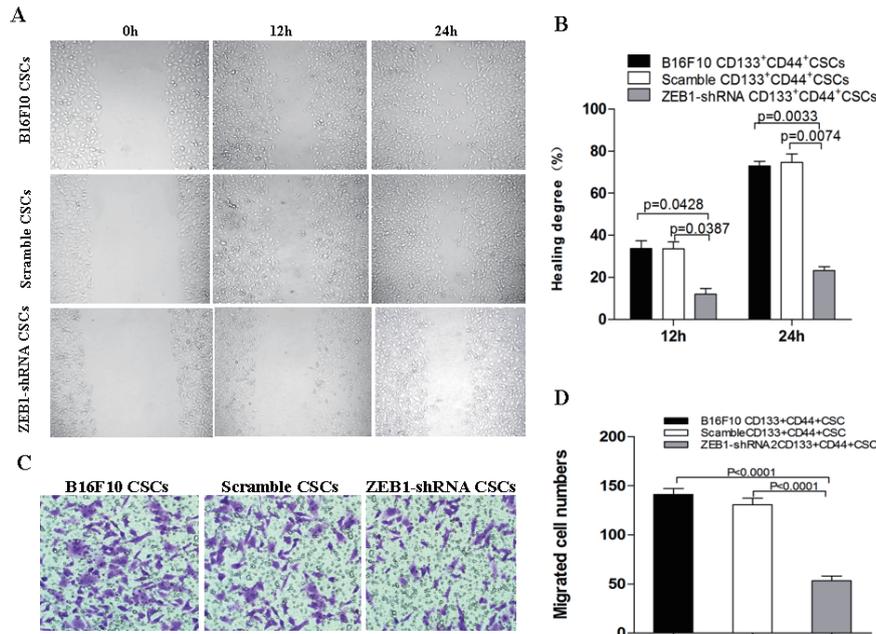
Figure 2. Short hairpin ZEB1-B16F10 CD133+CD44+ CSCs reduces the ability of migration and invasion *in vitro*. (A) The wound-healing assay shows that the migration ability in B16F10 ZEB1-shRNA-CD133+CD44+ CSCs was decreased compared with that of B16F10 CD133+CD44+ CSCs and B16F10 scramble-CD133+CD44+ CSCs. **(C)** The invasive ability of B16F10 ZEB1-shRNA-CD133+CD44+ CSCs was markedly decreased compared with that of B16F10 CD133+CD44+ CSCs and B16F10 scramble-CD133+CD44+ CSCs in the invasive assay. **(B and D)** Between- group differences in the healing degree, and in the invasive cells; all differences were statistically significant; refer to the statistically significant differences as indicated.
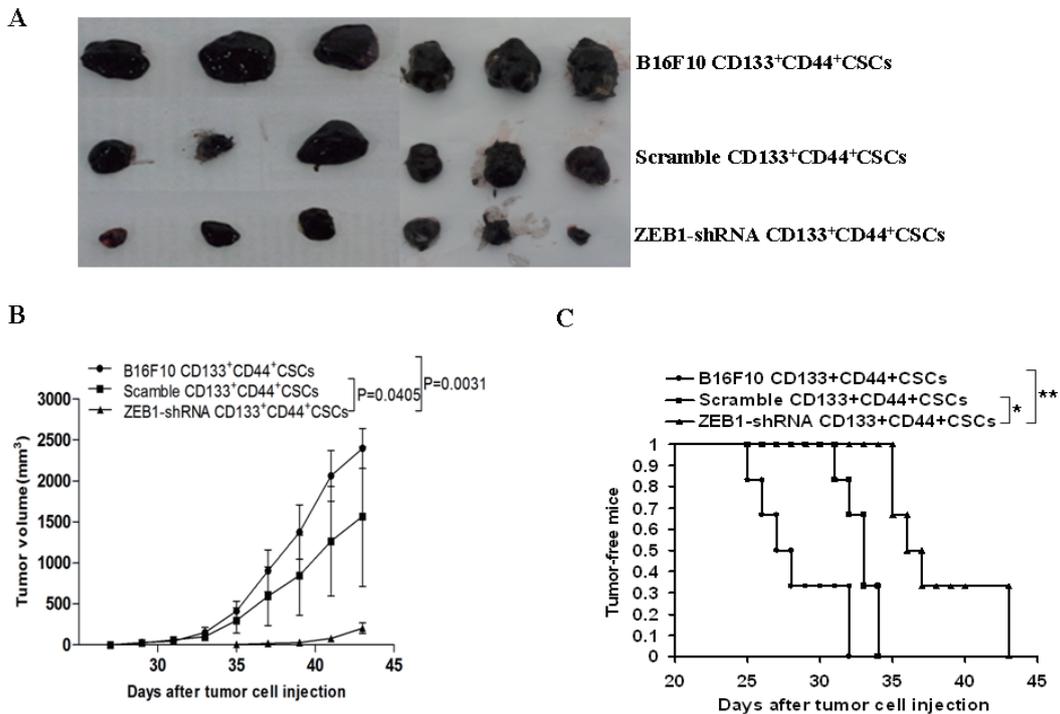
Figure 3. The knockdown of ZEB1 in B16F10 CD133+CD44+ CSCs inhibits the tumorigenicity and tumor progression in mice. (A) The representative images show the tumor sizes stripped from the mice 43 days after mice were injected with the 5 × 10^5 B16F10 ZEB1-shRNA-CD133+CD44+ CSCs, B16F10 CD133+CD44+ CSCs and B16F10 scramble-CD133+CD44+ CSCs, respectively. **(B)** Tumor growth dynamic state in mice injected with the above different cells. **(C)** Days of tumor-free mice injected with the above different cells.

CD133+CD44+ CSCs ($p < 0.0001$) when these cells were cultured for 48 h (Figure 2D).

This findings implied that the maintenance of the B16F10 CD133+CD44+ CSC-like properties, including self-renewal (colony forming and proliferative activity) and drug resistance as well as metastasis (the ability of migration and invasion), may mainly depend on ZEB1 expression or not.

3.2. Decrease of ZEB1 expression in B16F10 CD133$^+$CD44$^+$ CSCs inhibits tumorigenicity and metastasis in mice

Having found the effects of down-regulated ZEB1 expression on cellular biological behaviors that exhibit the B16F10 CD133$^+$CD44$^+$ CSC-like properties *in vitro*, we wanted to know if these effects would inhibit tumorigenicity and metastatic potential of B16F10 shZEB1-CD133$^+$CD44$^+$ CSCs in the mouse model. Images in Figure 3A indicate that the tumor sizes on day 43 after the mice were injected with B16F10 cells. We found that all 6 mice developed tumors in 35 days after being injected with 5×10^5 B16F10 shZEB1-CD133$^+$CD44$^+$ CSCs, however, the tumor volume, the time of tumor occurrence, and the tumor-free mice days were significantly different from the other mice, which was statistically significant compared with the B16F10-scramble-CD133$^+$CD44$^+$ CSCs group ($p < 0.05$) and the B16F10-CD133$^+$CD44$^+$ CSCs group ($p < 0.01$), respectively. Figure 3B presents the dynamic state changes of tumor volumes in B16F10 melanoma bearing mice, while Figure 3C exhibits the B16F10 melanoma bearing mouse survival days in the three groups were obviously different from each other. These differences were statistically significant in shZEB1-CD133$^+$CD44$^+$ CSCs in contrast with B16F10-scramble-CD133$^+$CD44$^+$ CSCs ($p < 0.05$), and B16F10-scramble-CD133$^+$CD44$^+$ CSCs ($p < 0.05$), respectively.

Consistently, the down-regulation of ZEB1 expression in B16F10-CD133$^+$CD44$^+$ CSCs markedly reduced tumor lung metastasis. This efficacy was assessed by observation of lung tumor nodes 43 days after mice were injected with the various cells (Figure 4A). Representative images of lung tissues show tumor nodes in the different mice, which was statistically significant between the B16F10 shZEB1-CD133$^+$CD44$^+$ CSC group and the B16F10 CD133$^+$CD44$^+$ CSC group ($p = 0.007$), or between the B16F10 shZEB1-CD133$^+$CD44$^+$ CSC group and the B16F10 scramble-CD133$^+$CD44$^+$ CSC group ($p = 0.0232$) (Figure 4B). Notably, a few metastatic tumor cells were seen in lung tissue sections from the mice injected with the B16F10 shZEB1-CD133$^+$CD44$^+$ CSCs as analyzed by HE staining (Figure 4C). However, a lot of metastatic tumor cells were found in the lung tissue sections from the mice injected with the B16F10 CD133$^+$CD44$^+$ CSCs or B16F10 scramble-CD133$^+$CD44$^+$ CSCs as are shown in
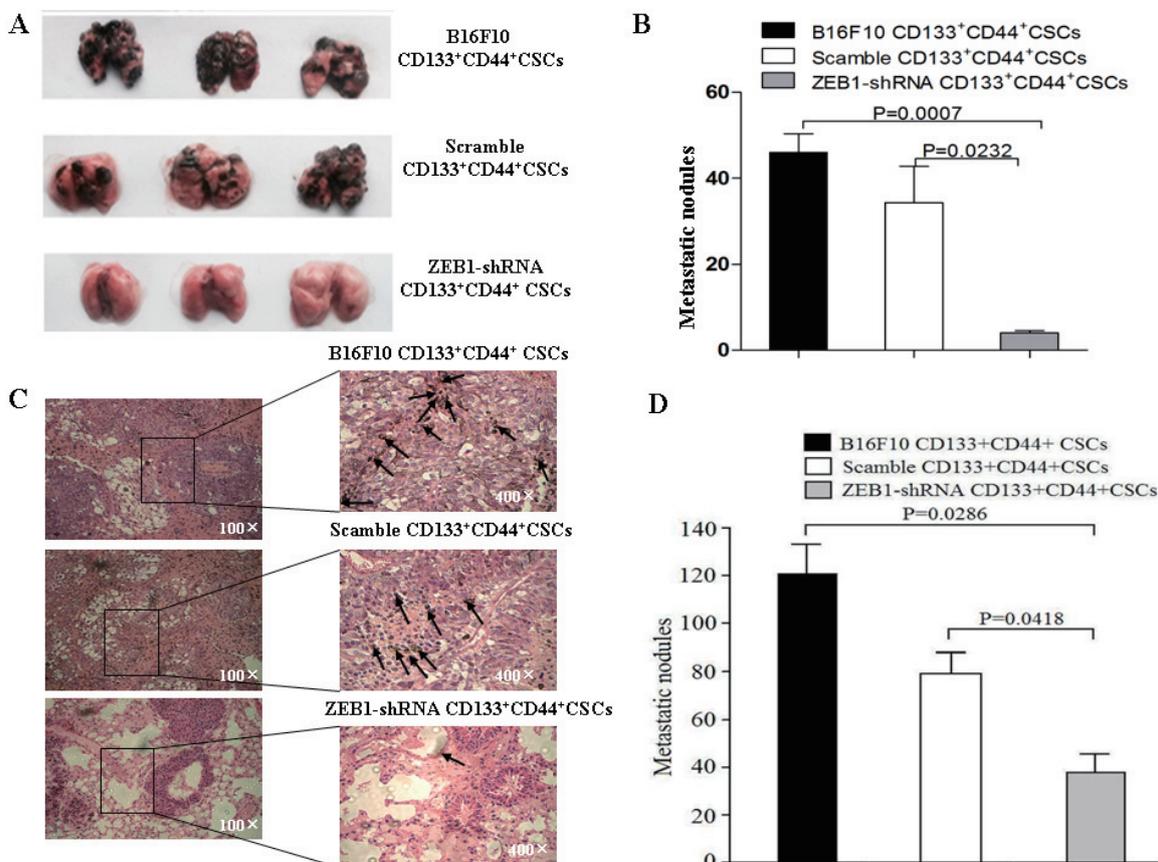
Figure 4. The knockdown of ZEB1 in B16F10 CD133$^+$CD44$^+$ CSCs inhibits tumor lung metastasis in mice. (A) Images show tumor metastatic nodes in mouse lungs stripped from the mice 43 days after mice were injected with 5×10^5 B16F10 ZEB1-shRNA-CD133$^+$CD44$^+$ CSCs, B16F10 CD133$^+$CD44$^+$ CSCs and B16F10 scramble-CD133$^+$CD44$^+$ CSCs, respectively. **(B)** Quantification analysis of lung tumor metastatic node counts. **(C)** Tissue sections derived from the mice 43 days after mice were injected with the above different cells, respectively. Arrows point to the metastatic focus (400×). **(D)** Between-group differences in the tumor metastatic focus in the different lung sections; refer to the statistically significant differences as indicated.

Figures 4C and 4D. From these results, we concluded that the B16F10 CD133$^+$CD44$^+$ CSC-like properties were significantly inhibited in the *in vivo* mouse model.

3.3. *Impacts of down-regulation of ZEB1 in B16F10 CD133$^+$CD44$^+$ CSCs on EMT-related molecular*

expression in tumor tissues

To evaluate the functional significance of the decrease of ZEB1 expression, we tested the expression of ZEB1, E-cadherin, N-cadherin, and vimentin in the tumor tissues from B16F10 melanoma bearing mice
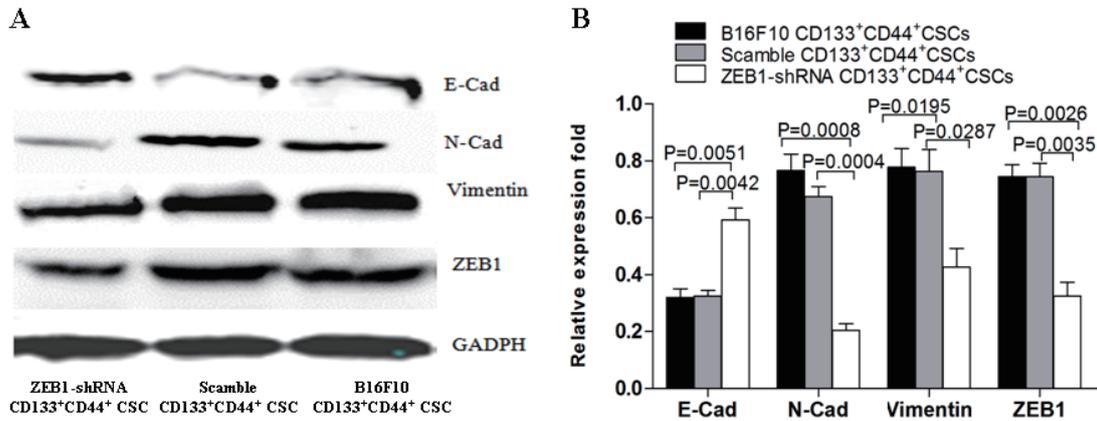
Figure 5. Detection of tumor EMT markers by Western blot. (A) The expression of E-cadherin, N-cadherin, vimentin, and ZEB1 in tumor tissues from mice injected with 5×10^5 B16F10 ZEB1-shRNA-CD133$^+$CD44$^+$ CSCs, B16F10 CD133$^+$CD44$^+$ CSCs and B16F10 Scramble-CD133$^+$CD44$^+$ CSCs, respectively. **(B)** Quantification analysis of molecular expression; refer to the statistically significant differences as indicated.
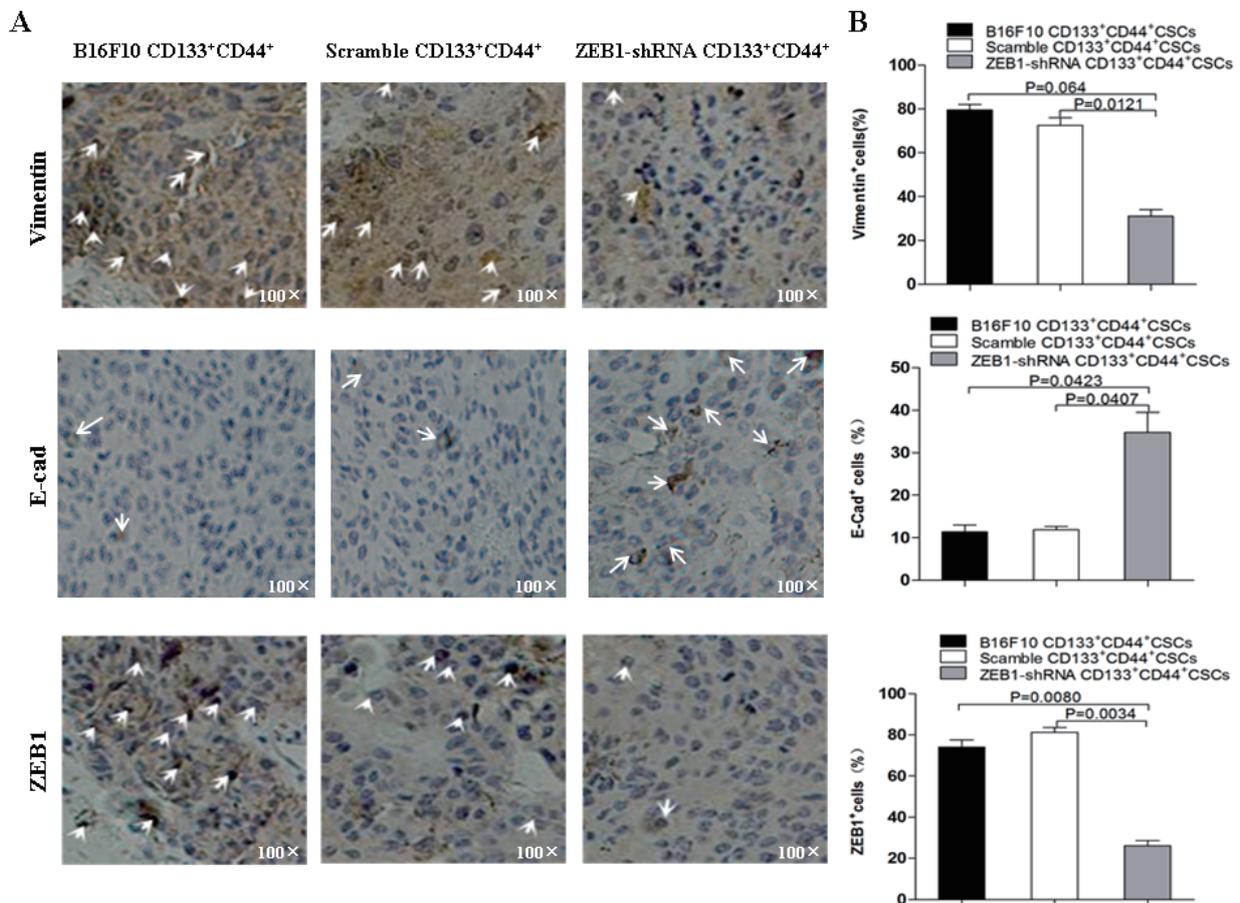
Figure 6. Detection of tumor EMT markers by immunohistochemistry. (A) The expression of vimentin, E-cadherin, and ZEB1 in tumor tissues from mice injected with 5×10^5 B16F10 ZEB1-shRNA-CD133$^+$CD44$^+$ CSCs, B16F10 CD133$^+$CD44$^+$ CSCs and B16F10 scramble-CD133$^+$CD44$^+$ CSCs, respectively. Arrows point to positive cells that expressed the EMT associated molecules (100×). **(B)** The semi-quantification analysis of molecular expression; refer to the statistical differences as indicated.

by Western blot analysis. Figure 5A shows E-cadherin expression in the B16F10 shZEB1-CD133$^+$CD44$^+$ CSCs was markedly higher than that of both B16F10 CD133$^+$CD44$^+$ CSCs and B16F10 scramble-CD133$^+$CD44$^+$ CSCs. There were significant differences between the B16F10 shZEB1-CD133$^+$CD44$^+$ CSCs and the B16F10 CD133$^+$CD44$^+$ CSCs (p = 0.0051), and between the B16F10 shZEB1-CD133$^+$CD44$^+$ CSCs and the B16F10 scramble-CD133$^+$CD44$^+$ CSCs (p = 0.0042). Whereas the ZEB1, N-cadherin, and vimentin indicated much lower expression in the B16F10 shZEB1-CD133$^+$CD44$^+$ CSCs than either B16F10 CD133$^+$CD44$^+$ CSCs or B16F10 scramble-CD133$^+$CD44$^+$ CSCs, which was statistically significant as is shown in Figure 5B.

Similarly, the results of the immu¬nohistochemistry in panels A and C of Figure 6 show the E-cadherin expression in B16F10 shZEB1-CD133$^+$CD44$^+$ CSCs was significantly increased while expression of vimentin and ZEB-1 was decreased compared with B16F10 CD133$^+$CD44$^+$ CSCs and B16F10 scramble-CD133$^+$CD44$^+$ CSCs, which was statistically significant as is shown in Figure 6B. These results demonstrated that the increased expression of E-cadherin coupled with the decreased expression of vimentin and ZEB-1 may have inhibited the EMT process of B16F10 shZEB1-CD133$^+$CD44$^+$ CSCs in the mouse model.

4. Discussion

It is known that there are a subset of cells within a tumor with "stem-like" properties. These cells represent a distinct tumor subpopulation known as CSCs that are responsible for tumor initiation, progression, metastasis, therapeutic resistance and relapse (*29*). In this study, we focused on the melanoma B16F10 CD133$^+$CD44$^+$ CSC-like properties, and wanted to know whether the inhibition of the B16F10 CSC-like properties would alter cellular tumorigenicity and metastasis potential. We selected the transcription factor ZEB1 as a target to inhibit the B16F10 CSC-like properties because this is the role of ZEB1 and is tightly related with the melanoma' CSC-like properties as described by previous reports (*5,6,17,18,30*).

Since self-renewal is one of the main B16F10 CSC-like properties, we first assessed the clone formation capability and proliferative activity of B16F10 shZEB1-CD133$^+$ CD44$^+$ CSCs. We found that knockdown of ZEB1 not only markedly decreased clone formation capability in common plate and soft agar media, and proliferative activity of B16F10 CD133$^+$CD44$^+$ CSCs, but also significantly reduced the drug resistance to epirubicin as well as the ability of migration and invasion *in vitro* compared to B16F10 CD133$^+$CD44$^+$ CSCs and scramble-CD133$^+$CD44$^+$ CSCs. The data from this study demonstrated that the knockdown of ZEB1 in B16F10 CD133$^+$CD44$^+$ CSCs reduced the

ability for self-renewal, migration and invasion, which may represent the decrease of tumor cell invasiveness and stem-like properties, suggesting inhibitory roles on B16F10 CD133$^+$CD44$^+$ CSC-like properties. More importantly, the knockdown of ZEB1 in B16F10 CD133$^+$CD44$^+$ CSCs inhibited the tumorigenicity and distant lung metastasis potential. According to the CSC hypothesis, the tumorigenicity and metastasis potential represent mainly CSC-like properties in epithelial originated tumor cells (*31,32*). Consistent with the previously reported findings (*2,5,6,17*), our current study demonstrated that B16F10 CD133$^+$CD44$^+$ CSCs had a multipotent, self-renewal capacity and strong tumorigenesis, while the decrease of ZEB1 expression in B16F10 CD133$^+$CD44$^+$ CSCs caused reduction of CSC-like properties, which may be good evidence that ZEB1 serves as a crucial factor to maintain CSC-like properties.

Metastasis is associated with poor prognosis for melanoma, which is responsible for about 90% of skin cancer-related mortality. The capacity of cancer cells to undergo EMT is now considered a hallmark of tumor metastasis (*11,31*). For this purpose, we tested EMT related molecular expression in the tumor tissues. Apparently, B16F10 shZEB1-CD133$^+$CD44$^+$ CSCs exhibited significantly decreased ZEB1 expression compared with the control cells in the tumor tissues analyzed by Western blot and immu¬nohistochemistry assays. In addition, the expression of E-cadherin and vimentin, which are characteristic molecules of EMT that are closely associated with typical phenotype changes of EMT in tumor cell growth and metastasis (*15,33,34*), was significantly inhibited in the tumor tissues from the mice injected with B16F10 shZEB1-CD133$^+$ CD44$^+$ CSCs. These positive consistent data allow us to suppose that the reduction of tumor cell lung metastasis mainly is due to inhibition of the EMT processes of B16F10 shZEB1-CD133$^+$CD44$^+$ CSCs.

In conclusion, the present study provides a better understanding of ZEB1 roles in melanoma B16F10 CD133$^+$CD44$^+$ CSCs. These data demonstrate that the decrease of ZEB1 expression resulted in inhibitory effects on the B16F10 CD133$^+$CD44$^+$ CSC-like properties, and reduced the tumorigenesis and metastatic potential in the melanoma mouse model. These findings support the use of knockdown of ZEB1 approaches in future melanoma clinical trials.

Acknowledgements

References

1. Chin L, Garraway LA , Fisher DE. Malignant melanoma: Genetics and therapeutics in the genomic era. Genes Dev. 2006; 20:2149-2182.

2. Dou J, Pan M, Wen P, Li Y, Tang Q, Chu L, Zhao F, Jiang C, Hu W, Hu K, Gu N. Isolation and identification of cancer stem-like cells from murine melanoma cell lines. Cell Mol Immunol. 2007; 4:467-472.

3. Sztiller-Sikorska M, Koprowska K, Jakubowska J, Jakubowska J, Zalesna I, Stasiak M, Duechler M, Czyz ME. Sphere formation and self-renewal capacity of melanoma cells is affected by the microenvironment. Melanoma Res. 2012; 22:215-224.

4. Schatton T, Murphy GF, Frank NY, Yamaura K, Waaga-Gasser AM, Gasser M, Zhan Q, Jordan S, Duncan LM, Weishaupt C, Fuhlbrigge RC, Kupper TS, Sayegh MH, Frank MH. Identification of cells initiating human melanomas. Nature. 2008; 451:345-349.

5. Dou J, Gu N. Emerging strategies for the identification and targeting of cancer stem cells. Tumour Biol. 2010; 31:243-253.

6. He X, Wang J, Zhao F, Yu F, Chen D, Cai K, Yang C, Chen J, Dou J. Antitumor efficacy of viable tumor vaccine modified by heterogenetic ESAT-6 antigen and cytokine IL-21 in melanomatous mouse. Immunol Res. 2012; 52:240-249.

7. Jukic DM, Rao UN, Kelly L, Skaf JS, Drogowski LM, Kirkwood JM, Panelli MC. Microrna profiling analysis of differences between the melanoma of young adults and older adults. J Transl Med. 2010; 8:27.

8. Kreiseder B, Orel L, Bujnow C, Buschek S, Pflueger M, Schuett W, Hundsberger H, de Martin R, Wiesner C. α-Catulin downregulates E-cadherin and promotes melanoma progression and invasion. Int J Cancer. 2013; 132:521-530.

9. Rangel MC, Karasawa H, Castro NP, Nagaoka T, Salomon DS, Bianco C. Role of Cripto-1 during epithelial-to- mesenchymal transition in development and cancer. Am J Pathol. 2012; 180:2188-2200.

10. Kemper K, de Goeje PL, Peeper DS, van Amerongen R. Phenotype switching: Tumor cell plasticity as a resistance mechanism and target for therapy. Cancer Res. 2014; 74:5937-5941.

11. Laurenzana A, Biagioni A, Bianchini F, Peppicelli S, Chillà A, Margheri F, Luciani C, Pimpinelli N, Del Rosso M, Calorini L, Fibbi G. Inhibition Of uPAR-TGF β crosstalk blocks MSC-dependent EMT in melanoma cells. J Mol Med (Berl). 2015; 93:783-794.

12. Sztiller-Sikorska M, Koprowska K, Majchrzak K, Hartman M, Czyz M. Natural compounds' activity against cancer stem-like or fast-cycling melanoma cells. PLoS One. 2014; 9:e90783.

13. Scheel C, Weinberg RA. Cancer stem cells and epithelial-mesenchymal transition: Concepts and molecular links. Semin Cancer Biol. 2012; 22:396-403.

14. Zhang H, Cai K, Wang J, Wang X, Cheng K, Shi F, Jiang L, Zhang Y, Dou J. MiR-7, inhibited indirectly by lincRNA HOTAIR, directly inhibits SETDB1 and reverses the EMT of breast cancer stem cells by downregulating the STAT3 pathway. Stem Cells. 2014;

15. Ulrike B, Schubert J, Wellner U, Schmalhofer O, Vincan E, Spaderna S, Brabletz T. A reciprocal repression between ZEB1 and members of the miR-200 family promotes EMT and invasion in cancer cells. EMBO Rep. 2008; 9:582-589.

16. Thiery JP, Acloque H, Huang RY, Nieto MA. Epithelial-mesenchymal transitions in development and disease. Cell. 2009; 139:871-890.

17. Dou J, He X, Liu Y, Wang Y, Zhao F, Wang X, Chen D, Shi F, Wang J. Effect of downregulation of ZEB1 on vimentin expression, tumour migration and tumourigenicity of melanoma B16F10 cells and CSCs. Cell Biol Int. 2014; 38:452-461.

18. Kreiseder B, Orel L, Bujnow C, Buschek S, Pflueger M, Schuett W, Hundsberger H, de Martin R, Wiesner C. α-Catulin downregulates E-cadherin and promotes melanoma progression and invasion. Int J Cancer. 2013; 13:521-530.

19. Chen D, Wang J, Zhang Y, Chen J, Yang C, Cao W, Zhang H, Liu Y, Dou J. Effect of down-regulated transcriptional repressor ZEB1 on the epithelial-mesenchymal transition of ovarian cancer cells. Int J Gynecol Cancer. 2013; 23:1357-1366.

20. Dou J, Jiang C, Wang J, Zhang X, Zhao F, Hu W, He X, Li X, Zou D, Gu N. Using ABCG2-molecule-expressing side population cells to identify cancer stem-like cells in a human ovarian cell line. Cell Biol Int. 2011; 35:227-234.

21. Chen J, Wang J, Zhang Y, Chen D, Yang C, Kai C, Wang X, Shi F, Dou J. Observation of ovarian cancer stem cell behavior and investigation of potential mechanisms of drug resistance in three-dimensional cell culture. J Biosci Bioeng. 2014; 118:214-222.

22. Dou J, Wen P, Hu W, Li Y, Wu Y, Liu C, Zhao F, Hu K, Wang J, Jiang C, He X, Gu N. Identifying tumor stem-like cells in mouse melanoma cell lines by analyzing the characteristics of side population cells. Cell Biol Int. 2009; 33:807-815.

23. Mosmann TR. Colorimetric assay for cellular growth and survival: Application to proliferation and cytotoxicity assays. J Immunol Methods. 1983; 65:55-63.

24. Shen B, Chu E S, Zhao G, Man K, Wu CW, Cheng JT, Li G, Nie Y, Lo CM, Teoh N, Farrell GC, Sung JJ, Yu J. PPAR gamma inhibits hepatocellular carcinoma metastases *in vitro* and in mice. Br J Cancer. 2012; 106:1486-1494.

25. Ngora H, Galli UM, Miyazaki K, Zöller M. Membrane-bound and exosomal metastasis-associated C4.4A promotes migration by associating with the $\alpha_6\beta_4$ integrin and MT1-MMP. Neoplasia. 2012; 14:95-107.

26. Mikesh LM, Kumar M, Erdag G. Evaluation of molecular markers of mesenchymal phenotype in melanoma. Melanoma Res. 2010; 20:485-495.

27. Hu WH, Wang J, Dou J, He X, Zhao F, Jiang C, Yu F, Hu K, Chu L, Li X, Gu N. Augmenting therapy of ovarian cancer efficacy by secreting IL-21 human umbilical cord blood stem cells in nude mice. Cell Transplatation. 2011; 20:669-680.

28. Yang X, Lin X, Zhong X, Kaur S, Li N, Liang S, Lassus H, Wang L, Katsaros D, Montone K, Zhao X, Zhang Y, Bützow R, Coukos G, Zhang L. Double-negative feedback loop between reprogramming factor LIN28 and microRNA let-7 regulates aldehyde dehydrogenase 1-positive cancer stem cells. Cancer Res. 2010; 70:9463-

9472.

29. Yu Y, Ramena G, Elble RC. The role of cancer stem cells in relapse of solid tumors. Front Biosci (Elite Ed). 2012; 4:1528-1541.

30. Liu SJ, Tetzlaff MT, Liu A, Liegl-Atzwanger B, Guo J, Xu X. Loss of microRNA-205 expression is associated with melanoma progression. Lab Invest. 2012; 92:1084-1096.

31. Zimmerer RM, Korn P, Demougin P, Kampmann A, Kokemüller H, Eckardt AM, Gellrich NC, Tavassol F. Functional features of cancer stem cells in melanoma cell lines. Cancer Cell Int. 2013; 13:78.

32. Patrawala L, Calhoun T, Schneider-Broussard R, Zhou J, Claypool K, Tang DG. Side population is enriched in tumorigenic, stem-like cancer cells, whereas ABCG2+ and ABCG2- cancer cells are similarly tumorigenic. Cancer Res. 2005; 65:6207-6219.

33. Wang X, Zhao F, He X, Wang J, Zhang Y, Zhang H, Ni Y, Sun J, Wang X, Dou J. Combining TGF-β1 knockdown and miR200c administration to optimize antitumor efficacy of B16F10/GPI-IL-21 vaccine. Oncotarget. 2015; 6:12493-12504.

Alexaki VI, Javelaud D, Van Kempen LC, *et al*. GLI2-Mediated Melanoma Invasion and Metastasis. J Natl Cancer Inst. 2010; 102:1148-1159.

The risk factors for suboptimal CD4 recovery in HIV infected population: an observational and retrospective study in Shanghai, China

Fengdi Zhang[1], Meiyan Sun[1], Jianjun Sun[1], Liqian Guan[1], Jiangrong Wang[1], Hongzhou Lu[1,2,3,*]

[1] Department of Infectious Disease, Shanghai Public Health Clinical Center, Fudan University, Shanghai, China;
[2] Department of Infectious Disease, Huashan Hospital Affiliated to Fudan University, Shanghai, China;
[3] Department of Internal Medicine, Shanghai Medical College, Fudan University, Shanghai, China.

Summary   Although the initiation of antiretroviral therapy (ART) has promoted the reconstitution of CD4+ T-cell count in the HIV infected population, not all patients can achieve the normalization of their immunologic functions. We analysed the variables associated with immunologic recovery, which is commonly regarded as the increase of CD4 to 350 cell/μL after a year of ART. We collected data from 3,485 patients attending a university-based HIV clinic from June 2005 to July 2014 in Shanghai, China. Logistic regression test was performed to analyse the risk factors for suboptimal CD4+ recovery following yearlong ART. The CD4+ T-cell of 723 participants (41.5% of the 1744 subjects) showed more than 350 cell/μL after one year of ART. Compared with baseline CD4 > 350 cell/μL, patients with baseline CD4 ≤ 200 cell/μL or 200 < CD4 ≤ 350 cell/μL were 42.6, 4.5 times more likely to be incomplete CD4 recovery, respectively. The risk of suboptimal immunologic recovery among patients with regimen including AZT or d4T were 2.1, 2.4 times higher compared with TDF, respectively. In our study, between optimal CD4 recovery group and suboptimal recovery group, there were no significant differences in age, gender, marital status, transmission routes, WHO stage, and CD4 recovery rates. As for the dynamic CD4 change, we found the CD4 recovery rates were 49.9% and 61.8% in the second and third year of ART, respectively. Patients who had a low level of CD4+ T-cell count (< 200 cell/μL) during the initiation of ART exhibited more difficulties recovering to a normal level. Furthermore, the regimen, including AZT or d4T, was not beneficial to CD4 recovery. So, more efforts should be made to guarantee the early diagnosis and timely treatment for HIV/AIDS patients, and simultaneously optimize antiretroviral therapy.

Keywords: HIV, antiretroviral therapy, CD4 recovery, suboptimal immunologic response, risk factors

1. Introduction

For many years, HIV infection has been a serious public health burden worldwide (*1-6*). The CD4+ T cell plays a critical role in the pathogenesis of the HIV infection. As the main target cells of HIV, after being infected, CD4+ T-cell count reduces significantly and leads to the deconstruction of T-cell immune response, which consequently causes immunodeficiency and increases incidences of opportunistic infections and tumours. Two hundreds cells per microliter of CD4 count is a critical point in clinical practice because patients with CD4 counts above 200 cell/μL have lower risk of clinical events (*7,8*).

Highly active antiretroviral therapy (HAART) for HIV infection is among the greatest successes of modern medicine, having remarkably prolonged the expected life span of HIV-infected individuals (*9-13*). With HAART, HIV infection can be prevented from

Address correspondence to:
Dr. Hongzhou Lu, Shanghai Public Health Clinical Center, Fudan University, No.2901, Caolang Road, Jinshan District, Shanghai, China.
E-mail: luhongzhou@fudan.edu.cn

transforming into clinical AIDS. As a result, what was commonly considered as a fatal disease is now regarded as a chronic condition. However, after the initiation of HAART, the outcome of some patients remained unsatisfactory, with the possible occurrence of virologic failure and suboptimal immunologic response (SIR). Currently, there is no consensus on the definition of suboptimal immunologic response, but certain studies have recommended that immunologic response failure can be identified as not managing to increase CD4 counts to more than 350 cell/μL or 500 cell/μL within a specific time period (*e.g.*, 4 to 7 years) (*7*).

Given the fact that incomplete CD4 recovery still occurs after the initiation of HAART, risk factors for this outcome should be analysed. According to published data (*8,14-18*), predictors for suboptimal CD4 recovery are as follows: CD4 < 200 cell/μL at the initiation of ART, older age, co-infected with hepatitis C virus, HIV-2, human T-cell leukaemia virus, regimen of ART, persistent immune activation, loss of the regenerative potential of the immune system and concomitant medical conditions. However, limited studies mainly focused on the risk factors for incomplete immunologic recovery in China, which is a resource-limited place. Therefore, in this context, we conducted an observational and retrospective study to evaluate the influence factors of CD4+ T-cell count recovery rate of the HIV positive population in East China.

2. Materials and Methods

2.1. *Study design, subjects and inclusion criteria*

We conducted the cohort study of HIV-infected patients who attended the clinic affiliated with Fudan University, from June 2005 to July 2014 in Shanghai, China. Participants were only enrolled if they were HIV positive and on stable ART. Their CD4 count and virus load were not considered. Besides, all participants were not infected with the hepatitis B virus or the hepatitis C virus. Our study conformed to the principles of the Declaration of Helsinki and the current Guideline of Diagnosis and Treatment of AIDS. Every enrolled patient was offered a written informed consent form.

2.2. *Data collection*

The patients' data was firstly collected from their charts, and afterwards a professional staff, majoring in Hospital Information Management, manually entered the data into a national electronic database. In addition, the clinicians routinely checked the data to ensure accuracy and consistency.

2.3. *ART therapy*

ART management at our hospital complied with the

Chinese National Antiretroviral Therapy Guidelines. Based on the present situation in China, first-line regimen includes a combination of two nucleoside reverse transcriptase inhibitors (NRTIs): lamivudine (3TC) and zidovudine (AZT) or tenofovir (TDF) or stavudine (d4T) and a nonnucleotide reverse transcriptase inhibitor (NNRTI): efavirenz (EFV) or nevirapine (NVP). In the second-line regimen, a protease inhibitor, preferably lopinavir/ritonavir (LPV/r), is used to substitute for the nonnucleotide reverse transcriptase inhibitor. Approximately every three months, we monitored the ART therapy with CD4+ T-cell count. Apart from the T lymphocyte immunity test, the blood routine examination and blood biomedical assay were also conducted. The patients received the virus load test at the sixth month of ART, and then the test was to be conducted annually. To observe the changing trend of CD4 counts, we gathered follow-up data every three months during the first year, and every six months from the second to the third year.

2.4. *CD4+ T-cell count measurement*

Blood samples for CD4+ T-Cell count measurement were analysed with CYTOMICS-FC500 at the Shanghai Public Health Clinical Centre affiliated with Fudan University. In our study, we defined the baseline CD4+ T cell count as the most recent test performed within one month before ART was initiated.

2.5. *Analysis and statistics*

Data analysis was conducted by the IBM SPSS version 19.0 (IBM SPSS, Inc., Armonk, NY, USA). Continuous variables were described using mean and standard deviation (SD), while categorical variables were described by numbers and percentages. The chi square test was used for categorical variables and the t test was used for continuous variables. We used the logistic regression test to analyse the risk factors for suboptimal CD4 recovery after HAART initiation. The confounding factors included: age, gender, marital status, infection route, treatment regimen, WHO stages, initiation of ART timing and baseline CD4 cell counts. All hypothesis testing was two-sided, with a level of α = 0.05.

3. Results

3.1. *Characteristics of the participants*

1,744 participants, with a mean age of 37.3 years old (min 18, max 88), were enrolled in this study (Figure 1). Most subjects were male and nearly half of the participants were single, while 40% of the participants were married or cohabiting with others. When it comes to the infection routes, the majority of participants
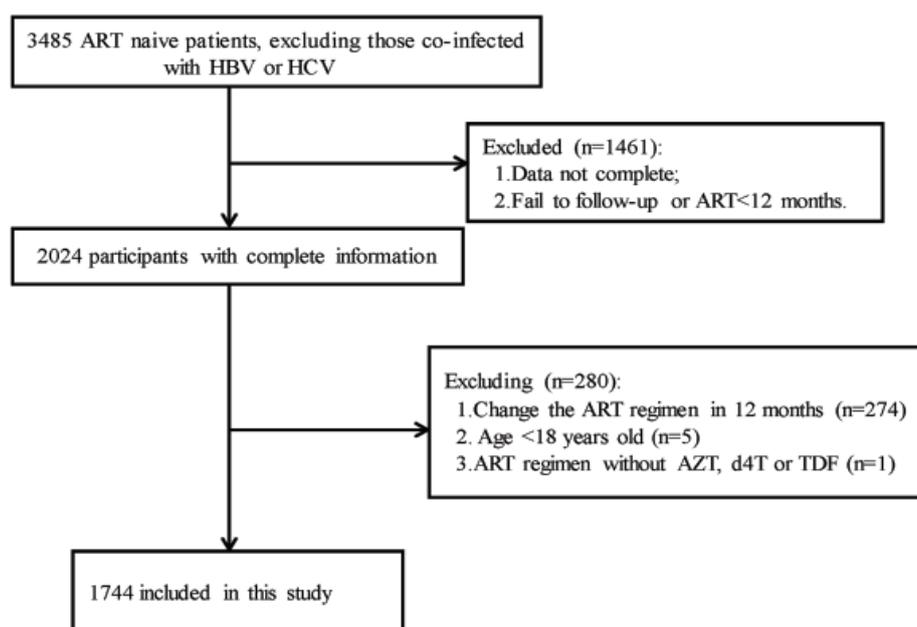
Figure 1. Flow chart of the study. Inclusion criteria of the participants in HIV voluntary consult and test clinic of SHAPHC.

were infected *via* sexual transmission: 1,017 (58.3%) were homosexual men (MSM) and 395 (22.6%) were heterosexual transmission. Blood transfusion and intravenous drug users (IDU) accounted for 1.7% and 1.5%, respectively. Those who did not know how they became infected with HIV accounted for 15.8%. Of all the participants, a fairly large proportion was at the third WHO stage. As for the timing of ART initiation, 1,187 subjects (68.1%) started ART within six months from the time they were diagnosed as being HIV positive. The mean CD4 count of our participants before they received ART was about 202 cell/µL. After one year of ART, the mean CD4 count was 340 cell/µL, with an increase of some 140 cell/µL. The most commonly used regimen in our study was two NRTIs + 1 NNRTI, in which AZT + 3TC + EFV was received by more than half of the participants (Table 1).

3.2. Prevalence and risk factors for suboptimal CD4+ T-cell recovery

One year after the initiation of ART, the CD4+ T-cell count of 723 subjects (41.5% of all 1,744 participants) was above 350 cell/µL, which was defined as the recovered group. While the CD4+ T-cell count of the remaining 1,021 participants failed to achieve the same level; it was defined as the unrecovered group. There was no significance in age between the two above groups ($p = 0.207$). There was also no difference in gender ($p = 0.461$) and marital status ($p = 0.061$) between the two above groups. However, through the chi-square test, we found that the transmission routes of the two groups had discrepancy ($p < 0.001$). Specifically, the rate of those infected with HIV

Table 1. Characteristics and analysis of the demographics of the 1,744 participants

Variable	Number (%) in 1,744 participants
Age at start of ART (Mean ± S.D.)	37.3 ± 12.0
Gender	
Male	1588 (91.1)
Female	156 (8.9)
Marital status	
Single	901 (51.7)
Married/cohabiting	692 (39.7)
Divorced/separated	120 (6.9)
Widowed	15 (0.9)
Unknown	16 (0.9)
Infectious routes	
Blood transfusion	30 (1.7)
IDU	26 (1.5)
MSM	1017 (58.3)
Heterosexual transmission	395 (22.6)
Unknown	276 (15.8)
CD4 count (Mean ± S.D.)	
At baseline	202.4 ± 166.1
At 1 year of ART	339.7 ± 181.5
Timing of the initiation of ART	
Less than 6 months	1187 (68.1)
7-12 months	151 (8.7)
13-24 months	173 (9.9)
More than 24 months	233 (13.4)
ART regimen	
AZT+3TC+EFV	1039 (59.6)
d4T+3TC+NVP	66 (3.8)
d4T+3TC+EFV	195 (11.2)
TDF+3TC+EFV	247 (14.2)
TDF+3TC+LPV/r	22 (1.3)
AZT+3TC+NVP	118 (6.8)
AZT+3TC+LPV/r	42 (2.4)
Others	15 (0.9)
WHO stage	
Stage 1	12 (0.7)
Stage 2	26 (1.5)
Stage 3	1282 (73.5)
Stage 4	424 (24.3)

Table 2. The risk factors for incomplete CD4 recovery after the first year's ART by logistic regression test

Factors	Recovered (*n* = 723)	Unrecovered (*n* = 1021)	*p* value	Univariate Analysis		Multivariate Analysis	
				Odds ratio (95% CI)	*p* value	Adjusted OR (95% CI)	*p* value
Age group (Mean ± S.D.)	36.0 ± 12.0	38.3 ± 12.0	0.207[#]				
18-44 yr., *n* (%)	569 (78.7)	718 (70.3)		0.708 (0.464-1.080)	0.109		
45-59 yr., *n* (%)	118 (16.3)	239 (23.4)		1.111 (0.699-1.766)	0.657		
≥ 60 yr., *n* (%)	36 (5.0)	64 (6.3)		Reference			
Gender			0.461				
Male, *n* (%)	654 (90.5)	934 (91.5)		1.124 (0.807-1.565)	0.490		
Female, *n* (%)	69 (9.5)	87 (8.5)		Reference			
Married status			0.061				
Married/cohabiting, *n* (%)	268 (37.1)	424 (41.5)		1. 184 (0.974-1.439)	0.090		
Unmarried/no cohabiting, *n* (%)	455 (62.9)	597 (58.5)					
Infectious route			< 0.001				
MSM, *n* (%)	455 (62.9)	562 (55.0)		Reference		Reference	
Heterosexual transmission, *n* (%)	156 (16.0)	239 (23.4)		1.227 (0.969-1.555)	0.089	0.905 (0.665-1.231)	0.525
Unsexual transmission, *n* (%)	112 (15.5)	220 (21.5)		1.548 (1.196-2.004)	0.001	0.827 (0.578-1.185)	0.302
Treatment regimen			< 0.001				
Including AZT, *n* (%)	526 (72.8)	674 (66.0)		1.409 (1.084-1.831)	0.010	2.052 (1.480-2.846)	< 0.001
Including d4T, *n* (%)	53 (7.3)	215 (21.1)		4.490 (3.064-6.581)	< 0.001	2.400 (1.531-3.762)	< 0.001
Including TDF, *n* (%)	144 (20.0)	132 (12.9)		Reference		Reference	
WHO stage			0.157				
Stage 1, 2, *n* (%)	20 (2.8)	18 (1.8)		Reference			
Stage 3, 4, *n* (%)	703 (97.2)	1003 (98.2)		1.574 (0.827-2.997)	0.168		
Timing of the initiation of ART			0.005				
Less than 6 months, *n* (%)	465 (64.3)	722 (70.7)		1.354 (1.105-1.660)	0.003	1.116 (0.879-1.418)	0.368
More than 6 months, *n* (%)	258 (35.7)	299 (29.3)		Reference		Reference	
Baseline CD4 count			0.033[#]				
(cell/μl) mean ± S.D.	285.4 ± 196.1	143.7 ± 107.5					
CD4 ≤ 200, *n* (%)	115 (15.9)	682 (66.8)		47.552 (24.675-91.641)	< 0.001	42.597 (21.927-82.752)	< 0.001
200 < CD4 ≤ 350, *n* (%)	518 (71.6)	328 (32.1)		5.155 (2.715-9.788)	< 0.001	4.519 (2.367-8.627)	< 0.001
CD4 > 350, *n* (%)	90 (12.4)	11 (1.1)		Reference		Reference	

[#] These p values were calculated by *t*-test. The others were analyzed by chi-square test.

through MSM was slightly higher in the recovered group than in the unrecovered group (62.9% *vs*. 55.0%). On the contrary, the rate of heterosexual transmission and unsexual transmission, 16.0% and 15.5%, respectively, in the recovered group was lower than that of the uncovered group, 23.4% and 21.5%, respectively.

The rate of different ART regimens was also diverse between the recovered group and the unrecovered group: the regimen included AZT (72.8% *vs*. 66.0%), d4T (7.3% *vs*. 21.1%) and TDF (20.0% *vs*. 12.9%). Surprisingly, no difference was found in the WHO stage between the two groups (*p* = 0.157). In view of the timing of ART initiation, the proportion of participants who initiated ART earlier (≤ 6 months from being diagnosed with HIV infection) was approximately 64% in the recovered group as compared to about 71% in the unrecovered group. The baseline CD4 count of the two groups showed significant differences (*p* = 0.033).

When we conducted the univariate logistic analysis, we found that among all the variables, only the ART regimen and the baseline CD4+ T-cell count were associated with suboptimal CD4+ T-cell recovery. Furthermore, the multivariate analysis showed that the lower baseline CD4+ T-cell count and the regimen including AZT and d4T, were higher risk factors for CD4+ T-cell unrecovery (Table 2).

3.3. *Follow-up situation of participants*

Among all the 1,744 participants, the CD4+ T-cell count of only 101 participants was above 350 cell/μL at baseline. After a year of ART, the CD4 count of 723 subjects was above this level. The data corresponding to the second year of ART decreased by 793 because some patients had not reached the second year of their ART, or we failed to follow up due to certain personal or impersonal factors. In the remaining 951 subjects, 476 people had a CD4+ T-cell count above 350 cell/μL. We had 455 subjects with complete information at the third year of ART, and among them 281 participants had CD4 count above 350 cell/μL (Figure 2A).

At the baseline, only 5.8% of the participants had a CD4+ T-cell count above 350 cell/μL and the CD4 recovery rate increased to 41.5% after a year of ART. After eliminating the participants with missing data, the CD4 recovery rate increased to 49.9% and 61.8% in the second and third years of ART, respectively (Figure 2B).

4. Discussion

In this study, we analysed the risk factors for incomplete CD4 recovery in the HIV-infected population of East China. We found that the ART regimen and the baseline
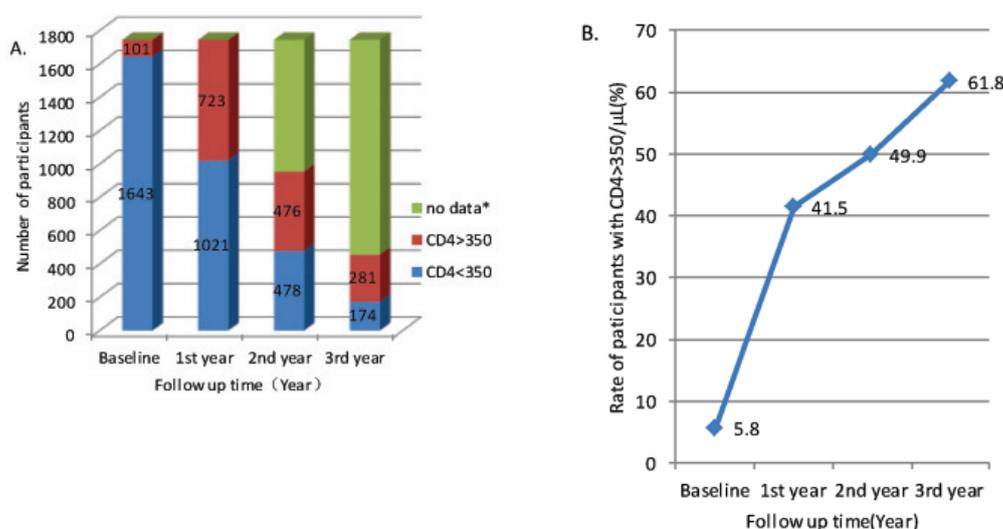
Figure 2. Review of participants' follow-up for 3 years. (A), Proportion of participants with different CD4 level or without data. **(B)**, Trend of CD4 recovery rate. * Participants who had received ART less than 3 years or without follow-up information.

of CD4+ T-cell count could impact immunological restoration. AZT, d4T and TDF are commonly used among HIV infectors in China. However, compared with TDF, the regimen including AZT and d4T were more likely to suppress the recovery of CD4+ T-cell. Those with higher baseline CD4+ T-cell count are more likely to achieve full immunological recovery.

Through statistical analysis, we drew the same conclusion that the lower baseline CD4 count is adverse to immunologic restoration. Compared with those whose baseline CD4 > 350 cell/µL, patients with CD4 between 200 and 350 cell/µL or CD4 < 200 cell/µL at ART initiation were more likely to have suboptimal immunologic responses, with the odds ratio of 42.597 (95% CI: 21.927-82.752) and 4.519 (95% CI: 2.367-8.627), respectively. All of the above results were similar with the results about predictors for incomplete CD4 recovery after HAART initiation mentioned in the US AIDS guidelines (7).

Our study also found that ART regimen could impede CD4 recovery to some extent. As different ART regimens are applied in different countries, we studied ART regimens concerning 3TC, d4T, AZT, and TDF, which are commonly used for patients and free of charge in China. Compared with the ART regimen including TDF, we found that the regimens including AZT and d4T impeded CD4 recovery, and the odds ratio were 2.052 (95% CI: 1.480-2.846) and 2.400 (95% CI: 1.531-3.762), respectively. Our result is similar to the study conducted in 2006 by Gallant JE, *et al.* and the study conducted in Senegal by G. Batista, *et al* (*8,19*). The incomplete CD4 recovery among patients with regimen including AZT or d4T can be explained by the fact that both these drugs have myelotoxicity, and there is a smaller increase of total lymphocyte count when AZT and d4T are included in an ART regimen (*20-22*). Li TS' study has demonstrated that the

thymus function of adults will gradually decline with the increase of age. It is well known that the maturity of T lymphocytes is in the thymus, thus aging undoubtedly affects CD4+ T-cell count (*23*). However, our univariate analysis showed that age was not associated with CD4+ T-cell recovery, which was inconsistent with the results in the guideline of the USA. The main reason is that the number of elder subjects (> 60 years) was not large enough comparing with other age groups (chi-square test, $p = 0.246$).

Nowadays, there is no specific standard for the early therapy of HIV/AIDS, but the current study indicated that early therapy is superior to delayed therapy, resulting in better virus suppression, less confection with other diseases, lower morbidities and better CD4+ T-cell recovery (*24*). It is difficult to determine when these patients became infected with HIV, so we substituted the diagnosis date for the infection time. We defined early therapy as initiating ART regimen less than six months from the date they received diagnosis reports, and delayed therapy was defined as more than six months from the time of confirmed diagnosis. However, in our study, we found that the timing of ART initiation was not a risk factor for incomplete CD4+ T-cell recovery (univariate analysis, OR = 1.116, 95% CI: 0.879-1.418, $p = 0.368$). Therefore, a credible way needs to be established to verify the exact time of infection for the accurate analysis of the relationship between the timing of ART initiation and treatment efficacy.

Although a high degree of concern is paid to the CD4+ T-cell recovery in the field of HIV/AIDS research, various conclusions have been obtained from different studies. An urban cohort study conducted in sub-Saharan Africa indicated that if the CD4 recovery criterion is stipulated at the cut-off of 200 cell/µL, then the recovery rates would be 57%, 58%, and 81%

BioScience Trends. 2015; 9(5):335-341.

at the sixth, twelfth, and twenty-forth months of ART, respectively (*25*). Another study conducted in Senegal declared that if suboptimal immune reconstitution is defined as the increase of CD4 count less than 50 cell/μL in patients with virologic suppression more than six months, then the recovery rate would be 84.5% after a year of ART (*8*). Our cohort study showed that the CD4 recovery rates were 41.5%, 49.9%, and 61.8% after twelve, twenty-four, and thirty-six months of ART, separately. Apparently, in the same follow-up time, the immune reconstitution rate will be higher if the recovery standard is set at a lower point. Obviously, with the longer period of having ART, the immune reconstitution of patients is more promising.

However, our study still had two limitations. Firstly, not all of the participants had their HIV-RNA levels measured at the baseline due to the high cost of the test. This test was free of charge after a year of ART. 2,241 patients out of the 3,485 participants had HIV-RNA level tests, with 2,179 people having their HIV-RNA levels lower than 1.0×10^3 copies/mL. Therefore, we can come to the conclusion that we had a satisfactory virologic suppression (97.2%). Secondly, the information of some patients was lost or incomplete due to certain reasons during the second and third years from the initiation of ART. In turn, this set limitations for us to observe the dynamic changes in CD4 recovery of all of the participants and evaluate the exact recovery rate.

In conclusion, we carried out an observational, retrospective and cohort research to study the risk factors for suboptimal CD4 recovery in the HIV infected population of Shanghai, China. We discovered that patients who had a low level of CD4+ T-cell count (< 200 cell/μL) at the initiation of ART had more difficulties recovering to the normal level. Furthermore, the regimen including AZT or d4T impedes CD4 recovery. Actually, the CD4 recovery rate is not satisfactory in our settings. To decrease the incidence of opportunistic infection and mortality in the HIV infected population, we should endeavour to facilitate the normalization of their CD4+ T-cell count. At the same time, more efforts should be made to guarantee the early diagnosis and early treatment for HIV/AIDS patients as well as optimizing antiretroviral therapy.

Acknowledgements

References

1. Oram S, Stockl H, Busza J, Howard LM, Zimmerman C. Prevalence and risk of violence and the physical, mental, and sexual health problems associated with human trafficking: Systematic review. PLoS Med. 2012; 9:e1001224.
2. Turan JM, Nyblade L. HIV-related stigma as a barrier to achievement of global PMTCT and maternal health goals: A review of the evidence. AIDS Behav. 2013; 17:2528-2539.
3. Bobkova M. Current status of HIV-1 diversity and drug resistance monitoring in the former USSR. AIDS Rev. 2013; 15:204-212.
4. Hoare J, Ransford GL, Phillips N, Amos T, Donald K, Stein DJ. Systematic review of neuroimaging studies in vertically transmitted HIV positive children and adolescents. Metab Brain Dis. 2014; 29:221-229.
5. Gelu-Simeon M, Sobesky R, Haim-Boukobza S, Ostos M, Teicher E, Fontaine H, Salmon-Ceron D, Meyer L, Trinchet JC, Paule B, Samuel D, Lewin M, Duclos-Vallee JC. Do the epidemiology, physiological mechanisms and characteristics of hepatocellular carcinoma in HIV-infected patients justify specific screening policies? AIDS. 2014; 28:1379-1391.
6. van Rensburg HC. South Africa's protracted struggle for equal distribution and equitable access – still not there. Hum Resour Health. 2014; 12:26.
7. National Institutes of Health. Guidelines for the Use of Antiretroviral Agents in HIV-1-Infected Adults and Adolescents. *https://aidsinfo.nih.gov/guidelines* (accessed May 5, 2015).
8. Batista G, Buve A, Ngom Gueye NF, Manga NM, Diop MN, Ndiaye K, Thiam A, Ly F, Diallo A, Ndour CT, Seydi M. Initial suboptimal CD4 reconstitution with antiretroviral therapy despite full viral suppression in a cohort of HIV-infected patients in Senegal. Med Mal Infect. 2015; 45:199-206.
9. Samuel R, Bettiker R, Suh B. Antiretroviral therapy 2006: Pharmacology, applications, and special situations. Arch Pharm Res. 2006; 29:431-458.
10. Manfredi R, Sabbatani S. A novel antiretroviral class (fusion inhibitors) in the management of HIV infection. Present features and future perspectives of enfuvirtide (T-20). Curr Med Chem. 2006; 13:2369-2384.
11. Calza L, Manfredi R, Pocaterra D, Chiodo F. Risk of premature atherosclerosis and ischemic heart disease associated with HIV infection and antiretroviral therapy. J Infect. 2008; 57:16-32.
12. Hester EK. HIV medications: An update and review of metabolic complications. Nutr Clin Pract. 2012; 27:51-64.
13. Hazuda DJ. HIV integrase as a target for antiretroviral therapy. Curr Opin HIV AIDS. 2012; 7:383-389.
14. Davies MA, Ford N, Rabie H, Fatti G, Stinson K, Giddy J, Tanser F, Technau KG, Sawry S, Eley B, Wood R, Mofenson LM, Keiser O, Boulle A. Reducing CD4 monitoring in children on antiretroviral therapy with virologic suppression. Pediatr Infect Dis J. 2015; 12:250-255.
15. Kasahara TM, Hygino J, Andrade RM, Monteiro C, Sacramento PM, Andrade AF, Bento CA. Poor functional immune recovery in aged HIV-1-infected patients following successfully treatment with antiretroviral therapy. Hum Immunol. 2015; 15:299-303.
16. Kolber MA, Saenz MO, Tanner TJ, Arheart KL, Pahwa S, Liu H. Intensification of a suppressive HAART regimen increases CD4 counts and decreases CD8+ T-cell activation. Clin Immunol. 2008; 126:315-321.

17. Pinzone MR, Di Rosa M, Cacopardo B, Nunnari G. HIV RNA suppression and immune restoration: Can we do better? Clin Dev Immunol. 2012; 2012:515962.

18. Nakanjako D, Ssinabulya I, Nabatanzi R, Bayigga L, Kiragga A, Joloba M, Kaleebu P, Kambugu AD, Kamya MR, Sekaly R, Elliott A, Mayanja-Kizza H. Atorvastatin reduces T-cell activation and exhaustion among HIV-infected cART-treated suboptimal immune responders in Uganda: A randomised crossover placebo-controlled trial. Trop Med Int Health. 2015; 20:380-390.

19. Gallant JE, DeJesus E, Arribas JR, Pozniak AL, Gazzard B, Campo RE, Lu B, McColl D, Chuck S, Enejosa J, Toole JJ, Cheng AK, Study G. Tenofovir DF, emtricitabine, and efavirenz *vs.* zidovudine, lamivudine, and efavirenz for HIV. N Engl J Med. 2006; 354:251-260.

20. DeJesus E, Herrera G, Teofilo E, Gerstoft J, Buendia CB, Brand JD, Brothers CH, Hernandez J, Castillo SA, Bonny T, Lanier ER, Scott TR, Team CNAS. Abacavir versus zidovudine combined with lamivudine and efavirenz, for the treatment of antiretroviral-naive HIV-infected adults. Clin Infect Dis. 2004; 39:1038-1046.

21. Huttner AC, Kaufmann GR, Battegay M, Weber R, Opravil M. Treatment initiation with zidovudine-containing potent antiretroviral therapy impairs CD4 cell count recovery but not clinical efficacy. AIDS. 2007; 21:939-946.

22. Domingo P, Cabeza Mdel C, Torres F, Salazar J, Gutierrez Mdel M, Mateo MG, Martinez E, Domingo JC, Fernandez I, Villarroya F, Ribera E, Vidal F,Baiget M. Association of thymidylate synthase polymorphisms with acute pancreatitis and/or peripheral neuropathy in HIV-infected patients on stavudine-based therapy. PLoS One. 2013; 8:e57347.

23. Li T, Wu N, Dai Y, Qiu Z, Han Y, Xie J, Zhu T, Li Y. Reduced thymic output is a major mechanism of immune reconstitution failure in HIV-infected patients after long-term antiretroviral therapy. Clin Infect Dis. 2011; 53:944-951.

24. Le T, Wright EJ, Smith DM, He W, Catano G, Okulicz JF, Young JA, Clark RA, Richman DD, Little SJ, Ahuja SK. Enhanced CD4+ T-cell recovery with earlier HIV-1 antiretroviral therapy. N Engl J Med. 2013; 368:218-230.

25. Nakanjako D, Kiragga A, Ibrahim F, Castelnuovo B, Kamya MR, Easterbrook PJ. Sub-optimal CD4 reconstitution despite viral suppression in an urban cohort on antiretroviral therapy (ART) in sub-Saharan Africa: Frequency and clinical significance. AIDS Res Ther. 2008; 5:23.

Original Article

Serum concentrations of Flt-3 ligand in rheumatic diseases

Kayo Nakamura*, Noriko Nakatsuka*, Masatoshi Jinnin**, Takamitsu Makino, Ikko Kajihara, Katsunari Makino, Noritoshi Honda, Kuniko Inoue, Satoshi Fukushima, Hironobu Ihn

Department of Dermatology and Plastic Surgery, Faculty of Life Sciences, Kumamoto University, Kumamoto, Japan.

Summary	Fms-like tyrosine kinase 3 (Flt-3) is a cytokine receptor expressed on the surface of bone-marrow progenitor of hematopoietic cells. Flt-3 ligands are produced by peripheral blood mononuclear cells, and found in various human body fluids. Flt-3 signal is involved in the regulation of vessel formation as well as B cell differentiation, suggesting that Flt-3 signal contributes to the pathogenesis of vascular abnormalities and immune dysregulation in rheumatic diseases. The aim of the present study is to examine serum Flt-3 ligand levels in patients with various rheumatic diseases, and to evaluate the possibility that serum Flt-3 ligand levels can be a useful disease marker. Sera were obtained from 20 dermatomyositis (DM) patients, 36 systemic sclerosis (SSc) patients, 10 systemic lupus erythematosus (SLE) patients, 10 scleroderma spectrum disorder (SSD) patients, 4 mixed connective tissue disease (MCTD) patients, and 12 normal subjects. Flt-3 ligand levels were determined with ELISA. Serum Flt-3 ligand levels were significantly elevated in patients with DM, SSc, SSD and MCTD compared to those in normal subjects. DM patients with elevated Flt-3 ligand levels were accompanied with significantly increased CRP levels and increased frequency of heliotrope rash than those with normal levels. In addition, SSc patients with elevated Flt-3 ligand levels showed significantly reduced frequency of nailfold bleeding. Serum Flt-3 ligand levels can be a marker of cutaneous manifestation in DM and a marker of microangiopathy in SSc. Clarifying the role of Flt-3 ligand in rheumatic diseases may lead to further understanding of these diseases and new therapeutic approaches.

Keywords: Flt-3, dermatomyositis, systemic sclerosis, systemic lupus erythematosus

1. Introduction

Immune dysfunction and vascular abnormalities are thought to be the common features in rheumatic diseases including rheumatoid arthritis (RA), polymyositis/dermatomyositis (PM/DM), systemic sclerosis (SSc), systemic lupus erythematosus (SLE), mixed connective tissue disease (MCTD) or Sjögren's syndrome (SjS) (*1,2*). For example, autoantibodies, Raynaud's phenomenon, nailfold bleeding (NFB) and skin ulcers are frequently seen in various rheumatic diseases. These vascular abnormalities are characterized by uncontrolled regeneration of the vasculature and

vascular losses due to defective maintenance of the vasculature (*3*). However, the mechanism is hardly understood, and needs to be clarified.

Fms-like tyrosine kinase 3 (Flt-3), also known as CD135, is a cytokine receptor expressed on the surface of bone marrow-derived hematopoietic progenitor cells. Activation of the receptor has been reported to regulate vessel formation as well as the blood cell differentiation. For example, Flt-3 signal is thought to play roles in the angiogenesis of malignant tumors, the process of B cell differentiation, immune response to virus infection, and aging (*4-7*). Furthermore, Flt-3 mutations are found in patients with leukemia (*8*). Thus, there is a possibility that Flt-3 signal is involved in the pathogenesis of vascular abnormalities and immune dysregulation in rheumatic diseases as well as similar dysregulation of immunity and angiogenesis such as malignancy, infection and aging.

On the other hand, Flt-3 ligands, approximately 30 kDa transmembrane glycoproteins, are produced

---
*These authors contributed equally to this works.
**Address correspondence to:*
Dr. Masatoshi Jinnin, Department of Dermatology and Plastic Surgery, Faculty of Life Sciences, Kumamoto University, 1-1-1 Honjo, Kumamoto 860-8556, Japan.
E-mail: mjin@kumamoto-u.ac.jp

by peripheral blood mononuclear cells (*9*), and can be found as soluble homodimeric proteins in various human body fluids including serum. So far, several previous studies have suggested the significance of Flt-3 ligand levels in autoimmune arthritis such as RA and primary Sjogren's syndrome: there was a significant correlation between serum Flt-3 ligand levels and disease activity in RA patients (*10,11*). However, the expression of Flt-3 ligand in other rheumatic diseases has yet to be elucidated. Therefore, in this study, we examined serum Flt-3 ligand levels in patients with various rheumatic diseases, and tried to evaluate the possibility that serum levels of Flt-3 ligand can be a useful disease marker.

2. Materials and Methods

2.1. *Clinical assessment and patient material*

Patients with SSc and SLE fulfilled the criteria proposed by the American College of Rheumatology (ACR) (*12,13*). All SSc patients were grouped into diffuse cutaneous SSc (dcSSc) and limited cutaneous SSc (lcSSc) according to the classification system proposed by LeRoy *et al*. (*14*). The concept of scleroderma spectrum disorder (SSD) was originally proposed by Maricq *et al*. to unify typical SSc, early forms of SSc and closely related disorders (*15,16*). After that, Ihn *et al*. redefined SSD as patients that did not fulfill the ACR criteria of SSc but were thought to develop SSc in the future, and proposed a new diagnostic method (*17*). Classical DM patients were diagnosed based on the criteria proposed by Bohan and Peter (*18,19*). Patients with clinically and histopathologically typical cutaneous lesions but without myositis were diagnosed as clinically amyopathic DM (CADM) according to the previous criteria (*20*). MCTD patients had clinical features of SLE, SSc and PM/DM and anti-U1RNP antibodies, but did not satisfy the criteria for these connective tissue diseases (*12,13,18,19*), and were diagnosed according to the criteria of Alarcón-Segovia (*21,22*).

Sera were obtained from randomly chosen 15 classical DM patients (age range: 27-86 years, mean ± SD: 54.1 ± 18.4; disease duration range: 1-24 months, mean ± SD: 7.4 ± 7.5), 5 CADM patients (age range: 33-81 years, mean ± SD: 61.4 ± 19.4; disease duration range: 1-108 months, mean ± SD: 31.2 ± 38.5), 36 patients with SSc (13 dcSSc and 23 lcSSc, age range: 24-85 years, mean ± SD: 62.2 ± 14.6; disease duration range: 1-768 months, mean ± SD: 75.0 ± 151.7), 10 SSD patients (age range: 44-75 years, mean ± SD: 54.9 ± 10.7; disease duration range: 1-120 months, mean ± SD: 27.9 ± 40.1), 10 SLE patients (age range: 23-57 years, mean ± SD: 35.0 ± 11.9; disease duration range: 2-84 months, mean ± SD: 21.3 ± 27.6) and 4 MCTD patients (age range: 44-73 years, mean ± SD:

59.8 ± 12.6; disease duration range: 24-228 months, mean ± SD: 123.0 ± 83.4). Clinical and laboratory data reported in this study were obtained at the time of serum sampling. None of the patients received systemic treatments such as steroid or immunosuppressant at the serum sampling.

Control serum samples were also collected from 12 normal subjects (age range = 32-81 years, mean ± SD: 47.1 ± 16.4). All serum samples were stored at − 80°C prior to use. Institutional review board approval and written informed consent were obtained before patients and healthy volunteers were entered into this study according to the Declaration of Helsinki.

2.2. *Nailfold bleeding*

Nailfold bleeding (NFB) was evaluated macroscopically by the presence of splinter hemorrhages of the nailfold capillaries in more than one finger by 2 investigators in a blinded manner.

2.3. *Serum concentrations of Flt-3 ligand*

Levels of serum Flt-3 ligand were measured with a specific ELISA kit (R&D Systems, Minneapolis, MN, USA) (*23*). Briefly, anti-Flt-3 ligand monoclonal antibodies were precoated onto microtiter wells. Aliquots of serum were added to each well, followed by the addition of peroxidase-conjugated antibodies to Flt-3 ligand. Color was developed with hydrogen peroxide and tetramethylbenzidine peroxidase, and the absorbance at 450 nm was measured. Wavelength correction was performed by absorbance at 540 nm. The concentration of Flt-3 ligand in each sample was determined by interpolation from a standard curve.

2.4. *Statistical analysis*

Statistical analysis was carried out with Mann-Whitney U test for the comparison of medians, and Fisher's exact probability test for the analysis of frequency. *p* values less than 0.05 were considered significant. Receiver operating characteristic (ROC) curve analysis was performed to evaluate the diagnostic performance of Flt-3 ligand levels using GraphPad Prism ver. 5.01 (MDF software, Tokyo, Japan).

3. Results

3.1. *Serum concentrations of Flt-3 ligand in patients with various rheumatic diseases*

The serum Flt-3 ligand levels in patients with various rheumatic diseases are shown in Figure 1. Serum samples were obtained from 20 DM patients (including 5 CADM patients), 36 SSc patients, 10 SSD patients, 10 SLE patients, 4 MCTD patients, and 12 normal

subjects. SSD patients did not fulfill the criteria of SSc but were thought to develop SSc in the future, while CADM patients had typical cutaneous lesions of DM but lacked myositis (*15-17,20*).
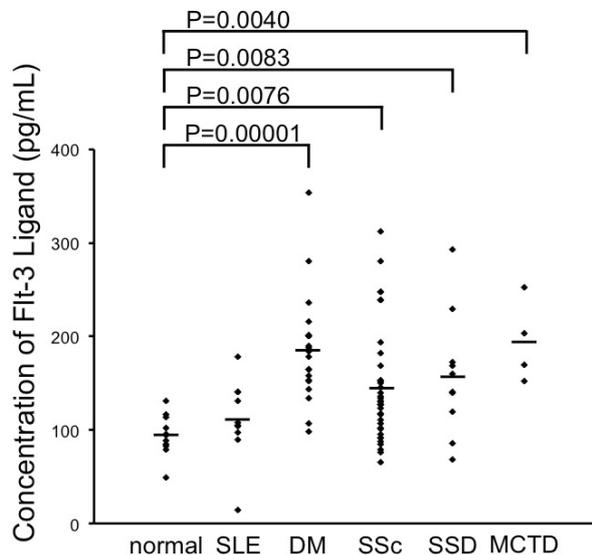

Figure 1. The serum levels of Flt-3 ligand in rheumatic diseases. Levels of Flt-3 ligand in sera of patients with systemic lupus erythematosus (SLE, *n* = 10), dermatomyositis (DM, *n* = 20), systemic sclerosis (SSc, *n* = 36), scleroderma spectrum disorder (SSD, n = 10), mixed connective tissue disease (MCTD, *n* = 4) and normal subjects (*n* = 12) were analyzed with ELISA. Bars show the means.

The mean age of normal subjects was 47.1 years, and the ratio of female was 75.0%. Summary of clinical/laboratory features in patients with these rheumatic diseases enrolled in this study are shown in Tables and Supplemental Tables. For example, in DM patients, the mean age at the serum sampling was 56.0 years, and mean CK levels were 2,400.8 IU/L (normal values; 57-284 IU/L for male and 45-176 IU/L for female) (Table 1). Among the rheumatic diseases, DM patients had elevated serum Flt-3 ligand concentration (mean ± SD: 185.1 ± 57.4 pg/mL), and there was a statistically significant difference in the values between DM patients and normal subjects (94.4 ± 21.0 pg/mL, *p* = 0.000011, Figure 1). According to the manufacturer's data, mean normal serum Flt-3 ligand level was 93.9 pg/mL, which is consistent with our results. In ROC curve analysis for serum Flt-3 ligand levels to distinguish DM patients from normal subjects, the area under the curve (AUC) was 0.9708 (95% confidence interval; 0.9219-1.020, Figure 2A): AUC more than 0.9 means that the level of Flt-3 ligand is useful for diagnosis of DM patients. When the most optical cut-off point was set at 132.8 pg/mL according to the Youden index (0.90), the sensitivity was 90.0% and the specificity was 100.0%. There were no significant differences between patients with classical DM and CADM (189.9 ± 52.4 *vs.* 170.8 ± 55.0 pg/mL, *p* = 0.51, Figure 2B).

Levels of serum Flt-3 ligand also showed significant elevation in patients with SSc compared to in normal

Table 1. Correlation of serum Flt-3 ligand levels with clinical/serological features in patients with dermatomyositis

Items	All patients (*n* = 20)	Serum Flt-3 ligand	
		Patients with elevated Flt-3 ligand levels (*n* = 10)	Patients with normal Flt-3 ligand levels (*n* = 10)
Age at the time of serum sampling (mean years)	56.0	61.9	50.0
Gender (ratio of female, %)	60.0	50.0	70.0
Duration of disease (mean months)	13.4	6.3	20.3
Type (DM:CADM)	15:5	8:2	7:3
Clinical features			
Gottron's sign (%)	83.3	100.0	70.0
Heliotrope rash (%)	75.0	100.0*	50.0
Laboratory features			
IgG (mg/dL)	1379.2	1365.4	1392.9
CK (IU/L)	2400.8	2155.2	2646.4
Myoglobin (ng/mL)	694.6	602.6	786.7
Aldolase (U/L)	37.0	21.6	50.7
CRP (mg/dL)	0.83	1.48*	0.19
Organ involvement			
Muscle weakness (%)	76.5	87.5	66.7
Interstitial kung disease (%)	35.3	42.6	30.0
Dysphasia (%)	30.8	40.0	20.0
Joint (%)	28.6	50.0	20.0
ANA specificity			
ANA (+)	50.0	70.0	30.0
(levels, index)	48.6	67.3	20.5
Anti-Jo-1 (%)	10.0	10.0	10.0
(levels, IU/mL)	1.68	1.74	1.61

The cut-off vale was set at the mean + 4SD of the value in healthy control subjects. DM, dermatomyositis; CADM, clinicallyamyopathic dermatomyositis; CK, creatin kinase; ANA, antinuclear antibodies; Anti-Jo-1, Anti-Jo-1 antibodies. * *p* < 0.05, versus patients with normal Flt-3 ligand levels using Fisher's exact probability test.
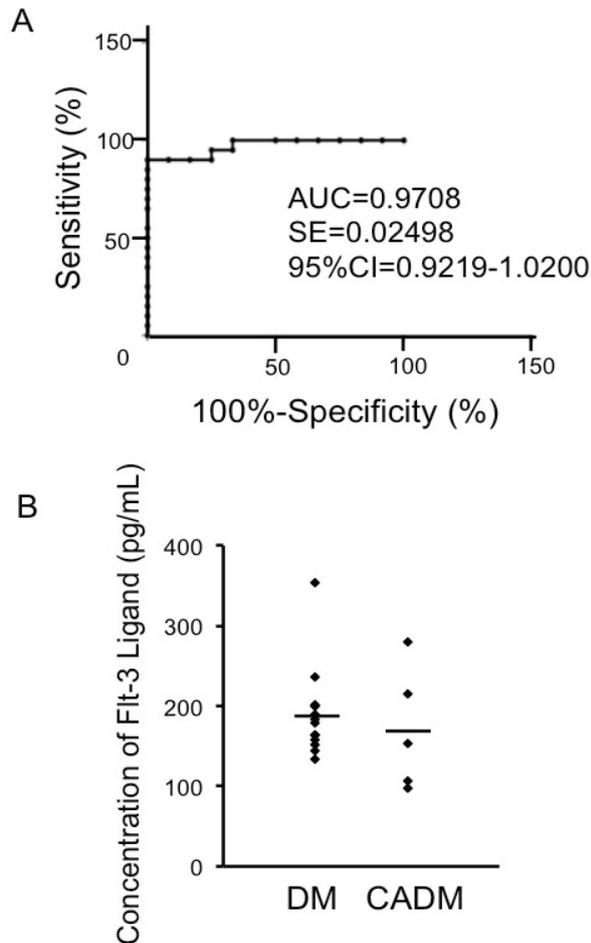
Figure 2. The serum levels of Flt-3 ligand in dermatomyositis. (A) Receiver operating characteristic (ROC) curve for serum Flt-3 ligand to distinguish dermatomyositis (DM) patients from normal subjects. AUC; areas under curves, SE; standard error, CI; confidence interval. **(B)** Levels of Flt-3 ligand in sera of patients with classical DM (*n* = 15) and clinically amyopathic DM (CADM, *n* = 5) were analyzed with ELISA. Bars show the means.

Figure 3. The serum levels of Flt-3 ligand in systemic sclerosis. (A) Receiver operating characteristic (ROC) curve for serum Flt-3 ligand to distinguish systemic sclerosis (SSc) patients from normal subjects. AUC; areas under curves, SE; standard error, CI; confidence interval. **(B)** Levels of Flt-3 ligand in sera of patients with diffuse cutaneous SSc (dcSSc, *n* = 13) and limited cutaneous SSc (lcSSc, *n* = 23) were analyzed with ELISA. Bars show the means.

subjects (144.7 ± 60.9 *vs*. 94.4 ± 21.0 pg/mL, *p* = 0.0026). In ROC curve analysis for serum Flt-3 ligand levels to distinguish SSc patients from normal subjects, AUC was 0.7928 (95% confidence interval; 0.6655-0.9202, Figure 3A): AUC more than 0.7 indicates sufficient diagnostic performance of serum Flt-3 ligand levels. When the most optical cut-off point was set at 114.8 pg/mL by the Youden index (0.56), the sensitivity and specificity were 63.9% and 91.7%, respectively. We could not find any significant differences in Flt-3 ligand levels between dcSSc patients and lcSSc patients (139.8 ± 69.1 *vs*. 147.6 ± 57.3 pg/mL, *p* = 0.72, Figure 3B).

Patients with SSD and MCTD also showed significantly higher serum Flt-3 ligand levels than normal subjects (157.7 ± 65.9 *vs*. 94.4 ± 21.0 pg/mL, *p* = 0.0083 and 194.3 ± 44.1 vs. 94.4 ± 21.0 pg/mL, *p* = 0.0040, respectively) (Supplemental Tables 1 and 2, *http://www.biosciencetrends.com/docindex. php?year=2015&kanno=5*). On the other hand, serum Flt-3 ligand levels were slightly higher in patients

with SLE compared with normal subjects, but the difference was not statistically significant (111.0 ± 43.3 *vs*. 94.4 ±21.0 pg/mL, *p* = 0.25) (Supplemental Table 3, *http://www.biosciencetrends.com/docindex. php?year=2015&kanno=5*).

Taken together, significant increases of serum Flt-3 ligand levels were found in patients with DM, SSc, SSD, and MCTD. When the cut-off value was set at the mean + 2SD of Flt-3 ligand levels in normal subjects (136.4 pg/mL), all the values in normal subjects were below the cut-off. On the other hand, increased serum Flt-3 ligand levels were found in 17 of the 20 DM patients (85.0%), 14 of the 36 SSc patients (38.9%), 7 of the 10 SSD patients (70.0%), all of the 4 MCTD patients (100.0%) and 3 of the 10 SLE patients (30.0%). Furthermore, when the cut-off was set at mean + 4SD of values in normal subjects (178.5 pg/mL), increased serum Flt-3 ligand levels were seen in 10 of the 20 DM patients (50.0%), 8 of the 36 SSc patients (22.2%), 2 of the 10 SSD patients (20.0%), and 2 of the 4 MCTD patients (50.0%).

Table 2. Correlation of serum Flt-3 ligand levels with clinical/serological features in patients with systemic sclerosis

Items	All patients (*n* = 36)	Serum Flt-3 ligand	
		Patients with elevated Flt-3 ligand levels (*n* = 14)	Patients with normal Flt-3 ligand levels (*n* = 22)
Age at the time of serum sampling (mean years)	62.2	64.9	60.3
Gender (ratio of female, %)	77.7	75.0	77.2
Duration of disease (mean months)	75.0	58.2	86.6
Type (diffuse:limited)	13:23	6:8	7:15
m-TSS	11.0	11.6	10.5
Clinical features			
Pitting scars (%)	43.8	50.0	40.0
Ulcers (%)	32.0	20.0	40.0
Nailfold bleeding (%)	48.7	26.7*	63.6
Raynaud's phenomenon (%)	90.3	100.0	84.2
Telangiectasia (%)	23.1	18.2	26.7
Contracture of phalanges (%)	85.7	100.0	77.8
Calcinosis (%)	5.9	0.0	10.0
Diffuse pigmentation (%)	28.6	42.9	21.4
Short SF (%)	75.0	85.7	70.6
Sicca symptoms (%)	53.9	45.5	60.0
Laboratory features			
CRP (mg/dL)	0.75	0.95	0.57
Organ involvement			
Pulmonary fibrosis (%)	37.1	35.7	38.1
Mean %VC (%)	102.9	100.0	104.9
Mean %DLCO (%)	87.0	85.1	88.4
Pulmonary hypertension (%)	28.1	27.0	29.0
Esophagus (%)	20.6	35.7	10.0
Heart (%)	29.4	28.6	30.0
Kidney (%)	0.0	0.0	0.0
Joint (%)	57.9	71.4	50.0
Thrombosis (%)	0.0	0.0	0.0
ANA specificity			
Anti-topo I (%)	27.8	21.4	31.8
(levels, IU/mL)	36.7	33.8	39.6
Anti-centromere (%)	38.9	50.0	31.8
(levels, IU/mL)	74.5	73.0	76.1
Anti-U1 RNP (%)	16.7	21.4	13.6
(levels, IU/mL)	10.4	12.9	7.9
Anti-SS-A (%)	30.6	57.1	13.6
(levels, IU/mL)	28.0	22.6	32.3

The cut-off vale was set at the mean + 2SD of the value in healthy control subjects. m-TSS, modified Rodnan's total skin thickness score; SF, sublingual frenulum; VC, vital capacity; DLco, diffusion capacity for carbon monooxidase; ANA, antinuclear antibodies; Anti-topo I, anti-topoisomerase I antibody; Anti-centromere, anti-centromere antibodies; Anti-U1 RNP, anti-U1 RNP antibodies; Anti-SS-A, anti-SS-A antibodies. * $p < 0.05$ versus patients with normal Flt-3 ligand levels using Fisher's exact probability test.

3.2. *Correlation of serum Flt-3 ligand levels with clinical manifestations and laboratory data in patients with DM or SSc*

Then we examined correlation of serum Flt-3 ligand levels with clinical and serological features of patients with DM or SSc. As shown in Table 1, when Flt-3 ligand levels > mean + 4SD of the values in normal subjects (178.5 pg/mL) were regarded as elevated, DM patients with elevated Flt-3 ligand levels tended to be accompanied with heliotrope rash at a significantly higher prevalence than those with normal levels (100.0% *vs.* 50.0%, *p* = 0.029). Furthermore, C-reactive protein (CRP) levels (normal values; < 0.3 mg/dL) in DM patients with elevated Flt-3 ligand levels were significantly higher than in those without (1.48 *vs.* 0.19 mg/dL, *p* = 0.019). We could not find any significant

differences between patients with and without elevated Flt-3 ligand levels in terms of the frequency of Gottron's sign, the levels of muscle enzymes, or the positive rates and the levels of antinuclear antibody (ANA) and Jo-1 antibody. Duration of disease (between the onset of symptoms and the first hospital visit) was slightly shorter in patients with elevated Flt-3 ligand levels, but not statistically significant.

On the other hand, when SSc patients were divided into two groups according to the cut-off value (136.4 pg/dL, mean + 2SD of normal subjects), patients with elevated Flt-3 ligand levels showed a significantly reduced prevalence of NFB as compared to those with normal levels (26.7 *vs.* 63.6%, *p* = 0.027, Table 2). There were no significant differences between patients with elevated Flt-3 ligand levels and those with normal levels in the frequency of major organ involvements

or other vascular involvements including Raynaud's phenomenon, thrombosis, pitting scar or telangiectasia. Furthermore, CRP levels were not significantly different between the two groups. The positive rates and the levels of antibodies against topoisomerase I, centromere, U1 RNP or SS-A were not significantly different between patients with and without elevated Flt-3 ligand levels. Duration of disease was shorter in patients with elevated Flt-3 ligand levels, albeit insignificant.

4. Discussion

We demonstrated several novel findings in this study. First, levels of serum Flt-3 ligand were significantly elevated in patients with DM, SSc, SSD, and MCTD compared to normal subjects. Second, SSc patients with elevated Flt-3 ligand levels showed significantly reduced prevalence of NFB compared to those with normal levels. And lastly, in DM patients, those with elevated Flt-3 ligand levels were accompanied with significantly increased CRP levels and increased frequency of heliotrope rash than those with normal levels.

NFB is one of the earliest vascular events in SSc, and the main factor of the diagnostic criteria for SSD. Although we also performed capillaroscopy on several SSc patients with or without increased serum Flt-3 ligand levels, we could not find any significant differences in the frequency of capillaroscopic findings including bleeding, dilated loops and giant loops between the two groups, probably because the number of patients determined was limited and insufficient to allow statistically based conclusions. Considering the significant elevation of Flt-3 ligand levels in SSD patients and the reduced frequency of NFB in SSc patients with elevated Flt-3 ligand levels, there is a possibility that Flt-3 ligand may start to elevate at the prodromal stage of SSc, and have suppressive effect on NFB. Increased Flt-3 ligand levels may activate Flt-3 signal, and may stimulate vascular formation to repair vascular abnormalities of NFB in these patients.

Although patients in this study were randomly chosen, DM patients showed high CK levels (2,400.8 IU/L) and high CRP levels (0.83 mg/dL) on average. Thus, one of the reasons why DM patients showed the elevated serum Flt-3 ligand values is possibly due to their high disease activities at the sampling point. Higher CRP levels and a higher frequency of heliotrope rash in DM patients with elevated Flt-3 ligand levels indicated that an abnormal increase of Flt-3 ligand may be correlated with the disease activity and the formation of the skin lesions. Crowson *et al.* previously reported that skin lesions of DM showed more severe endothelial injury, telangiectasia, and deposition of fibrin or C5b-9 on vessels than those of lupus erythematosus, whereas the density of superficial vascular plexus was lower

in lesions of DM compared to lupus erythematosus (*24*). Several investigators also have demonstrated a marked reduction of capillary number in the involved muscles of DM (*25,26*). These results indicate that vascular abnormalities are present in DM, and play a role in the pathogenesis of skin lesions. Given that Flt-3 signals may be mediated in the vessel formation process, and that uncontrolled activation of angiogenic factors rather than their inactivation is thought to cause vascular abnormalities in rheumatic diseases (*27,28*). The excessive expression of Flt-3 ligands in DM may also induce dysregulation of the vessel formation, resulting in the formation of heliotrope rash. Consistently, MCTD patients included in this study were accompanied with heliotrope rash, and showed the highest Flt-3 ligand levels among rheumatic diseases, although we could not determine ROC curve analysis or the association with clinical/laboratory findings due to the small number of the patients. On the other hand, although SLE patients are sometimes accompanied with a variety of microangiopathy phenotypes, weaker changes of vessels in SLE than in DM as described above may explain the lower serum Flt-3 ligand levels in SLE.

Taken together, our results suggested that Flt-3 signal may play a different role in each rheumatic disease. Telangiectasia and endothelial injury are commonly observed both in skin lesions of DM including heliotrope rash and in the microangiopathy such as NFB (*24,29*), which may be associated with increased Flt-3 ligand levels in patients with DM or SSc. However, there are also several differences between these two abnormalities (*e.g.* distribution or the presence of bleeding). Further researches on the similarities and the dissimilarities are needed in the future.

On the other hand, we had expected that the association of serum Flt-3 ligand levels and immunodysfunction in patients with DM or SSc, but the positive rates and the levels of ANA or other antibodies were not significantly different between patients with and without elevated serum Flt-3 ligand levels.

As the limitation of this study, because the onset ages of SSc, DM, SLE, and MCTD were usually different (*30,31*), the patients were not age-matched. There was no correlation between serum Flt-3 ligand levels and the age of individuals included in this study ($r = 0.399$). Furthermore, Kinn *et al.* have reported that the expression levels of Flt-3 ligand in healthy skin did not show any significant correlation with aging (*7*), and Metcalf *et al.* have suggested that Flt-3 ligand levels in peripheral blood mononuclear cells were similar between adult people and old people (*32*). Thus, the direct correlation between aging and serum Flt-3 ligand levels is not obvious. However, the mean ages of both SSc and DM patients were higher than that of SLE patients, and the levels of Flt-3 ligand in SSc and DM

were higher than those in SLE. Additionally, the mean age of DM or SSc patients with elevated Flt-3 ligand levels tended to be older than the counterpart. Because normal aging is usually associated with minimal/chronic inflammation coined by inflammaging, there is a possibility that the difference of Flt-3 ligand levels can be explained by aging factor. Future studies to measure circulating levels of Flt-3 or Flt-3 ligand in normal aging as well as malignancy or viral infection are needed. On the other hand, albeit insignificant, disease duration of the elevated Flt-3 ligand groups in both SSc and DM patients was shorter than the counterpart. This result suggests that these patients may have more severe symptoms. These points should also be clarified in the future by larger studies.

In conclusion, serum Flt-3 ligand levels may be a marker of cutaneous manifestations in DM patients and a marker of microangiopathy in SSc patients. Clarifying the role of Flt-3 ligand in rheumatic disease by systematic approach is required for further understanding of the diseases and new therapeutic approaches.

Acknowledgements

References

1. Lyons R, Narain S, Nichols C, Satoh M, Reeves WH. Effective use of autoantibody tests in the diagnosis of systemic autoimmune disease. Ann N Y Acad Sci. 2005; 1050:217-228.
2. Szekanecz Z, Koch AE. Vascular involvement in rheumatic diseases: 'vascular rheumatology'. Arthritis Res Ther. 2008; 10:224.
3. Mulligan-Kehoe MJ, Simons M. Vascular disease in scleroderma: Angiogenesis and vascular repair. Rheum Dis Clin North Am. 2008; 34:73-79.
4. Wilhelm SM, Carter C, Tang L, *et al*. BAY 43-9006 exhibits broad spectrum oral antitumor activity and targets the RAF/MEK/ERK pathway and receptor tyrosine kinases involved in tumor progression and angiogenesis. Cancer Res. 2004; 64:7099-7109.
5. Li LX, Goetz CA, Katerndahl CD, Sakaguchi N, Farrar MA. A Flt3- and Ras-dependent pathway primes B cell development by inducing a state of IL-7 responsiveness. J Immunol. 2010; 184:1728-1736.
6. Smith JR, Thackray AM, Bujdoso R. Reduced herpes simplex virus type I latency in Flt-3 ligand-treated mice is associated with enhanced numbers of natural killer and dendritic cells. Immunology 2001; 102:352-358.
7. Kinn PM, Holdren GO, Westermeyer BA, Abuissa M, Fischer CL, Fairley JA, Brogden KA, Brogden NK. Age-dependent variation in cytokines, chemokines, and

8. Nakao M, Yokota S, Iwai T, Horiike S, Kashima K, Sonoda Y, Fujimoto T, Misawa S. Internal tandem duplication of the flt3 gene found in acute myeloid leukemia. Leukemia. 1996; 10:1911-1918.
9. Stirewalt DL, Radich JP. The role of FLT3 in haematopoietic malignancies. Nat Rev Cancer. 2003; 3:650-665.
10. Tobón GJ, Renaudineau Y, Hillion S, Cornec D, Devauchelle-Pensec V, Youinou P, Pers JO. The Fms-like tyrosine kinase 3 ligand, a mediator of B cell survival, is also a marker of lymphoma in primary Sjögren's syndrome. Arthritis Rheum. 2010; 62:3447-3456.
11. Ramos MI, Perez SG, Aarrass S, Helder B, Broekstra P, Gerlag DM, Reedquist KA, Tak PP, Lebre MC. FMS-related tyrosine kinase 3 ligand (Flt3L)/CD135 axis in rheumatoid arthritis. Arthritis Res Ther. 2013; 15:R209.
12. Subcommittee for scleroderma criteria of the American rheumatism association diagnostic and therapeutic criteria committee. Preliminary criteria for the classification of systemic sclerosis (scleroderma). Arthritis Rheum. 1980; 23:581-590.
13. Hochberg MC. Updating the American College of Rheumatology revised criteria for the classification of systemic lupus erythematosus. Arthritis Rheum. 1997; 40:1725.
14. LeRoy EC, Black C, Fleischmajer R, Jablonska S, Krieg T, Medsger TA, Rowell N, Wollheim F. Scleroderma (systemic sclerosis): Classification, subsets and pathogenesis. J Rheumatol. 1988; 15:202-205.
15. Maricq HR, Weinrich MC, Keil JE, Smith EA, Harper FE, Nussbaum AI, Leroy EC, McGregor AR, Diat F, Rosal EJ. Prevalence of scleroderma spectrum disorders in the general population of South Carolina. Arthritis Rheum. 1989; 32:998-1006.
16. Maricq HR, Mcgregor AR, Diat F, Smith EA, Maxwell DB, LeRoy EC, Weinrich MC. Major clinical diagnoses found among patients with Raynaud phenomenon from the general population. J Rheumatol. 1990; 17:1171-1176.
17. Ihn H, Sato S, Tamaki T, Soma Y, Tsuchida, Ishibashi Y, Takehara K. Clinical evaluation of scleroderma spectrum disorders using a points system. Arch Dermatol Res. 1992; 284:391-395.
18. Bohan A, Peter JB. Polymyositis and dermatomyositis (first of two parts). N Engl J Med. 1975; 292:344-347.
19. Bohan A, Peter JB. Polymyositis and dermatomyositis (second of two parts). N Engl J Med. 1975; 292:403-407.
20. Sontheimer RD. Cutaneous features of classic dermatomyositis and amyopathic dermatomyositis. Curr Opin Rheumatol. 1999; 11:475-482.
21. Alarcón-Segovia, D, Delezé M, Oria, CV, Sanchez-Guerrero J, Gómez-Pacheco L, Cabiedes J, Fernández L, Ponce de León S. Antiphospholipid antibodies and the antiphospholipid syndrome in systemic lupus erythematosus a prospective analysis of 500 consecutive patients. Medicine. 1989; 68:353-365.
22. Ihn H, Yamane K, Yazawa N, Kubo M, Fujimoto M, Sato S, Kikuchi K, Tamaki K. Distribution and antigen specificity of anti-U1RNP antibodies in patients with systemic sclerosis. Clin Exp Immunol. 1999; 117:383-387.
23. Papadaki HA, Damianaki A, Pontikoglou C, Pyrovolaki K, Eliopoulos DG, Stavroulaki E, Eliopoulos GD.

Increased levels of soluble flt-3 ligand in serum and long-term bone marrow culture supernatants in patients with chronic idiopathic neutropenia. Br J Haematol. 2006; 132:637-639.

24. Crowson AN, Maqro CM. The role of microvascular injury in the pathogenesis of cutaneous lesions of dermatomyositis. Hum Pathol. 1996; 27:15-19.

25. Dalakas MC. Review: An update on inflammatory and autoimmune myopathies. Neuropathol Appl Neurobiol. 2011; 37:226-242.

26. Mammen AL. Dermatomyositis and polymyositis: Clinical presentation, autoantibodies, and pathogenesis. Ann NY Acad Sci. 2010; 1184:134-153.

27. Distler O, Distler JHW, Scheid A, Acker T, Hirth A, Rethage J, Michel BA, Gay RE, Müller-Ladner U, Matucci-Cerinic M, Plate KH, Gassmann M, Gay S. Uncontrolled expression of vascular endothelial growth factor and its receptors leads to insufficient skin angiogenesis in patients with systemic sclerosis. Circ Res. 2004; 95:109-116.

28. Jinnin M, Makino T, Kajihara I, Honda N, Makino K, Ogata A, Ihn H. Serum levels of soluble vascular endothelial growth factor receptor-2 in patients with systemic sclerosis. Br J Dermatol. 2010; 162:751-758.

29. Walker JG, Stirling J, Beroukas D, Dharmapatni K, Haynes DR, Smith MD, Ahern MJ, Roberts-Thomson PJ. Histopathological and ultrastructural features of dermal telangiectasias in systemic sclerosis. Pathology. 2005; 37:220-225.

30. Ohta A, Nagai M, Nishina M, Tomimitsu H, Kohsaka H. Age at onset and gender distribution of systemic lupus erythematosus, polymyositis/dermatomyositis, and systemic sclerosis in Japan. 2013; 23:759-764.

31. Maldonado ME, Perez M, Pignac-Kobinger J, Marx ET, Tozman EM, Greidinger EL, Hoffman RW. Clinical and immunologic manifestations of mixed connective tissue disease in a Miami population compared to a Midwestern US caucasian population. J Rheumatol. 2008; 35:429-437.

32. Metcalf TU, Cubas RA, Ghneim K, Cartwright MJ, Grevenynghe JV, Richner JM, Olagnier DP, Wilkinson PA, Cameron MJ, Park BS, Hiscott JB, Diamond MS, Wertheimer AM, Nikolich-Zugich J, Haddad EK. Global analyses revealed age-related alterations in innate immune responses after stimulation of pathogen recognition receptors. Aging Cell. 2015; 14:421-432.

BST
BioScience Trends

Guide for Authors

1. Scope of Articles

BioScience Trends is an international peer-reviewed journal. BioScience Trends devotes to publishing the latest and most exciting advances in scientific research. Articles cover fields of life science such as biochemistry, molecular biology, clinical research, public health, medical care system, and social science in order to encourage cooperation and exchange among scientists and clinical researchers.

2. Submission Types

Original Articles should be well-documented, novel, and significant to the field as a whole. An Original Article should be arranged into the following sections: Title page, Abstract, Introduction, Materials and Methods, Results, Discussion, Acknowledgments, and References. Original articles should not exceed 5,000 words in length (excluding references) and should be limited to a maximum of 50 references. Articles may contain a maximum of 10 figures and/or tables.

Brief Reports definitively documenting either experimental results or informative clinical observations will be considered for publication in this category. Brief Reports are not intended for publication of incomplete or preliminary findings. Brief Reports should not exceed 3,000 words in length (excluding references) and should be limited to a maximum of 4 figures and/or tables and 30 references. A Brief Report contains the same sections as an Original Article, but the Results and Discussion sections should be combined.

Reviews should present a full and up-to-date account of recent developments within an area of research. Normally, reviews should not exceed 8,000 words in length (excluding references) and should be limited to a maximum of 100 references. Mini reviews are also accepted.

Policy Forum articles discuss research and policy issues in areas related to life science such as public health, the medical care system, and social science and may address governmental issues at district, national, and international levels of discourse. Policy Forum articles should not exceed 2,000 words in length (excluding references).

Case Reports should be detailed reports of the symptoms, signs, diagnosis, treatment, and follow-up of an individual patient. Case reports may contain a demographic profile of the patient but usually describe an unusual or novel occurrence. Unreported or unusual side effects or adverse interactions involving medications will also be considered. Case Reports should not exceed 3,000 words in length (excluding references).

News articles should report the latest events in health sciences and medical research from around the world. News should not exceed 500 words in length.

Letters should present considered opinions in response to articles published in BioScience Trends in the last 6 months or issues of general interest. Letters should not exceed 800 words in length and may contain a maximum of 10 references.

3. Editorial Policies

Ethics: BioScience Trends requires that authors of reports of investigations in humans or animals indicate that those studies were formally approved by a relevant ethics committee or review board.

Conflict of Interest: All authors are required to disclose any actual or potential conflict of interest including financial interests or relationships with other people or organizations that might raise questions of bias in the work reported. If no conflict of interest exists for each author, please state "There is no conflict of interest to disclose".

Submission Declaration: When a manuscript is considered for submission to BioScience Trends, the authors should confirm that 1) no part of this manuscript is currently under consideration for publication elsewhere; 2) this manuscript does not contain the same information in whole or in part as manuscripts that have been published, accepted, or are under review elsewhere, except in the form of an abstract, a letter to the editor, or part of a published lecture or academic thesis; 3) authorization for publication has been obtained from the authors' employer or institution; and 4) all contributing authors have agreed to submit this manuscript.

Cover Letter: The manuscript must be accompanied by a cover letter signed by the corresponding author on behalf of all authors. The letter should indicate the basic findings of the work and their significance. The letter should also include a statement affirming that all authors concur with the submission and that the material submitted for publication has not been published previously or is not under consideration for publication elsewhere. The cover letter should be submitted in PDF format. For example of Cover Letter, please visit http://www.biosciencetrends.com/downcentre.php (Download Centre).

Copyright: A signed JOURNAL PUBLISHING AGREEMENT (JPA) form must be provided by post, fax, or as a scanned file before acceptance of the article. Only forms with a hand-written signature are accepted. This copyright will ensure the widest possible dissemination of information. A form facilitating transfer of copyright can be downloaded by clicking the appropriate link and can be returned to the e-mail address or fax number noted on the form (Please visit Download Centre). Please note that your manuscript will not proceed to the next step in publication until the JPA Form is received. In addition, if excerpts from other copyrighted works are included, the author(s) must obtain written permission from the copyright owners and credit the source(s) in the article.

Suggested Reviewers: A list of up to 3 reviewers who are qualified to assess the scientific merit of the study is welcomed. Reviewer information including names, affiliations, addresses, and e-mail should be provided at the same time the manuscript is submitted online. Please do not suggest reviewers with known conflicts of interest, including participants or anyone with a stake in the proposed research; anyone from the same institution; former students, advisors, or research collaborators (within the last three years); or close personal contacts. Please note that the Editor-in-Chief may accept one or more of the proposed reviewers or may request a review by other qualified persons.

Language Editing: Manuscripts prepared by authors whose native language is not English should have their work proofread by a native English speaker before submission. If not, this might delay the publication of your manuscript in BioScience Trends.

The Editing Support Organization can provide English proofreading, Japanese-English translation, and Chinese-English translation services to authors who want to publish in BioScience Trends and need assistance before submitting a manuscript. Authors can visit this organization directly at http://www.iacmhr.com/iac-eso/support.php?lang=en. IAC-ESO was established to facilitate manuscript preparation by researchers whose native language is not English and to help edit works intended for international academic journals.

4. Manuscript Preparation

Manuscripts should be written in clear, grammatically correct English and submitted as a Microsoft Word file in a single-column format. Manuscripts must be paginated and typed in 12-point Times New Roman font with 24-point line spacing. Please do not embed figures in the text. Abbreviations should be used as little as possible and should be explained at first mention unless the term is a well-known abbreviation (*e.g.* DNA). Single words should not be abbreviated.

Title Page: The title page must include 1) the title of the paper (Please note the title should be short, informative, and contain the major key words); 2) full name(s) and affiliation(s) of the author(s), 3) abbreviated names of the author(s), 4) full name, mailing address, telephone/fax numbers, and e-mail address of the corresponding author; and 5) conflicts of interest (if you have an actual or potential conflict of interest to disclose, it must be included as a footnote on the title page of the manuscript; if no conflict of

interest exists for each author, please state "There is no conflict of interest to disclose"). Please visit Download Centre and refer to the title page of the manuscript sample.

Abstract: The abstract should briefly state the purpose of the study, methods, main findings, and conclusions. For article types including Original Article, Brief Report, Review, Policy Forum, and Case Report, a one-paragraph abstract consisting of no more than 250 words must be included in the manuscript. For News and Letters, a brief summary of main content in 150 words or fewer should be included in the manuscript. Abbreviations must be kept to a minimum and non-standard abbreviations explained in brackets at first mention. References should be avoided in the abstract. Key words or phrases that do not occur in the title should be included in the Abstract page.

Introduction: The introduction should be a concise statement of the basis for the study and its scientific context.

Materials and Methods: The description should be brief but with sufficient detail to enable others to reproduce the experiments. Procedures that have been published previously should not be described in detail but appropriate references should simply be cited. Only new and significant modifications of previously published procedures require complete description. Names of products and manufacturers with their locations (city and state/country) should be given and sources of animals and cell lines should always be indicated. All clinical investigations must have been conducted in accordance with Declaration of Helsinki principles. All human and animal studies must have been approved by the appropriate institutional review board(s) and a specific declaration of approval must be made within this section.

Results: The description of the experimental results should be succinct but in sufficient detail to allow the experiments to be analyzed and interpreted by an independent reader. If necessary, subheadings may be used for an orderly presentation. All figures and tables must be referred to in the text.

Discussion: The data should be interpreted concisely without repeating material already presented in the Results section. Speculation is permissible, but it must be well-founded, and discussion of the wider implications of the findings is encouraged. Conclusions derived from the study should be included in this section.

Acknowledgments: All funding sources should be credited in the Acknowledgments section. In addition, people who contributed to the work but who do not meet the criteria for authors should be listed along with their contributions.

References: References should be numbered in the order in which they appear in the text. Citing of unpublished results, personal communications, conference abstracts, and theses in the reference list is not recommended but these sources may be mentioned in the text. In the reference list, cite the names of all authors when there are fifteen or fewer authors; if there are sixteen or more authors, list the first three followed by *et al.* Names of journals should be abbreviated in the style used in PubMed. Authors are responsible for the accuracy of the references. Examples are given below:

Example 1 (Sample journal reference): Inagaki Y, Tang W, Zhang L, Du GH, Xu WF, Kokudo N. Novel aminopeptidase N (APN/CD13) inhibitor 24F can suppress invasion of hepatocellular carcinoma cells as well as angiogenesis. Biosci Trends. 2010; 4:56-60.

Example 2 (Sample journal reference with more than 15 authors): Darby S, Hill D, Auvinen A, *et al.* Radon in homes and risk of lung cancer: Collaborative analysis of individual data from 13 European case-control studies. BMJ. 2005; 330:223.

Example 3 (Sample book reference): Shalev AY. Post-traumatic stress disorder: diagnosis, history and life course. In: Post-traumatic Stress Disorder, Diagnosis, Management and Treatment (Nutt DJ, Davidson JR, Zohar J, eds.). Martin Dunitz, London, UK, 2000; pp. 1-15.

Example 4 (Sample web page reference): Ministry of Health, Labour and Welfare of Japan. Dietary reference intakes for Japanese. *http://www.mhlw.go.jp/houdou/2004/11/h1122-2a.html* (accessed June 14, 2010).

Tables: All tables should be prepared in Microsoft Word or Excel and should be arranged at the end of the manuscript after the References section. Please note that tables should not in image format. All tables should have a concise title and should be numbered consecutively with Arabic numerals. If necessary, additional information should be given below the table.

Figure Legend: The figure legend should be typed on a separate page of the main manuscript and should include a short title and explanation. The legend should be concise but comprehensive and should be understood without referring to the text. Symbols used in figures must be explained.

Figure Preparation: All figures should be clear and cited in numerical order in the text. Figures must fit a one- or two-column format on the journal page: 8.3 cm (3.3 in.) wide for a single column, 17.3 cm (6.8 in.) wide for a double column; maximum height: 24.0 cm (9.5 in.). Please make sure that the symbols and numbers appeared in the figures should be clear. Please make sure that artwork files are in an acceptable format (TIFF or JPEG) at minimum resolution (600 dpi for illustrations, graphs, and annotated artwork, and 300 dpi for micrographs and photographs). Please provide all figures as separate files. Please note that low-resolution images are one of the leading causes of article resubmission and schedule delays. All color figures will be reproduced in full color in the online edition of the journal at no cost to authors.

Units and Symbols: Units and symbols conforming to the International System of Units (SI) should be used for physicochemical quantities. Solidus notation (*e.g.* mg/kg, mg/mL, $mol/mm^2/min$) should be used. Please refer to the SI Guide www.bipm.org/en/si/ for standard units.

Supplemental data: Supplemental data might be useful for supporting and enhancing your scientific research and BioScience Trends accepts the submission of these materials which will be only published online alongside the electronic version of your article. Supplemental files (figures, tables, and other text materials) should be prepared according to the above guidelines, numbered in Arabic numerals (*e.g.*, Figure S1, Figure S2, and Table S1, Table S2) and referred in the text. All figures and tables should have titles and legends. All figure legends, tables and supplemental text materials should be placed at the end of the paper. Please note all of these supplemental data should be provided at the time of initial submission and note that the editors reserve the right to limit the size and length of Supplemental Data.

5. Submission Checklist

The Submission Checklist will be useful during the final checking of a manuscript prior to sending it to BioScience Trends for review. Please visit Download Centre and download the Submission Checklist file.

6. Online Submission

Manuscripts should be submitted to BioScience Trends online at http://www.biosciencetrends.com. The manuscript file should be smaller than 5 MB in size. If for any reason you are unable to submit a file online, please contact the Editorial Office by e-mail at office@biosciencetrends.com.

7. Accepted Manuscripts

Proofs: Galley proofs in PDF format will be sent to the corresponding author via e-mail. Corrections must be returned to the editor (proof-editing@biosciencetrends.com) within 3 working days.

Offprints: Authors will be provided with electronic offprints of their article. Paper offprints can be ordered at prices quoted on the order form that accompanies the proofs.

Page Charge: Page charges will be levied on all manuscripts accepted for publication in BioScience Trends ($140 per page for black white pages; $340 per page for color pages). Under exceptional circumstances, the author(s) may apply to the editorial office for a waiver of the publication charges at the time of submission.

(*Revised February 2013*)

JOURNAL PUBLISHING AGREEMENT (JPA)

Manuscript No.:

Title:

Corresponding Author:

The International Advancement Center for Medicine & Health Research Co., Ltd. (IACMHR Co., Ltd.) is pleased to accept the above article for publication in BioScience Trends. The International Research and Cooperation Association for Bio & Socio-Sciences Advancement (IRCA-BSSA) reserves all rights to the published article. Your written acceptance of this JOURNAL PUBLISHING AGREEMENT is required before the article can be published. Please read this form carefully and sign it if you agree to its terms. The signed JOURNAL PUBLISHING AGREEMENT should be sent to the BioScience Trends office (Pearl City Koishikawa 603, 2-4-5 Kasuga, Bunkyo-ku, Tokyo 112-0003, Japan; E-mail: **office@biosciencetrends.com**; Tel: **+81-3-5840-8764**; Fax: **+81-3-5840-8765**).

1. Authorship Criteria
As the corresponding author, I certify on behalf of all of the authors that:
1) The article is an original work and does not involve fraud, fabrication, or plagiarism.
2) The article has not been published previously and is not currently under consideration for publication elsewhere. If accepted by BioScience Trends, the article will not be submitted for publication to any other journal.
3) The article contains no libelous or other unlawful statements and does not contain any materials that infringes upon individual privacy or proprietary rights or any statutory copyright.
4) I have obtained written permission from copyright owners for any excerpts from copyrighted works that are included and have credited the sources in my article.
5) All authors have made significant contributions to the study including the conception and design of this work, the analysis of the data, and the writing of the manuscript.
6) All authors have reviewed this manuscript and take responsibility for its content and approve its publication.
7) I have informed all of the authors of the terms of this publishing agreement and I am signing on their behalf as their agent.

2. Copyright Transfer Agreement
I hereby assign and transfer to IACMHR Co., Ltd. all exclusive rights of copyright ownership to the above work in the journal BioScience Trends, including but not limited to the right 1) to publish, republish, derivate, distribute, transmit, sell, and otherwise use the work and other related material worldwide, in whole or in part, in all languages, in electronic, printed, or any other forms of media now known or hereafter developed and the right 2) to authorize or license third parties to do any of the above.

I understand that these exclusive rights will become the property of IACMHR Co., Ltd., from the date the article is accepted for publication in the journal BioScience Trends. I also understand that IACMHR Co., Ltd. as a copyright owner has sole authority to license and permit reproductions of the article.

I understand that except for copyright, other proprietary rights related to the Work (*e.g.* patent or other rights to any process or procedure) shall be retained by the authors. To reproduce any text, figures, tables, or illustrations from this Work in future works of their own, the authors must obtain written permission from IACMHR Co., Ltd.; such permission cannot be unreasonably withheld by IACMHR Co., Ltd.

3. Conflict of Interest Disclosure
I confirm that all funding sources supporting the work and all institutions or people who contributed to the work but who do not meet the criteria for authors are acknowledged. I also confirm that all commercial affiliations, stock ownership, equity interests, or patent-licensing arrangements that could be considered to pose a financial conflict of interest in connection with the article have been disclosed.

Corresponding Author's Name (Signature):

Date: